W-PM-Sym-1 FLUORESCENCE INTENSITY SPECTROSCOPY MAPS MOLECULAR DYNAMICS OF CELLULAR CHEMISTRY. Watt W. Webb, Applied Physics, Cornell University, Ithaca, NY 14853-2501.

Fluctuation spectroscopy and transient analysis of temporal variations of spatial distributions of fluorescent molecular markers of receptors and ligands map receptor distributions and probe the dynamics of their motion and their reactions. Bright markers and electro-optical image analysis facilitate tracking of the motion of individual receptor molecules on the cell surface. We find that congestion of the dense populations of proteins on cell surfaces alters the statistical thermodynamics of these 2-dimensional solutions, and we infer that diffusion is impeded; consequently, the dynamics of transmembrane signals generated by the binding of extracellular ligands to sparse cell surface receptors appear to be slowed. Fluorescent indicators of intracellular chemistry, second messenger activity, pH and polarizable ion concentration can map the dynamics of the diverse cellular responses to membrane signals. They have revealed spatial waves, temporally coherent spatially inhomogeneous limit cycle oscillations of second messengers and complex transient vesicle traffic. As time permits we shall illustrate these cellular dynamics with recent results of research in our group and our collaborators sponsored by the NSF, NIH, ONE and the Biotechnology Program at Cornell.

W-PM-Sym-2 **LUMINESCENCE DIGITAL IMAGING MICROSCOPY** *Thomas M. Jovin, Donna J. Arndt-Jovin, Michel Robert-Nicoud, Thorsten Schormann, Gerard Marriott, and Robert M. Clegg.* Department of Molecular Biology, Max Planck Institute for Biophysical Chemistry, Postfach 2841, 3400 Göttingen, Federal Republic of Germany.

We have applied optical microscopy based on light emission (prompt and delayed fluorescence, phosphorescence) in studies of cellular structures and of processes during the cell cycle, differentiation, and development. Two new technologies have been used [1]: (i) a high performance scientific CCD camera system, and (ii) a confocal laser scanning system.

A new method (photobleaching FRET-Digital Imaging Microcopy, *pbFRET-DIM*) has been developed for spatially resolved proximity measurements by exploiting the high dynamic range, sensitivity, and linearity of the CCD camera in the determination of resonance energy transfer (FRET). Only images of the donor emission before and during photobleaching are required to calculate energy transfer images. Data have been acquired for lectin binding sites, cell surface components involved in exocytosis [2], and for chromatin. The CCD camera has also been adapted for the measurement of delayed luminescence (fluorescence, phosphorescence) by incorporating choppers in the excitation and emission paths of the microscope. Sites of DNA replication in living cells can be visualized by this technique.

Confocal laser scanning microscopy offers a number of advantages for the localization and quantitation of fluorescence labeled targets and probes. Most important is the rejection of interfering signals emanating from out-of-focus and adjacent structures. The "optical sectioning" of the specimen and 3-D reconstruction of numerous cellular structures and systems have been carried out using laser excitation from 351 to 528 nm. References: [1] T. M. Jovin & D. J. Arndt-Jovin, *Ann. Rev. Biophys. Biophys. Chem.* **18** (1989). [2] See also abstract of U. Kubitscheck et al.

W-PM-Sym-3 ^{13}C NMR STUDIES OF DIABETES AND MUSCULAR FATIGUE. R.G. Shulman, D.L. Rothman, T. Jue, T. Price, M.J. Avison, R.A. DeFronzo* and G.I. Shulman, Yale University, New Haven, CT; *present address: University of Texas Health Science Center at San Antonio, TX.

Previous studies have shown that the carbon nuclei in glycogen are 100% visible in ^{13}C NMR despite its high molecular weight. This has been used to interpret a variety of animal studies, following glycogen synthesis and degradation in rat hearts and livers.

In humans we have been able to observe glycogen in both liver and muscle in the natural abundance ^{13}C NMR spectra. In both tissues the signal-to-noise of the glycogen C_1 peak was $\sim$30 at 2.1T, in 13 minutes of accumulation, while the muscle glycogen peak with a small coil was $\sim$40:1 at 4.7T. It has been possible to follow hepatic glycogen repletion after a fast and muscle glycogen depletion during aerobic exercise. In the exercise experiments the correlation of glycogen consumption with fatigue is being investigated.

1-^{13}C (99% enriched) and insulin have been infused into humans to the hyperglycemic, hyperinsulemic conditions needed for muscle glycogen synthesis. Under these conditions normal healthy subjects start glycogen synthesis within 25 minutes while the type II diabetics do not start glycogen synthesis until much later. The 1-^{13}C glycogen peak gives the rate of glycogen synthesis after quantitating its intensity and correcting for degree of labeling.

W-PM-Sym-4 SPIN LABEL OXIMETRY. James S. Hyde[1], Witold K. Subczynski[2], and Akihiro Kusumi[3]. [1]National Biomedical ESR Center, Dept. of Radiology, The Medical College of Wisconsin, Milwaukee, WI USA, [2]Dept. of Biophysics, Institute of Molecular Biology, Jagiellonian University, Krakow, Poland, [3]Dept. of Pure and Applied Sciences, College of Arts and Sciences, University of Tokyo, Meguro-Ku, Tokyo 153, Japan.

Spin Label Oximetry is the measurement of oxygen concentration, diffusion, and collision frequency by the effect of Heisenberg exchange between molecular oxygen and nitroxide radical spin labels on the EPR properties of the spin labels. Four aspects will be discussed. (1) Cellular respiration. Bimolecular collisions of oxygen with labels that uniformly sample the extracellular medium permit the determination of the effective V_{Max} and K_M. (2) The permeability of the cell membrane to oxygen. Using measurements of the bimolecular collision frequency of oxygen with lipid-type labels, the permeability coefficient has been calculated. (3) The effect of bimolecular colli- sions with spin labels is to change the effective spin-lattice relaxation time T_1 of the label. The ability to change T_1 without affecting other rates in a heterogeneous system has been found to be useful in measuring these other rates. In this third aspect, oxygen serves as a purely technical means for changing T_1. (4) We observe a wide range of bimolecular collision frequencies of oxygen with spin labels at various sites in membrane proteins, which may yield information on protein dynamics.

There is an analogy between spin label oximetry and the study of bimolecular collisions of paramagnetic metals with spin labels. Also, collisions between ^{14}N- and ^{15}N-containing spin labels can be measured with our techniques. We are, in fact, developing an EPR-based alternative to fluorescence quenching methodology.

W-PM-Sym-5 X-RAY SPECTROSCOPY AND MAPPING OF SUBCELLULAR COMPOSITION, A.P. Somlyo, PA Musc. Inst. Univ. of PA, Phila., PA, and Dept. of Physiol., Univ. of VA, Charlottesville, VA.

X-ray spectra generated by irradiation of a microvolume with fast electrons provide information about its composition at a spatial resolution of at least 10nm (1-2). In conjunction with rapid freezing and cryoultramicrotomy, electron probe microanalytic spectroscopy (EPMA) permits the in situ measurement of the composition of cell organelles without the translocation of diffusible elements that occur during cell fractionation. The practically attainable limit of detectability (for calcium) in ultra thin cryosections is 0.3mmol/kg (3). The collection of spectra from individual object points, while scanning the electron beam, can be used to generate X-ray maps showing the elemental distribution within cells and organelles. These methods have been used to answer the question whether mitochondria or the endoplasmic reticulum play a significant role in the regulation of cytoplasmic Ca^{2+} in nonmuscle cells, to quantitate the monovalent ionic composition of the sarcoplasmic reticulum (SR) and the ionic movements associated with calcium release during contraction in striated (e.g. 4) and in smooth muscle, and to measure subcellular ionic composition related to diverse problems such as visual transduction, pathology of mitochondrial calcium and magnesium transport, localization of calcium in sickle cells, eurokarytic and bacterial membranes and spores. Some of the results of these studies and brief summary of further potential of X-ray and electron energy loss spectroscopy in biology will be presented. Supp. by grant HL15835 to PA Musc Inst. 1) Somlyo, A.P. & Shuman, H. Ultramicroscopy 8:219, 1982. 2) LeFurgey, A., Bond, M. & Ingram, P. Ultramicroscopy 24:185, 1988. 3) Somlyo, A.P. Cell Calcium 6:197-212, 1985. 4) Somlyo, A.V., McClellan, G., Gonzalez-Serratos, H. and Somlyo, A.P. J. Biol. Chem. 260:6801-6807, 1985.

W-PM-Min-1 FROM FEMTOSECONDS TO BIOLOGY: MECHANISM OF THE LIGHT-DRIVEN PROTON PUMP IN BACTERIORHODOPSIN. Richard A. Mathies, Chemistry Department, University of California, Berkeley CA 94720.

Bacteriorhodopsin is an intrinsic membrane protein that is found in the purple membrane of *Halobacterium halobium*. Light absorption by its all-*trans* retinal prosthetic group drives the pigment through a photoreaction cycle that pumps protons outside the cell. The primary photochemical reaction is an excited-state, 13-*trans* to 13-*cis* double bond isomerization of the chromophore that has recently been directly observed using femtosecond (10^{-15} s) transient absorption spectroscopy (Mathies et al., Science *240*:777, 1988). The elucidation of the structure of retinal in the intermediates of bacteriorhodopsin is a prerequisite for defining the molecular mechanism of proton pumping. To accomplish this we have used time-resolved resonance Raman spectroscopy to obtain vibrational spectra of the chromophore in bacteriorhodopsin's intermediates. Our recent work has focused on the structure of the chromophore in the M and N intermediates to define the molecular mechanism of the "reprotonation switch" which controls the connectivity of the Schiff base proton. The M intermediate contains a 13-*cis*, 14-s-*trans*, 15-*anti* Schiff base chromophore (Ames et al., Biochem., submitted), and the N intermediate is formed by simply protonating M (Fodor et al., Biochem. *27*:7097, 1988). These results eliminate chromophore based reprotonation switch mechanisms such as C_{14}-C_{15} bond rotation or inversion of the Schiff base nitrogen. An alternative "C-T Model" for the reprotonation switch in bacteriorhodopsin has been developed which is consistent with the known chromophore structures (Fodor et al., Biochem. *27*:7097, 1988). This model utilizes isomerization-driven protein conformational changes between a high-free energy "C-form" and a low-free energy "T-form" to regulate the connectivity of the Schiff base proton. This work, together with the results of linear dichroism experiments which indicate that the Schiff base N-H bond points toward the cytoplasm (S.W. Lin and R.A. Mathies, Biophys. Soc. abstract), will be used to discuss possible proton pumping mechanisms.

W-PM-Min-2 THE REACTION CYCLE OF THE SARCOPLASMIC RETICULUM Ca^{2+} PUMP. Wm. P. Jencks. Graduate Department of Biochemistry, Brandeis University, Waltham, MA 02254.

Coupling of ATP hydrolysis to the pumping of Ca^{2+} by the Ca ATPase of SR can be accounted for by changes in the chemical and vectorial specificities for catalysis in different chemical states of the enzyme: E·Ca_2 catalyzes reversible phosphoryl transfer between ATP and the enzyme and E catalyzes reversible phosphoryl transfer between Pi and the enzyme; the free enzyme binds and dissociates cytoplasmic Ca^{2+}, while phosphoenzyme dissociates and binds calcium inside the vesicle. Phosphorylation of the enzyme by bound ATP requires the binding of 2 Ca^{2+} and the change in specificity to dephosphorylation by water requires prior dissociation of 2 Ca^{2+}, consistent with the stoichiometry of 2 Ca^{2+} transported per ATP hydrolyzed. Phosphorylation by ATP occurs in two steps: a rate-limiting conformational change of E·ATP·Ca_2 followed by rapid, reversible phosphoryl transfer. Rapid phosphoryl transfer to ADP in the reverse direction gives a burst of phosphoenzyme disappearance and change in the direction of Ca^{2+} dissociation. Binding of exterior Ca^{2+} and phosphorylation by ATP are not inhibited by 20 mM interior Ca^{2+}, which might be expected to form "E_2·Ca_2" with Ca^{2+} bound to interior sites. Conformational changes occur in most steps of the reaction. Binding and dissociation of cytoplasmic Ca^{2+} do not proceed through a free, high-affinity intermediate "E_1". These and other properties of the reaction cycle are not consistent with the usual definitions of "E_1-E_2" and related models for active transport.

W-PM-Min-3 CORRELATIONS OF FUNCTION AND STRUCTURE IN THE SARCOPLASMIC RETICULUM ATPase. G. Inesi, D. Bigelow, T. Squier, I. Gryczynski and C. Sumbilla. Department of Biological Chemistry, Universty of Maryland School of Medicine, Baltimore, Maryland 21201.

Functional studies of the sarcoplasmic reticulum (SR) ATPase provide characterization of the catalytic and transport cycle, and allow mechanism-linked analysis of transport energetics. Another important aim is to unveil the roles of specific residues and of the protein conformation in the mechanism of vectorial catalysis. The substrate site is localized by ATP binding inhibition following FITC derivatization of Lys515, and by phosphoryl transfer from ATP to Asp351. Fluorescence energy transfer measurements with the ATPase covalently labeled at Cys670, Cys674, Cys344, Cys364 and Lys515, as well as TNP-AMP and Pr^{3+} bound to the nucleotide and calcium sites respectively, suggest that the cytoplasmic portion of the ATPase is folded to form a crevice for substrate binding. The nucleoside binding moiety of this site is not required for energy transduction, while phosphorylation of Asp351 is crucial. No large changes in secondary or tertiary structure within the cytoplasmic portion of the ATPase have been detected upon enzyme activation. Rather, fluorescence characterization of several tryptophan residues in hydrophobic regions demonstrates an increase of lifetimes and loss of anisotropy upon calcium binding. This reversible phenomenon, likely due to stabilization of clustered membrane helices, suggests that an interactive channel is involved in vectorial translocation of calcium. Involvement of hydrophobic domains is also evidenced by carbodiimide derivatization. The sensitivity of the transmembrane helices to calcium binding, and the reverse effect by enzyme phosphorylation, constitute an important device in the coupling mechanism.

W-PM-Min-4 CATION BINDING SITES ON THE Na/K PUMP. S.J.D. Karlish; Biochemistry Dept., Weizmann Institute of Science, Rehovot 76100, Israel.

The outstanding function-structure problem of cation pumps such as the Na/K-, H/K- and Ca-ATPases is the structure of the cation binding sites and detailed mechanism of cation binding, occlusion and movement through the protein. These pumps show a high degree of primary sequence homology and a similar predicted trans-membrane organization. The recent structural knowledge has lead to interesting (and some wild) speculation as to the nature of cation binding sites but there is as yet little or no real evidence.

I shall present experiments utilizing renal Na/K-ATPase and reconstituted vesicles, in conjunction with sensitive assays of cation transport and occlusion, which provide initial information as to the nature of cation binding residues. These include observations on electrogenic potentials and voltage-sensitivity of the reconstituted pumps, and inactivation of Rb(K) and Na occlusion on Na/K-ATPase by the hydrophobic carbodiimide DCCD. Together the experiments suggest that the cation binding and transporting domain of the Na/K-pump contains two negatively charged residues (asp,glu) in a non-aqueous environment and furthermore that the same residues are involved in binding, occlusion and transport of both Na and K(Rb) from either surface. Known features of the cation sites and trans-membrane path will be summarized and where possible these will be compared for the different cation pumps.

W-PM-Min-5 LIGANDS CONTROL THE Na/K PUMP'S TRANSPORT REACTION MECHANISM.
Joseph F. Hoffman, Department of Cellular and Molecular Physiology, Yale University School of Medicine, New Haven, CT 06510

W-PM-A1 **DIFFERENTIAL EFFECTS OF IP_3 AND Ca^{2+} INJECTIONS ON MEMBRANE CURRENTS OF *APLYSIA* NEURONS.**
Simon LEVY, Boston Univ. Sch. Med., Boston, Mass 02118.

I reported previously that injection of 1,4,5 inositol trisphosphate (IP_3) caused an increase in cytoplasmic Ca (Ca_i) that was spatially restricted to certain areas of identified *Aplysia* bursting neurons (*Biophys J* 51:424a, 1987). Since I found that the site of largest IP_3-induced Ca_i increase was generally near the plasma membrane, an important question is whether the sites of mobilized Ca^{2+} and Ca^{2+} influx are physically separate. Using double-barrelled Ca selective electrodes and a puffer electrode filled with high K^+-seawater, I induced a Ca_i increase by either pressure-injecting IP_3 intracellularly (using the 2nd barrel of the double-barrelled Ca electrode) or puffing high K^+ extracellularly. Both Ca_i increases were measured at the same site by the Ca selective barrel. The Ca_i increase induced by high K^+ was found to be much slower than the IP_3-induced Ca_i increase. The slower Ca_i increase probably reflects diffusion and buffering of the Ca^{2+} influx following depolarization by high K^+. This result could imply that entering Ca^{2+} and mobilized Ca^{2+} are intended to reach different target molecules. Injection of IP_3 was also found to induce distinct changes in holding current (Levy, *J Gen Physiol* 92:2a, 1988; Scholz *et al*, *J Neurophysiol* 60:86, 1988). To investigate whether the changes in holding current were primary or mediated by the Ca^{2+} released by IP_3, we used double-barrelled injecting electrodes which allow delivery of either Ca^{2+} or IP_3 at the *same* point (this is because the effects of IP_3 were found to be depth- and neuron-dependent). Side-by-side comparison of the currents induced by IP_3 and Ca^{2+} show that in most cells they are different both in waveform and time course: for example a rapid inward current induced by IP_3 *versus* an outward current induced by Ca^{2+}. This result implies that changes in membrane currents induced by IP_3 are not necessarily caused by mobilized Ca^{2+}.

W-PM-A2 TWO TYPES OF CHANNELS IN THE PLASMA MEMBRANE OF THE PITUITARY GONADOTROPH.
S.S. Stojilkovic, A. Stutzin, K.J. Catt, and E. Rojas, LCBG, NIDDK, and ERRB, NICHD, Bethesda, MD 20892

Measurements of the Ca^{2+} currents in cultured rat pituitary gonadotrophs were made using patch clamp techniques. Analysis of the inward Ca^{2+} currents, recorded in the presence of 5.2 mM Ca^{2+} (or Ba^{2+}), revealed a fast component, with activation-inactivation kinetics, and a delayed one with slower activation. The rate of inactivation of the first component was found to be voltage dependent. At -44 mV, a 5.5 mV change in potential induced an e-fold change in the fraction of Ca^{2+} channels available to conduct Ca^{2+} current. During long-lasting (100-200 msec) low-frequency depolarizing voltage clamp pulses, the size of the delayed component of the Ca^{2+} current remained constant. A comparison of the time constants for turning off the Ca^{2+} conductance showed that for brief pulses the tail currents could be described as the sum of two exponentials. For pulses of long duration (100 msec) a single exponential fitted the time course of the current tails. The differential effects of membrane potential on inactivation, and the different time constants for turning off the Ca^{2+} conductance, suggest the presence of two types of calcium channels in the membrane of the gonadotroph. We propose that the Ca^{2+} channel with activation-inactivation kinetics plays a major role in the control of Ca^{2+} entry required for the physiological response of the cell.

W-PM-A3 CALCIUM CURRENTS IN RAT PANCREATIC B-CELLS IN CULTURE. J. Hidalgo, M.-Y. Li, I. Atwater and E. Rojas. LCBG, NIH, Bethesda, MD 20892 (Introd. by V. Cena).
The patch voltage clamp technique was used to measure Ca^{2+} currents across the membrane of rat pancreatic B-cells. Cell cultures maintained for 2-10 days in a medium (CMRL 1066 from Gibco) supplemented with glucose (5.6 mM) secreted insulin in response to the sugar (11-33 mM) and to high K^+ (50 mM) in a bicarbonate-buffered Krebs solution at 37 °C.
Whole cell membrane currents (pipet solution (mM): 70 CsCl, Cs-glutamate, 10 Cs-Pipes, 5 Mg-ATP, 10 Cs-EGTA at pH 7) exhibited two distinct components, an early transient one and a delayed non-inactivating one. In the presence of a modified Krebs solution (mM: 120 Choline-Cl or TMA-Cl, 5 KCl, 1 $MgCl_2$, 2-6 $CaCl_2$, 5 CsHepes, pH = 7.4), the mid-point for the activation of the component with activation-inactivation kinetics (Ca-1) was ca. -45 mV and that of the delayed component (Ca-2) was 10 mV. With Ba^{2+} in place of Ca^{2+} in the external solution, only the delayed, non-inactivating, component was present in the records. The mean value of the maximum transient Ca^{2+} current (21 I-V curves from 5 cells) was -75 pA (Ca^{2+} = 4 mM) and that of the non-inactivating component was -125 pA. In the presence of glucose (11 mM) in the external solution single Ca^{2+}-channel currents (cell-attached configuration) measured with high (100 mM) Ca^{2+} or Ba^{2+} in the pipet ranged between 0.5 and 1.1 pA. Therefore, from the ratio "maximum whole cell membrane current/single Ca^{2+}-channel current" (i.e. 200/0.5) we estimate that an islet B-cell is equipped with about 400 Ca^{2+}-channels.

W-PM-A4 **COMPONENTS OF CALCIUM CURRENT IN DIFFERENTIATED PC12 CELLS AND NEONATAL RAT SYMPATHETIC NEURONS.** Mark R. Plummer, Diomedes E. Logothetis & Peter Hess, Dept. of Cellular & Molecular Physiology, Harvard Medical School, 25 Shattuck St., Boston, MA 02115

Differentiated PC12 cells and sympathetic neurons show a non-inactivating, dihydropyridine (DHP)-sensitive current at relatively positive holding potentials (-40 mV) and a partially inactivating, DHP-insensitive current at more negative holding potentials (-90 mV) when 20 mM Ba^{2+} is the charge carrier. 16 μM ω-Conotoxin (GVIA) inhibits the barium currents (by 50% in PC12 and by >70% in neonatal day 1-3 sympathetic neurons) and reveals three components: 1) Conotoxin-sensitive; 2) Conotoxin-resistant, DHP-sensitive, non-inactivating; and 3) Conotoxin-resistant, DHP-resistant, inactivating. The proportions of these three currents differ in the PC12 and sympathetic cells, but all three components can be found. Single channel recordings reveal at least two types of calcium channels. The first is the L-type channel (conductance = 26 pS, DHP-sensitive). The second channel is DHP resistant and is strongly inactivated at positive holding potentials but differs from the previously described N-type channel by its larger conductance (19-21 pS) and its much slower rate of inactivation. The difference in conductance may be explained by our finding that this channel can, especially in the sympathetic neurons, spend prolonged periods of time in a subconductance state of approximately 13 pS (arrows).

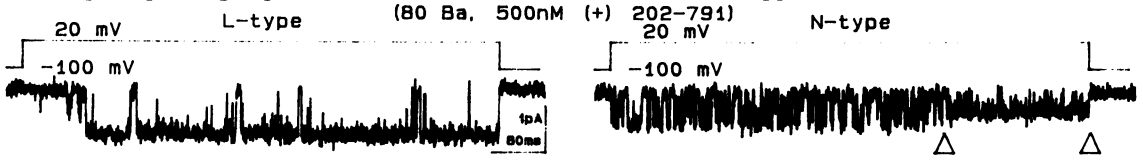

W-PM-A5 MEMBRANE CURRENTS OF *XENOPUS LAEVIS* OOCYTES INJECTED WITH RNA FROM RETINAS OF CARP AND MOUSE. Lawrence Pinto, Neurobiology Dept. Northwestern Univ., Evanston IL 60201, Akimichi Kaneko, National Institute for Physiological Sciences, Myodaiji, Okazaki, 444, JAPAN, Cathy Bowes and Deborah Farber, Jules Stein Institute, UCLA, Los Angeles.

We measured membrane currents with a two electode voltage clamp 3-7 days after injection of 50 nl of total RNA (1 μg/μl) extracted from retinas of adult carp or 9-11 day old C57BL/6J mice. Control oocytes were either uninjected or injected with distilled water. For oocytes injected with carp RNA, studied with 0.7 mM $[Ca^{2+}]_o$, depolarization (from a holding voltage, Vh, of -90mV) produced an outward current that was attenuated by 20 mM TEA, 1 mM Co^{2+}, or 500 μM DIDS. After offset of the depolarization an inward tail current flowed for 10 mM $[Ca^{2+}]_o$. This current was decreased by 500 μM DIDS. No TTX-sensitive currents were observed. Thus, $I_{K(V)}$, I_{Ca} and $I_{Cl(Ca)}$ flowed in the oocytes injected with RNA from carp retinas. For oocytes injected with mouse retinal RNA, depolarization (Vh = -90mV) also produced a DIDS-sensitive outward current, but in the presence of 40 mM Ba^{2+}, 10 mM Cs^{+}, and 20 mM TEA (0 Ca added) the current became inward for depolarizations to -10 to +20 mV. An inward tail current flowed after offset of the depolarizing pulse with 0.7 mM $[Ca^{2+}]_o$. This inward tail current was made larger by increasing $[Ca^{2+}]_o$, and was decreased by substitiution of Ba^{2+} or Co^{2+} for Ca^{2+} or addition of 400 μM DIDS. Thus, I_{Ca} and $I_{Cl(Ca)}$ also flowed in oocytes injected with mouse RNA, but I_{Ca} was more pronounced in the oocytes injected with mouse RNA than in the oocytes injected with carp RNA. Supported by NIH, NSF and JSPS.

W-PM-A6 **TRANSFORMATION BY c-raf MODIFIES KINETICS OF T-TYPE CA CURRENTS.** *Chinfei Chen, Michael J. Corbley*, Thomas M. Roberts* and Peter Hess.* Dept. of Cell. and Mol. Physiology, Neuroscience Program and Dana Farber Cancer Inst.*, Harvard Medical School, Boston, Ma 02115.

Normal 3T3 fibroblasts contain L- and T-type Ca channels with properties very similar to those found in excitable cells. Transformation by oncogenes specifically alters the density of T-type currents. Transformation induced by oncogene products localized in the cell membrane (c-H-*ras*, EJ-*ras*, v-*fms*, v-*src*, polyoma middle T) abolished T-type currents, while oncogene products mainly confined to the nucleus (polyoma large T, SV40 large T) reduced T-type current densities without affecting channel kinetics. The only proto-oncogene found in the cytoplasm of fibroblasts is c-*raf*, a serine-threonine kinase. At potentials which elicit T-type current in non-transformed cells (trace a), fibroblasts transformed by activated c-*raf* display a calcium current (trace b) with much slower activation and inactivation kinetics. However, the steady state kinetic properties, reversal potentials, current-voltage relationship and single channel conductance of this *raf*-related calcium current are very similar to those of the T-type current and strongly suggest that the *raf*-related calcium current is a kinetically modified T-type current. Although the mechanism by which transformation affects Ca channel expression is unclear, the fact that in all cases the effects specifically affect T-type Ca channels might suggest a yet unknown link between T-type Ca channel activity and the control of cell growth.

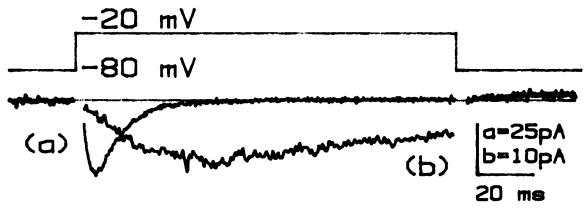

W-PM-A7 PHOTOAFFINITY LABELING OF DILTIAZEM BINDING POLYPEPTIDE IN PURIFIED SKELETAL MUSCLE CALCIUM CHANNEL PREPARATIONS. K. Naito, K. Itagaki, E. McKenna, A. Schwartz and P. Vaghy, Department of Pharmacology and Cell Biophysics, University of Cincinnati, OH 45267-0575.

Three distinct chemical groups of calcium antagonists act on voltage-dependent calcium channels. It has recently been demonstrated that two of these groups: 1,4-dihydropyridines (nifedipine-like drugs) and phenylalkylamines (verapamil-like drugs) specifically bind to a 165 KDa polypeptide (α_1 subunit) present in purified skeletal muscle calcium channel preparations. The primary structure of this polypeptide suggests that it alone or in combination with other subunits (α_2, β, γ, and δ) forms the voltage-dependent calcium channels. Covalent labeling of the purified receptor with the third group of calcium antagonists: benzothiazepines (diltiazem-like drugs) has not been reported. We have isolated calcium channels from digitonin solubilized rabbit skeletal muscle T-tubular membranes by lectin affinity chromatography and sucrose density gradient centrifugation. For covalent labeling of the benzothiazepine binding polypeptide, [^{3}H]-azidobutyril diltiazem, a newly synthesized photoaffinity probe (Tanabe Seiyaku Co., Ltd., Japan) was used in the absence and presence of excess concentration of unlabeled diltiazem. Our data suggest that diltiazem-like drugs also bind specifically to the α_1 subunit of the purified skeletal muscle voltage-dependent calcium channels. (Supported by NIH grant RO1 HL41088).

W-PM-A8 TISSUE SPECIFIC ISOFORMS OF THE α_1 SUBUNIT OF THE VOLTAGE DEPENDENT CALCIUM CHANNEL. W.J. Koch, D.F. Slish, A. Hui, G. Varadi, and A. Schwartz, Department of Pharmacology and Cell Biophysics, University of Cincinnati, Cincinnati, Ohio 45267-0575.

The L type voltage dependent calcium channel (VDCC) is an important regulator of the function of excitable tissues including cardiac, vascular smooth, and skeletal muscle and brain. The L type VDCC of skeletal muscle transverse tubular membranes has been purified and characterized. This channel contains five putative subunits termed α_1, α_2, β, γ, and δ. The α_1 subunit contains the binding domains for three classes of calcium channel modulators, phenylalkylamines, benzothiazepines, and 1,4-dihydropyridines, and is phosphorylated by protein kinases. Tissue specific α_1 isoforms have been isolated by screening rabbit heart, rat aorta and rat brain cDNA libraries with skeletal muscle cDNA clones. Several partial clones have been isolated which exhibit varying degrees of sequence homology with the skeletal muscle α_1 clones. Northern analysis using tissue specific cDNA clones shows major differences in the size and number of the hydribizing signals in the tissues studied. These immunological cross-reactivity data together with the reported experiments, electrophysiological studies and the well known tissue selective effects of calcium antagonists suggest the existence of tissue specific calcium channel isoforms. (Supported by T32 HL07382 and Berlex Fellowship.)

W-PM-A9 Isolation of a voltage dependent calcium channel from the squid central nervous system. Cherksey, B., Sugimori, M., Lin, J.-W. and R. Llinás. NYU Medical Center, New York, NY 10016.

FTX, a low molecular weight factor purified from American funnel-web spider venom, which specifically blocks the squid presynaptic calcium current (Sugimori, et al, 1988, Biol. Bull., in press) was used to construct an affinity chromatography gel. Solubilized squid optic lobe homogenate was reacted batchwise with the gel, the bound protein eluted and reconstituted into lipid vesicles by sonication/dialysis. When vesicles were preloaded with Quin-2,addition of Ca++ to the external medium produced a rapid, sustained increase in the fluorescence, not seen in control vesicles. Influx was blocked by 50 µM Cd++. FTX blocked in a dose-dependent and competitive manner with external Ca++. When a Nernst potential was established by valinomycin, the Ca++ influx into the vesicles was found to be voltage dependent. Vesicles were also fused with lipid bilayers formed across the tip of a patch-clamp micropipette. Two types of channel-like activity were found. The first was characterized by voltage-dependent openings of 1-3 msecs duration (mean). The opening probability, which was also voltage dependent, reached a maximum of 0.35 at a potential of 0 mV. The conductance was 15-20 pS in 80 mM Ba++ and 5-8 pS in 100 mM Ca++. Comparison of the macroscopic currents obtained by summing multiple pulses reproduced closely the macroscopic Ica in squid terminals (Llinás, et al. Biophys. J., 33, 289, 1981). When the cytoplasmic face of the protein was exposed to high concentrations of Ba++, extremely long mean open times (300 msec) of similar conductance were observed. In symmetric Ba++ solutions, replacement of the cytoplasmic solution with Cs+ resulted inconversion of long openings to short openings. High internal calcium (100 mM) did not change the opening-time mode. We conclude that using an affinity gel based on FTX, it has been possible to isolate and partially purify a calcium channel with the properties expected for the presynaptic channel.

W-PM-A10 DIHYDROPYRIDINE RECEPTOR GENE EXPRESSION: INDUCTION AND REPRESSION OF FUNCTIONAL "SLOW" CALCIUM CHANNELS INVOLVE A PRETRANSLATIONAL MECHANISM. Hue-Teh Shih, Helene Bigo, John M. Caffrey, Michael D. Schneider. Baylor College of Medicine, Houston, TX.

To establish whether formation of the dihydropyridine (DHP)-sensitive "slow" calcium channel in skeletal muscle is regulated by pretranslational mechanisms, DHP receptor (DHPR) mRNA abundance was analyzed by Northern hybridization, using synthetic oligonucleotides derived from the rabbit skeletal muscle DHPR cDNA. A 6.5 kb putative DHPR transcript was identified in differentiated mouse C2 myocytes and post-natal C3H mouse skeletal muscle. Little or no DHPR mRNA was detected in proliferating C2 cells, in agreement with our previous measurements of functional "slow" channels and DHP binding sites. DHPR mRNA was induced at least 10-fold after mitogen withdrawal, and was reversibly suppressed by 0.5 nM transforming growth factor ß, which we have shown to block the appearance of "slow" channels and DHPR. DHPR mRNA also was induced by mitogen withdrawal in BC3H1 myocytes, but not in BC3H1 cells stably transfected with a mutant *ras* allele that prevents muscle-specific gene expression. In contrast, DHPR gene expression was not prevented by incorporation of activated oncogenes (v-*erb*B, SV40:c-*myc*) which were permissive for myogenesis and Ca^{2+} channel expression. DHPR mRNA was detected in 2-day post-natal C3H mouse skeletal muscle and increased 14-fold by 2 months of age. In agreement with the finding that the density of "slow" Ca^{2+} channels did not increase after denervation (Gonoi & Hasegawa, *J. Physiol.* 401:617), DHPR mRNA abundance failed to change in soleus muscle 10 and 15 days after tibial nerve transection, despite marked up-regulation of the delta AChR transcript. Thus, developmental regulation of "slow" calcium channels, and the effects of growth factors and cellular oncogenes on calcium channel density measured by biophysical techniques and ligand binding, involve control at a pretranslational level. Furthermore, denervation exerts discordant effects on the genes encoding DHPR and an AChR sub-unit.

W-PM-B1 EVIDENCE FOR ATP-INDUCED MICROSECOND CROSS-BRIDGE ROTATION C.L. Berger, E.C. Svensson and D.D. Thomas, Dept. of Biochemistry, U of MN, Minn., MN 55455

We have used photolysis of caged ATP to obtain transient ST-EPR signals from maleimide spin-labeled myosin heads during maximal actin-activated ATPase activity. Our goal is to test the proposal that ATPase activity is coupled to rotational motion of cross-bridges (heads attached to actin). We have previously reported that ATP induces usec rotational motions of spin-labeled myosin heads in activated myofibrils and muscle fibers, but in these complex cycling systems, it is difficult to determine whether the motion is occurring when heads are attached to actin. In order to obtain data on heads that are attached to actin in the presence of saturating ATP, we have performed ST-EPR on acto-S1 at very low ionic strength, at 200 uM actin. Sedimentation experiments showed that 50-60% of the labeled S1 is bound to actin under these conditions. However, the ATPase activity is so high that only a few seconds are available for EPR data acquisition. Therefore, caged ATP was mixed with the sample in the dark, and approximately 1 mM ATP was produced by shining an intense pulse of UV light into the EPR cavity. The rigor ST-EPR signal level decreased rapidly to a steady-state level upon the release of ATP, then returned to the original level as the ATP was depleted. After correction for unbound S1, we conclude that S1 undergoes usec rotational motions when bound to actin during the ATPase cycle. It is likely that similar cross-bridge rotations occur during muscle contraction.

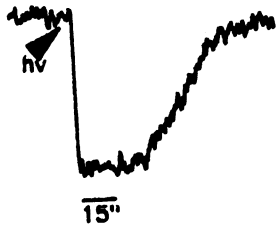

W-PM-B2 THE BIOCHEMICAL KINETICS AT HIGH S-1 CONCENTRATIONS: THE RELATIONSHIP BETWEEN K^a(ATPASE), K^s(ATPASE) AND K(BINDING). Leonard A. Stein and Vijay A. Harwalkar, Cardiology Division, Departments of Medicine and Physiology, SUNY at Stony Brook, Stony Brook, N.Y.11794

The actomyosin ATPase activity of skeletal myosin Subfragment-1 (S-1) can be studied either by treating S-1 as the enzyme, which is the most common way, or by treating actin as the enzyme by keeping the actin concentration low and varying the S-1 concentration. General agreement exists over the kinetic data associated with the actoS-1 ATPase activity when S-1 is treated as the enzyme, but this is not the case when actin is treated as the enzyme, and disagreement exists over whether both the V^amax and the K^a(ATPase) depend on the actin concentration, or if V^amax is approximately constant and only the K^a(ATPase) is actin dependent.

In the current work we have reinvestigated the steady state kinetics of actoS-1 using either actin or S-1 as the enzyme, and we have devised a mathematical scheme that brings the two realms of kinetics into one unified model. Let K(Binding) be the apparent dissociation constant of actin to S-1 during the steady state hydrolysis of ATP and V^smax and K^s(ATPase) be the kinetic constants for the situation where S-1 is treated as the enzyme. Furthermore, let V^amax and K^a(ATPase) be the same constants with actin as the enzyme. We find that if the proper range of actin and S-1 are chosen, these constants are related as follows:

$$V^a\text{max} = (K(\text{Binding})/K^s(\text{ATPase}))V^s\text{max}$$

$$K^a(\text{ATPase}) = K(\text{Binding}) + ((K(\text{Binding})/K^s(\text{ATPase}))-1)[\text{Actin}]$$

Hence we find that V^amax is independent of the actin concentration and that K^a(ATPase) has a simple linear dependence on the actin concentration. Data that support this model are presented.

W-PM-B3 THE BIOCHEMICAL KINETICS AT HIGH S-1 CONCENTRATIONS: THE RELATIONSHIP BETWEEN K^a(ATPASE), K^s(ATPASE) AND K(BINDING). Leonard A. Stein and Vijay A. Harwalkar, Cardiology Division, Departments of Medicine and Physiology,SUNY at Stony Brook, Stony Brook, N.Y.11794

The actomyosin ATPase activity of skeletal myosin Subfragment-1 (S-1) can be studied either by treating S-1 as the enzyme, which is the most common way, or by treating actin as the enzyme by keeping the actin concentration low and varying the S-1 concentration. General agreement exists over the kinetic data associated with the actoS-1 ATPase activity when S-1 is treated as the enzyme but this is not the case when actin is treated as the enzyme, and disagreement exists over whether both the V^amax and the K^a(ATPase) depend on the actin concentration, or if V^amax is approximately constant and only the K^a(ATPase) is actin dependent.

In the current work we have reinvestigated the steady state kinetics of actoS-1 using either actin or S-1 as the enzyme, and we have devised a mathematical scheme that brings the two realms of kinetics into a unified model. Let K(Binding) be the apparent dissociation constant of actin to S-1 during the steady state hydrolysis of ATP and V^smax and K^s(ATPase) be the kinetic constants for the situation where S-1 is treated as the enzyme. Furthermore let V^amax and K^a(ATPase) be the same constants with actin as the enzyme. We find that if the proper range of actin and S-1 are chosen, these constants are related as follows:

$$V^a\text{max} = (K(\text{Binding})/K^s(\text{ATPase}))V^s\text{max}$$

$$K^a(\text{ATPase}) = K(\text{Binding}) + ((K(\text{Binding})/K^s(\text{ATPase}))-1)[\text{Actin}]$$

Hence we find that V^amax is independent of the actin concentration and that K^a(ATPase) has a simple linear dependence on tha actin concentration. Data that support this model are presented.

W-PM-B4 LOCATION OF A CONTACT SITE BETWEEN ACTIN AND MYOSIN IN THE 3-D STRUCTURE OF THE ACTO-S1 COMPLEX. Andrzej A. Kasprzak, Patrick Chaussepied, and Manuel F. Morales, CVRI, University of California, San Francisco.

Using fluorescence energy transfer, we measured distances from a chromophore located in the vicinity of the actin-binding stretch 633-642 of myosin subfragment 1 (S1), to 5 points in the acto-S1 complex. Specific labeling of this part of the S1 heavy chain was achieved by first attaching the desired chromophore to a peptide, that by virtue of its charge complementarity specifically binds to this segment of S1 (Chaussepied & Morales, 1988, PNAS, *in press*), and then EDC-crosslinking the fluorescent antipeptide to S1. By employing this technique, antipeptides containing the 3 different labels were purified and specifically attached to S1: dansylaziridine (DNZ-***P***), iodoacetamidofluorescein (IAF-***P***) and monobromobimane (MBB-***P***). Based on the fluorescent lifetime decrease of the donors, the following distances were measured: (the donor→acceptor pairs are given in brackets): ***P***-Cys 707 (S1) [DNZ→ITMR], 50 Å; ***P***-Cys 697 (S1) [DNZ→MTMR], 47 Å; ADP(S1)-***P*** [ε-ADP·V_i→IAF], ≥59 Å; ADP (actin)-***P*** [ε-ADP→MBB], 40 Å; ***P***-Cys 374 (actin) [MBB→DAB], 47.4 Å; Cys 374-***P*** [1,5-IAEDANS→IAF], 59.4 Å. Addition of Mg·ATP had a small effect on the distance between the peptide and Cys 707, increasing it by ~4%, while it had a more pronounced effect on the distance between the peptide and Cys 697, where an increase of 15% was observed. The effect of actin on these two distances was negligible. These data enabled us 1) to place for the first time an interprotein contact in the 3-D map of the acto-S1 complex 2) to definitively exclude models of communication between the nucleotide and actin binding sites within S1, which involve direct contact or close proximity of these two loci of S1. (Supported by HL-16683, MDA (to PC) and AHA (to MFM)).

W-PM-B5 ANALYSIS OF A DROSOPHILA MELANOGASTER FLIGHT MUSCLE ACTIN MUTANT. Sparrow J.C.,[1] Reedy M.[2], Ball E.[1], Molloy J.E.[1], Hennessey E.S.[1], and D.C.S. White[1].

1. Department of Biology, University of York, Heslington, York, YO1 5DD, U.K.
2. Department of Anatomy, Duke University Medical Centre, Durham N.C. 27710, U.S.A.

We report a co-ordinated genetic, physiological and E.M. study of a flightless mutation (Act88F^{M342}) of the single actin gene expressed in the indirect flight muscle of Drosophila. DNA sequencing shows that the mutation causes a glutamic acid to lysine substitution in codon 93, making the mutant protein more basic. The mutant flight muscles contain normal amounts of actin and other muscle proteins. Mechanical experiments on single glycerinated fibers show that the mutant has about one half the stiffness under relaxing conditions seen in the wild-type and the response in activating solution is indistinguishable from that in relaxing solution. In the absence of ATP, the mutant develops a small rigor tension, and stiffness increases about three-fold over the relaxed state. The mutant muscle contains myofibrils which lack Z-discs. Thin filaments are formed and are marked by typical rigor crossbridges between thick and thin filaments in the absence of ATP in glycerinated fibers; the structure of these crossbridges appears similar to rigor bridges seen in wild-type Drosophila and Lethocerus. We conclude that the M3 42 mutant actin has functional actin binding sites that permit thin filament formation and myosin binding sites that can enable formation of rigor bonds, but may have lost the ability to bind to other proteins, such as α-actinin or capping proteins, whose interaction with thin filaments is required for the formation of Z-discs.

W-PM-B6 THE RATE OF Mant-ADP RELEASE FROM CROSS-BRIDGES OF SINGLE SKELETAL MUSCLE FIBERS. M.A. Ferenczi, S.K.A. Woodward, J.F. Eccleston. *N.I.M.R., Mill Hill, London NW7 1AA, U.K.*

The fluorescent ATP analogue 3'(2')-O-(N-methyl)anthraniloyl-ATP [1](Mant-ATP) supports force generation and shortening in muscle fibers. Solution studies demonstrate that the kinetics of Mant-ATP hydrolysis by subfragment 1 are similar to those of ATP and that Mant-ADP fluorescence is reduced by a factor of two upon dissociation from myosin. We were thus able to measure the rate of Mant-ADP release from single glycerinated fibers of rabbit psoas muscle. Fibers were incubated in a solution containing 50μM Mant-ATP, 2mM caged-ATP (P^3-1-(2-nitro)phenylethyladenosine 5'-triphosphate), 5mM $MgCl_2$, 30mM EGTA and the ionic strength made up to 0.2M with potassium propionate (pH 7.1) before transfer to a trough containing silicone oil on an epi-fluorescence microscope. The ATPase sites now contained bound Mant-ADP (K_{diss}~20μM). Caged-ATP was photolyzed rapidly (See Fig.) to release 500μM ATP within the muscle. Following an initial tension rise the fiber relaxed and fluorescence decreased with a rate constant of 1.8 s^{-1} and 3.3 s^{-1} at 12°C and 20°C respectively. The fluorescence change is caused by Mant-ADP dissociation from the ATPase sites. These rate constants suggest that in fibers ADP dissociation is considerably slower than from acto-subfragment 1 in solution [2]. Supported by the MRC and the EEC.

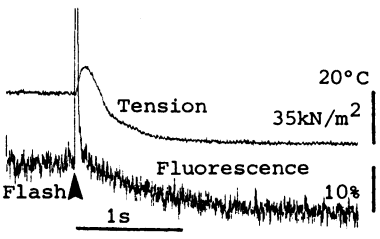

1. Hiratsuka, T. (1983). Biochim. Biophys. Acta 742: 496-508.
2. Siemankowski R.F. *et al.* (1985). Proc. Natl. Acad. Sci.USA 82: 658-662.

W-PM-B7 THE INHIBITORY EFFECTS OF PHOSPHATE AND ARSENATE ON MAXIMUM CALCIUM ACTIVATED FORCE ARE pH DEPENDENT IN SKINNED PSOAS BUT NOT CARDIAC PAPILLARY MUSCLE. Robert E. Godt, *Jose H. Leal-Cardoso, and Thomas M. Nosek. Dept. of Physiology & Endocrinology, Medical College of Ga., Augusta, GA. 30912-3000 and *Dept. of Physiology & Pharmacology, Fortaleza-Ceara, Brazil.

Many laboratories have demonstrated that phosphate (Pi) decreases maximum calcium activated force (Fmax) and calcium sensitivity of skinned skeletal and cardiac muscle. Thus an increase in Pi with fatigue or hypoxia accounts for at least part of the force depression observed in intact muscle under these conditions. However, whether the mono- or diprotonated form of Pi is responsible for these effects is controversial. To clarify this issue, we reexamined Pi's influence on contraction and compared it with that of arsenate (Asi), a structural analog of Pi. Procedures were as described previously (Nosek et al., 1987, Science 236:191) except that NaAcetate was used to adjust the ionic strength and 50 mM BES was used to buffer pH. Asi (0-30 mM, pH 7) decreased Fmax and the calcium sensitivity of both muscle types to a greater extent than Pi. Both Pi and Asi had greater effects on cardiac than skeletal muscle. The effect of the protonated state of Pi and Asi on Fmax was evaluated by measuring the response to 30 mM total Pi or Asi at pH 7.4, 7.0, and 6.6. In skeletal muscle we found that both Pi and Asi were more effective in decreasing Fmax as the pH was lowered and the concentration of the diprotonated forms increased. This was not, however, observed in cardiac muscle. These differences in the effects of Pi and Asi on Fmax in the two muscle types may be accounted for by differences in the structure of their myosin molecules. (Support: NIH grants AR 31636 (REG) and HL/AR 37022 (TMN)).

W-PM-B8 INFLUENCE OF INOTROPIC INTERVENTION ON CROSSBRIDGE ECONOMY DURING ISOMETRIC FORCE DEVELOPMENT IN GUINEA PIG PAPILLARY MUSCLES. G. Hasenfuss, Ch. Holubarsch, E.M. Blanchard, L.A. Mulieri and N.R. Alpert, Dept of Physiol and Biophys Univ of Vermont, Burlington VT 05405.

Isometric heat and force were measured in right ventricular guinea pig papillary muscles before (C) (Krebs-Ringer in mM: Na, 152; K, 3.6; Cl, 135; HCO_3, 25; Mg, 0.6; H_2PO_4, 1.3; SO_4, 0.6; Ca, 2.5; glucose, 5.6: gassed with 95/5, O_2/CO_2) and after the following inotropic interventions: 1) isoproterenol (I), 10^{-8} M, n = 5; 2) the phosphodiesterase inhibitor enoximone (E), 10^{-5} M, n=10; 3) ouabain (O), 10^{-6} M, n = 6; and 4) increase in extracellular calcium (Ca^{++}), 11 mM, n=6. Initial heat was partitioned into tension dependent heat (TDH) (crossbridge cycling) and tension independent heat (TIH) (calcium cycling) by the Gibbs shortening method. The ratio of TDH to isometric tension time integral (TDH/$\int$Pdt) was used as the index of reciprocal economy of isometric force development. Peak twitch force increased relative to C in response to each of the intropic agents: 1) I, 185%; 2) E, 46%; 3) O, 92%; and 4) Ca, 152%. TDH/$\int$Pdt (μcal/g cm s) for control and experimentals was: 1) C, 2.24 ± 0.60 - I, 5.18 ± 0.89, $p<0.01$; 2) C, 2.17 ± 0.63, - E 2.86 ± 0.79 $p<0.01$; 3) C, 2.16 ± 0.72 - O, 2.01 ± 0.40, ns; and 4) C, 2.24 ± 0.60 - Ca, 2.24 ± 0.45, ns. The decreases in economy following isoproterenol or enoxomine inotropic interventions are interpreted in terms of increases in cyclic AMP. The inotropic interventions that increase intracellular calcium (O and Ca) without an associated increase in cyclic AMP do not alter the economy. These results are discussed in terms of crossbridge kinetics. Supported in part by P01 HL 28001.

W-PM-B9 THE EFFECTS OF CROSSBRIDGES AND MAGNESIUM ON FIBER TnC. L.D. Yates & A.M. Gordon. *Department of Physiology and Biophysics, University of Washington, Seattle, WA 98195*

The highly cooperative nature of the relationship between force development and $[Ca^{2+}]$ in skinned skeletal muscle fibers would appear to arise from either cooperative Ca^{2+} binding, cooperative cross-bridge binding or via a mechanism in which both of these processes interact. We have investigated these possibilities using a fluorescent probe, rhodamine located at Cys-98 of TnC (TnCRHOD), to investigate thin filament activation in rabbit psoas muscle by following the linear dichroism. TnCRHOD was incorporated into single skinned muscle fibers by first partially extracting endogenous TnC, and then reincorporating the labeled species. The order parameter, b (Burghardt *et al.*, Proc. Natl. Acad. Sci. 80:7515, 1983), of relaxed fibers was -0.525 indicating that the probe is oriented within the fiber. The relative order was found to be affected by many factors; Ca^{2+}, cross-bridges, and Mg^{2+}. These effectors increased probe disorder. Ca^{2+} titration of fibers in rigor having no filament overlap (SL 4.0 μm) and 3 mM free Mg^{2+} increased probe disorder. This increase consisted of two transitions; one occurring at low Ca^{2+} levels (pK_1=7.26) and the other at higher levels of Ca^{2+} (pK_2=6.04). The second transition became more sensitive to Ca^{2+} through the presence of rigor cross-bridges in fibers having filament overlap. The addition of MgATP to fibers having overlap resulted in a Ca^{2+} titration curve in which probe order lagged force. This latter observation was found to be consistent with probe order being affected by only those cross-bridges in which both heads are bound. There was cooperativity in the second transition from fibers having no filament overlap and even greater cooperativity from those having overlap in the presence of MgATP. However, this cooperativity was lost through the presence of bound rigor cross-bridges in fibers having filament overlap. A reduction in the free Mg^{2+} from 3 mM to 44 μM resulted in both transitions being shifted to lower levels of Ca^{2+}. Interestingly, the reduced Mg^{2+} also resulted in the first transition having increased cooperativity . As such, these results suggest that other protein(s) are also affected by the low Mg^{2+}. These results reveal that the highly cooperative nature of the force-Ca^{2+} relationship probably occurs through an interaction between thin filament activation by Ca^{2+} and cross-bridge binding and that these effectors may influence the general properties of the thin filament in addition to their specific effect on TnC. Supported in part by NIH (NS08384 & HL31962) and MDA.

W-PM-C1 AUTOMATED SEQUENCE/STRUCTURE SEARCH ON PROTEIN STRUCTURES IN THE BROOKHAVEN PROTEIN DATA BANK

K. Namboodiri*, N. Pattabiraman#, A. Lowrey#, and B. P. Gaber*
*Bio/Molecular Engineering Branch, Code 6190 and #Laboratory for the Structure of Matter, Code 6030, Naval Research Laboratory, Washington, D.C., 20375.

Three-dimensional structure prediction and molecular modeling of proteins are important approaches in structural biology. The Brookhaven Protein Data Bank contains three-dimensional structures for proteins, but is not formatted for extensive similarity searches. However, the protein sequence database of the Protein Identification Resource (PIR) is the most widely used database for protein sequence similarity searches. Using the residues of all the protein structures available in the Brookhaven Protein Data Bank we have generated a new protein sequence database similar to the format of PIR. This allowed us to conduct automated searches, with or without mismatches, for protein sequences of unknown structures. Completely or partially matched protein fragments can be displayed using any molecular modeling program. This automated sequence/structure search procedure will be useful in modeling protein active sites, metal binding sites, fitting electron density maps and protein folding. Supported by the Office of Naval Research.

W-PM-C2 THREE-DIMENSIONAL STRUCTURE OF BRADYKININ IN SDS MICELLES: A STUDY USING NUCLEAR MAGNETIC RESONANCE, DISTANCE GEOMETRY AND RESTRAINED MOLECULAR MECHANICS AND DYNAMICS. Susannie C. Lee, Anne F. Russell and William D. Laidig, Procter & Gamble Company, Miami Valley Laboratories, P.O. Box 398707, Cincinnati, Ohio 45239-8707

The conformational properties of the pain-producing tissue hormone, bradykinin, have been determined by two-dimensional NMR techniques at 500 MHz. Proton resonance assignments of this 1280 Da nonapeptide were made by using 2-D homonuclear Hartmann-Hahn (HOHAHA) and rotating frame cross-relaxation (ROESY) experiments. Our studies indicate that bradykinin exists, in aqueous solution, either as a completely disordered structure or an an average of several conformations in fast exchange.

To gain a better understanding of the structural properties of bradykinin in a cell membrane receptor environment, various micellar systems were examined for their ability to stabilize a preferred conformation. The optimal system for this investigation was a mixture of bradykinin and perdeuterated sodium dodecyl sulfate (SDS) at a 1:5 molar ratio, as confirmed by the temperature-dependent behavior of the amide protons.

Detailed structural information for bradykinin in SDS was obtained from quantitative 2-D NOE analyses, distance geometry calculations (DISGEO) and restrained molecular mechanics and dynamics (CHARMm). The conformation of bradykinin in SDS micelles, as determined by these methods, is characterized by a beta-turn at residues 6-9. A comparison of the structures derived from distance geometry and restrained molecular mechanics and dynamics, will be presented.

W-PM-C3 AMIDE V OVERTONE ASSIGNMENT OF A CONFORMATION-SENSITIVE BAND IN THE UV RESONANCE RAMAN SPECTRA OF PEPTIDES AND PROTEINS

S. Krimm, Biophysics Research Division, University of Michigan, Ann Arbor, MI 48109, and S. Song and S.A. Asher, Department of Chemistry, University of Pittsburgh, Pittsburgh, PA 15260

Preresonance and resonance Raman spectra of N-methylacetamide, polypeptides, and proteins have shown the presence of a band (or bands), generally near 1400 cm^{-1} but varying in the range between 1300 and 1500 cm^{-1}, whose assignment and significance have been unclear. We have presented evidence (1) that this band can be assigned to the overtone of the amide V mode, the fundamental being normally strong in the infrared and very weak in the Raman. We give here the detailed arguments for this assignment, including confirmatory data from studies of (13)C(15)N-glycylglycine (2). Together with spectra of 218 nm-excited poly(L-glutamic acid) (1,3) and poly(L-lysine) (3), these results establish a sound basis for this assignment. Since the amide V mode is very sensitive to polypeptide chain conformation (4), the frequency and intensity of this overtone band provide a new sensitive probe of secondary structure in proteins. This research was supported by NSF grants DMB-8517812 and DMR-8806975 (S.K.) and NIH grant 1RO1GM30741-07 (S.A.A.).

1. S. Song, S.A. Asher, S. Krimm, and J. Bandekar, J. Am. Chem. Soc., in press.
2. S. Krimm, S. Song, and S.A. Asher, J. Am. Chem. Soc., submitted.
3. S. Song and S.A. Asher, J. Am. Chem. Soc., submitted.
4. S. Krimm and J. Bandekar, Adv. Protein Chem. 38, 181 (1986).

W-PM-C4 VIBRATIONAL CIRCULAR DICHROISM AS A SENSITIVE METHOD FOR STUDY OF PROTEIN CONFORMATION IN SOLUTION. P. Pancoska, S.C. Yasui, T.A. Keiderling, (Intr. by Pierre R. LeBreton), Department of Chemistry, University of Illinois at Chicago, Box 4348, Chicago, IL 60680.

Vibrational circular dichroism (VCD) spectra of large set of proteins, measured in amide I' region (1740 - 1560 cm^{-1}) are presented. Experimental conditions for routine VCD data collection of protein samples are discussed. Observed changes of sign, shape and magnitudes of VCD curves are correlated to different protein conformational types in terms of secondary structures. VCD spectra are shown to be more sensitive to variation in protein conformation than are related spectroscopic techniques--especially UV CD spectroscopy.

Multivariate statistical analysis of our protein data set provides evidence that 4 basis VCD curves are necessary for description of all the observed large changes in the set. Bandshape analysis of the experimental curves in terms of a restricted set of individual dichroic bands provides an alternative and consistent explanation of the structural specificity of the protein VCD spectra. The possibilities for quantitative analysis of these VCD curves in terms of secondary structure fractions will be discussed.

W-PM-C5 MOLECULAR MECHANISMS IN CALCIUM-BINDING PROTEINS: LESSONS FOR DESIGN. Harel Weinstein, Kenzi Hori, Joseph N. Kushick and Alan Factor. Department of Physiology and Biophysics, Mount Sinai School of Medicine, CUNY, NY 10029

To understand the molecular mechanisms in the function of Ca^{2+} channels and Ca^{2+}-dependent modulatory proteins, we explore the characteristics of Ca^{2+} binding in molecules with known structures. Theoretical approaches formulated in the computational methods of quantum chemistry and molecular mechanics are used to study the structural and electronic factors that determine the mechanisms of Ca^{2+} binding and its structural consequences. A first step was the development of suitable parameters for the calculation of interactions of Ca^{2+} with peptides and proteins with the CHARMM programs. Calculations on Calbindin, a 75 residues protein with 2 EF-hands, using the new Ca^{2+} parameters, yielded good agreement with data from crystallography, when the appropriate constraints were applied. Without Ca^{2+} the protein maintains the general tertiary structure, but significant changes are revealed in the secondary structures of the two Ca-binding loops and in the linker. With the Ca^{2+}, the coordination pattern in the crystal is generally well reproduced, but the linker remains distorted compared to the crystal structure. Inclusion of water molecules corrects the structure. Analysis of the Ca^{2+} binding ability of some proteins predicted to bind Ca on the basis of sequence homology with calmodulin, was done with simulated point mutations. Mutations of Loop II sequences constructed randomly yielded structures that did not bind Ca. Molecular dynamics at high temperatures explored the restrictions in the conformational space of the binding loops surrounded by the fixed protein structure. The linker segment between EF hands has a key role in the activity of the homologous binding proteins calmodulin and troponin C.

W-PM-C6 THE SOLVENT STRUCTURE IN PROTEIN CRYSTALS

Xiaodong Cheng and Benno P. Schoenborn
Center for Structural Biology, Department of Biology,
Brookhaven National Laboratory, Upton, NY 11973

In order to analyze hydrogen-bonding of solvent to protein, a solvent analysis procedure was developed that uses the average scattering density of solvent (1). The contribution of solvent to low-order structure factor terms has further been evaluated by dividing solvent space into shells extending outward from protein's surface. Two hydration layers in myoglobin crystals have thus been found. One layer of solvent molecules is located at a distance of 2.3 angstroms from the protein, and the other is 3.9 angstroms. These hydration patterns are consistent with the expected sterochemistry of Van der Waals contacts and hydrogen-bonding between bound water molecules and the protein's surface atoms.

With the known best parameters for the solvent shells, modified phases for observed low-order structure factors were calculated and used in Fourier maps to determine the locations of bound water and ion molecules. A detailed analysis of hydrogen-bonding within protein, protein to water and water to water was done using a modified least-square refinement.

This work was supported by the Office of Health and Environmental Research and calculations were performed under the supercomputing program of the United States Department of Energy.

(1) Schoenborn, B. P., J. Mol. Biol. 201, 741-749 (1988).

W-PM-C7 A SIMPLE MODEL FOR INTERACTING PROTEIN DOMAINS. John F. Brandts and Lung-Nan Lin, Univ. of Mass., Chem. Dept., Amherst, MA 01003 (Intr. by Ed Westhead).

Differential scanning calorimetry (DSC) is a useful technique for studying multidomain proteins since transitions for individual domains can frequently be separated along the temperature axis by deconvolution. Thermodynamic models now being used to interpret DSC data on multidomain proteins either ignore domain-domain interactions entirely (model of independent transitions) or implicitly assume they are always strong enough to impose a strict order to domain unfolding (model of sequential transitions). These models are therefore not capable of giving information on the actual strength of domain interaction and how this might change with conditions in order to provide the necessary crosstalk which acts to coordinate domain roles when carrying out functions for multidomain proteins. A new model is described which explicitly incorporates a pairwise interaction free energy, ΔG_{AB}, at the A-B domain interface. The model is made experimentally useful by making the simple assumption that the integrity of both domains is necessary to maintain the interaction. Under the most favorable circumstances, interpretation of DSC data using the model will: 1.) Provide numerical estimates of the absolute value of ΔG_{AB} for interacting domains. 2.) Provide estimates of changes in ΔG_{AB} brought about by changing solution conditions, introducing point mutations, etc. 3.) Recognize when ligand interactions with a binding domain are being influenced by a nearby regulatory domain, and provide numerical estimates of the increase (or decrease) in binding constant which is actually due to ligand-dependent changes in interactions between the binding domain and the regulatory domain. EAch of these applications will be illustrated using experimental DSC data on different multidomain proteins.

W-PM-C8 **ATTRIBUTION OF BINDING ENERGY IN ANTIGEN-ANTIBODY COMPLEXES McPC 603, D1.3, AND HyHEL-5** **J. Novotny, The Squibb Institute for Medical Research, Princeton, NJ 08540**

With X-ray coordinates of the antigen-antibody complexes McPC 603, D1.3, and HyHEL-5, the Gibbs free energy changes (ΔG) accompanying the respective noncovalent reactions were estimated. Calculations were based on an empirical Gibbs free energy function consisting of the following terms: hydrophobic force, solvent-modified electrostatics, changes in side chain conformational entropy, translational/rotational entropy changes, and cratic (dilutional) entropy. The calculated ΔG ranges matched the experimentally determined ΔG of McPC 603 and D1.3 complexes, and gave overestimates (i.e., more negative ΔG) in the case of HyHEL-5. Analysis of amino acid residue contributions towards the overall ΔG indicated that only a small number of residues contributes actively towards complex formation. In the antibodies, the bottom part of the antigen binding cavity dominates the energetics of binding. In lysozyme, the energetically most important residues define small (2-3 amino acids) "energetic" epitopes. Thus, a concept of protein antigenicity emerges that involves the active, attractive contributions mediated by the "energetic" epitopes, and the passive surface complementarity contributed by the surrounding contact area. The "energetic" epitopes include the essential antigenic positions determined experimentally and belong to the most protruding parts of lysozyme surface. They do not, however, coincide with backbone segments deemed to be exceptionally flexible. Least-squares superpositions of 6 antibody biding regions (KOL, NEW, J539, McPC 603, D1.3, HyHEL-5) indicate that the geometry of the VH-VL interface β-barrel is well conserved in both complexed and free antibodies, giving no indication of significant changes in domain-domain contacts among these different structures.

W-PM-C9 GENERATION AND EXAMINATION OF COMPACT, FOLDED PROTEIN CONFORMATIONS, David G. Covell and Robert L. Jernigan, Laboratory of Mathematical Biology, NCI, Bethesda, MD 20892.

Native protein conformations, small variants about these native forms, and folding intermediates, have been difficult to characterize, both experimentally and theoretically. The extremely broad conformational space available to a protein has lead to numerous unsuccessful efforts at locating energy minima of unverifiable quality. Here we restrict the size and shape of the available conformational space to be similar to the native state and generate all conformations upon a lattice in this space. Lattice points are defined by fitting α-carbon coordinates for each residue; quality of fits ranged from 1.4 to 1.6 A RMS deviation. All possible chain pathways are then enumerated on this fixed set of lattice points. Conformations are evaluated in terms of residue-specific non-bonded contact energies derived from 42 non-homologous globular proteins in the Protein Data Bank. Contact energies favor hydrophobic-hydrophobic residue interactions over hydrophobic-hydrophilic and hydrophilic-hydrophilic residue interactions. Native structures for avian pancreatic polypeptide, crambin, rubredoxin, pancreatic trypsin inhibitor and neurotoxin are always found within the best 3% of all conformers generated. This method is general and can be used to determine most favorable packing arrangements for folding of specific amino acid sequences within a restricted space, and to examine the critical elements of protein stability for known structures.

W-PM-D1 **DNA STRUCTURAL DATA FROM A DYNAMICS PROBE. THE EPR SPECTRA OF SPIN LABELED SINGLE STRANDED, HAIRPIN, AND DUPLEX DNA ARE DISTINGUISHABLE**

Andreas Spaltenstein, Bruce H. Robinson, and Paul B. Hopkins (Intr. by Leon Slutsky)

Department of Chemistry, University of Washington, Seattle, Washington 98195

Efforts to establish structure-function relationships involving nucleic acids have focused attention upon a variety of non-B conformations of DNA, for example A-, Z,-, bent, and hairpin-looped DNA. When such features are embedded within B-DNA, as would be the case *in vivo*, spectroscopic structural assignment is complicated because the region of interest constitutes only a small portion of the macromolecule. We have developed a new nitroxide spin labeled analog of thymidine (T*) which may be incorporated by automated chemical synthesis into deoxyoligonucleotides. EPR spectra of the spin labeled synthetic deoxyoligonucleotides (5')dTTTTTT*TTTTTT, (5')dCGCGAATTCGCGTTT*TTCGCGAATTCGCG, (5')dCGCGAATT*CGCGTTTTTCGCGAATTCGCG, and (5')dGCGAATT*CGCGCGCGC at pH 7.0 in 100 mM NaCl at 0° reveal the spin probe to be in dynamically distinct environments, exhibiting effective correlation times of 1.25, 3, 10, and 40 ns, respectively. The data are consistent with these deoxyoligonucleotides existing in solution as single strand, loop-labeled and stem-labeled hairpin, and duplex of indefinite length, respectively. The EPR signature of a spin labeled DNA is thus useful as a tool for solution structure characterization. The spin label method of structure evaluation may find use not only for preliminary characterization of small DNA's whose study by NMR or x-ray diffraction is contemplated, but also for site-specific investigation of DNA base sequences believed to possess unusual conformations within large DNA duplexes.

W-PM-D2 **ANISOTROPIC ROTATIONAL DIFFUSION OF MEMBRANE PROTEINS: SENSITIVITY OF CW-STEPR SPECTROSCOPY TO DIFFUSION MODELS AND TO DIFFUSION OF THE ANION EXCHANGE CHANNEL IN HUMAN ERYTHROCYTES.** A.H. Beth, C.E. Cobb, K. Balasubramanian, J.V. Staros, and B.H. Robinson. Departments of Molecular Physiology & Biophysics and Biochemsitry, Vanderbilt University, Nashville, TN 37232 and Department of Chemistry, University of Washington, Seattle, WA 98195.

The rotational correlation times of transmembrane proteins are predicted to be sensitive indicators of their effective size in the bilayer (Saffman & Delbrück, (1975) Proc. Natl. Acad. Sci. 72, 3111-3113). Thus, determination of the rotational diffusion characteristics of a membrane protein can provide information on its interactions with other membrane proteins and with membrane lipids. Spectroscopic methods including saturation transfer EPR (STEPR) using nitroxide spin labels have been employed in studies of membrane protein rotational diffusion in the μsec to msec correlation time range. A recurring problem in STEPR studies of spin labeled membrane proteins has been how to extract the elements of the anisotropic rotational diffusion tensor from experimental spectra. We have approached this problem by development of computational methods for modeling the effects of anisotropic rotational diffusion on STEPR line shapes. In the present work we have considered a uniaxial rotational diffusion model for a transmembrane protein and predicted the effects of changing $\tau_{||}$ (the rotational correlation time about the membrane normal axis) and Θ_t (the tilt of the nitroxide z-axis from the membrane normal axis) on computed STEPR line shapes. Results indicated that characteristic spectral features are discernable which are diagnostic of the diffusion model and the spin label binding geometry using input parameters from both $^{14}N,^{2}H$- and $^{15}N,^{2}H$-nitroxide spin labeled proteins. Moreover, for most binding geometries, line shapes from a uniaxial model cannot be satisfactorily approximated by an isotropic model at any correlation time nor by linear combinations of isotropic motional models having different rotational correlation times. We have applied this computational approach to preliminary analysis of the rotational diffusion of spin labeled anion exchange channels in intact human erythrocytes with encouraging results. First order analysis suggests 10 to 50 μsec for $\tau_{||}$ in the range of temperature from 37 to 2 °C. Supported by: HL34737, CA43720, DK31880, and DMB8706175.

W-PM-D3 ISOTOPE-DETECTED AMIDE HYDROGEN EXCHANGE KINETICS IN PROTEINS; DETERMINATION OF SLOW, INTERMEDIATE AND FAST RATES BY NMR USING ^{15}N INEPT EXPERIMENTS. Gillian D. Henry and Brian D. Sykes Department of Biochemistry, University of Alberta, Edmonton, Alberta, T6G 2H7, Canada.

Amide hydrogen exchange kinetics provided some of the initial insights into the dynamic aspects of protein structure and continues to be one of the more important experimental approaches. For larger proteins, individual amides may not be readily resolved even in two dimensions, and resonances may be difficult to assign. We have used the ^{15}N INEPT experiment (Morris and Freeman JACS 101:760) to determine individual rates over a variety of exchange regimes. These isotope-selective techniques are illustrated with M13 coat protein. The INEPT pulse sequence transfers magnetization from a nucleus of high γ (eg. ^{1}H) to one of low γ (eg. ^{15}N), thus if protonated protein is dissolved in H_2O, the exchange rate (k_{ex}) may be determined from the time-dependent decay of the INEPT signal. This method is suitable for the slowest amides in a protein. When the experiment is performed in $^{1}H_2O$, two more regimes become evident. If $k_{ex} \approx 2J_{NH}$ ($\approx$200 s^{-1}) polarization transfer does not occur efficiently as the relevant phase information is lost. This is useful for very rapidly exchanging amides. Alternatively, during normal ^{1}H-decoupled INEPT, saturation transfer from water may occur when $k_{ex} \cong 1/T_{1\ amide}$ ($\approx$2 s^{-1}) as both the amide and water are saturated during proton decoupling and $T_{1\ amide}$ is generally less than $T_{1\ water}$. These ^{15}N -directed experiments provide resolution not normally available for larger proteins and give access to very fast rates which cannot be determined by classic exchange out methods.

W-PM-D4 IN VIVO DEUTERIUM NMR STUDIES OF THE METABOLISM OF D AND L METHIONINE. Robert E. London, Scott A. Gabel, and Alex Funk (Intr. by Colin F. Chignell). Laboratory of Molecular Biophysics, National Institute of Environmental Health Sciences, NIH, Research Triangle Park, NC 27709.

The metabolism of the amino acid methionine is of interest both as a consequence of the central role of transmethylation reactions in the biochemistry of the cell, and due to the toxicity associated with excess dietary methionine. Questions about the extent to which transamination or transmethylation pathways contribute to the metabolism and toxicity of excess methionine have been the subject of debate. Despite a number of limitations on the use of deuterium as an NMR tracer in metabolic studies, the very low natural abundance, short spin lattice relaxation times, and ease of execution make ^{2}H NMR studies an attractive approach for in vivo analysis. Studies of the metabolism of [methyl-d_3]-L-methionine using a surface coil placed over the liver of an anesthetized rat show the rapid formation of [methyl-d_3]sarcosine and, over a longer period of time, the formation of deuterated N-trimethyl metabolites and a gradual increase in the intensity of the HDO resonance. These data indicate a major flux through the transmethylation pathway, and subsequent oxidation of the sarcosine deuterated methyl group. In vivo NMR studies of [methyl-d_3]-D-methionine exhibit similar metabolic transformations, indicating that D-methionine is rapidly converted into the L isomer. The formation of labeled sarcosine is dramatically reduced by prior administration of sodium benzoate, an inhibitor of D amino acid oxidase, indicating formation of the -keto acid followed by transamination to yield L-methionine. This apparent paradox of anabolic but not catabolic transamination is a consequence of the physiological irreversibility of the glutaminase II enzyme system involved.

W-PM-D5 A ^{13}C NMR STUDY OF THE METABOLISM OF [2-^{13}C]D-GLUCOSE IN HUMAN ERYTHROCYTES Michael C. Schrader, Virgil Simplaceanu, and Chien Ho
Department of Biological Sciences, Carnegie Mellon University, Pittsburgh, PA 15213.

We have used [2-^{13}C]D-glucose and ^{13}C NMR spectroscopy to determine the relative fluxes through the pentose phosphate pathway and glycolysis in human erythrocytes. Since the mature erythrocyte lacks mitochondria and the enzymes for gluconeogenesis, glucose is converted to lactate directly through these two pathways. When [2-^{13}C]D-glucose is metabolized via glycolysis, [2-^{13}C]lactate is generated. When metabolized via the pentose phosphate pathway, both [1,3-^{13}C]- and [3-^{13}C]lactate are formed. Taking into account the recycling of hexose 6-phosphate formed by the pentose phosphate pathway, the relative fluxes of these two pathways may be calculated from the rates of production of lactate labeled at C1, C2, and C3 positions. The advantages to using [2-^{13}C]D-glucose to determine these fluxes are that there is no interference from endogenous unlabeled metabolites and that the recycling of hexose 6-phosphate can be estimated. Using an adaptation of a model proposed by Katz and Wood [*J. Biol. Chem.* **235**: 2165-2177, (1960)], our present data indicate that there is a flux of approximately 8-12% through the pentose phosphate pathway in normal human erythrocytes. We are also using this technique to compare the percent flux through the pentose phosphate pathway in normal erythrocytes to those in sickle cell anemia.

[This work is supported by a grant from the National Institutes of Health (HL-24525). M.C.S. is supported by an M.D./Ph.D. fellowship awarded by the R.K. Mellon Foundation.]

W-PM-D6 **ROTATIONAL DIFFUSION OF PHOSPHORUS METABOLITES IN LENS TISSUE HOMOGENATES.** G.H. Caines, T. Schleich, P. N. Farnsworth*, and C.F. Morgan, Dept. of Chemistry, Univ. of California, Santa Cruz, CA 95064 and *Dept. of Physiology, New Jersey Medical School, Newark, NJ 07103.

Metabolic processes are believed to play a role in defining lens clarity, and thus, metabolic dysfunction is expected to ultimately lead to opacification, the condition of cataract. In this study we assess the rotational diffusion behavior of phosphorus containing metabolites by the technique of off-resonance rotating frame spin-lattice relaxation in lens tissue cortical and nuclear homogenates as a means of exploring the occurrence and extent of metabolite lens protein interactions. P-31 NMR spectra of juvenile (calf) lens homogenates were obtained at 10° C with a GE GN-300 (7.05 Tesla) spectrometer. Effective rotational correlation times ($\tau_{o,eff}$) for the major phosphorylated metabolites present in the bovine lens were derived from nonlinear least-squares analysis of intensity ratio vs. ω_e dispersion plots with the assumption of isotropic tumbling. Dipolar and chemical shift anisotropy relaxation contributions were assumed. Values of $\tau_{o,eff}$ vary from a low of 2.9 ns (GPC) to a high of 12.7 ns (ATP) for cortical homogenate, whereas for nuclear homogenate, values of 3.8 ns (GPC) to 35.3 ns (P_i) were obtained. This diversity of $\tau_{o,eff}$ values suggests the occurrence of differential binding affinities to lens macromolecules, most likely the lens proteins. A fast exchange model, between free and bound, was employed to yield the fraction of free (unbound) metabolite. Our results demonstrate that certain metabolites (PME, P_i, and GPC) exist in the cortex in a predominantly free (unbound) form, whereas other metabolites (e.g., ATP are largely bound. For the nucleus, GPC is predominantly free, but PME and P_i, by contrast, are substantially bound. (Supported by NIH grants EY 04033 and EY 05787)

W-PM-D7 COMPARISON OF THE MAJOR CYTOSOLIC WATER SOLUBLE PHOSPHODIESTER IN LENSES OF SEVERAL NON-MAMMALIAN SPECIES BY ^{31}P NMR. C. Tyler Burt[1], Sal Testeverde[2], and J.F. Levine[3]; [1]Laboratory of Molecular Biophysics, NIEHS, Research Triangle Park, NC 27709; [2]Biofish, Inc., Georgetown, MA; [3]Dept. of Microbiology, Pathology and Parasitology, College of Veterinary Medicine, NC State University, Raleigh, NC 27606

We report here the first total water soluble phosphorus profile of several different non-mammalian vertebrate lenses. They present a strong contrast to mammalian lenses. Fish lenses show the presence of threonine ethanolamine phosphodiester (TEP) in the millimolar range and its ^{31}P NMR characteristics are given. In addition, serine ethanolamine phosphodiester (SEP) is seen. Further, there are differences in the relative amount of the two compounds between fish species. Frog lens has not only SEP but TEP as well. This is the first report of TEP in an amphibian species. Representative reptilian lenses show a low level of SEP and relatively high amounts of ATP. Avian lenses, however, have no observable phosphodiester. Lenses from the rat show only glycerophosphorylcholine (GPC) and glycerolphosphorylethanolamine (GPE). No GPC or GPE was seen in the other species. These results are interpreted, in conjunction with the reported phosphodiesters in mammalian lenses, to imply a difference in regulation of phospholipid metabolism according to phyla.

W-PM-D8 **^{1}H-^{31}P CORRELATED (2D) NMR SPECTROSCOPY OF INTACT ORGANS.** T. Kushnir, O. Kaplan, N. Askenasy, G. Navon. School of Chemistry, Tel-Aviv University, Tel-Aviv 69978, Israel.

The assignment of ^{31}P NMR signals in intact organs has been traditionally performed by the analysis of the spectra of tissue extracts. There are however cases where this approach does not lead to definite identification. In our previous ^{31}P NMR studies of taurocholate-induced experimental pancreatitis a new transient signal appeared at -0.18 ppm. It was suggested that this compound can be a useful diagnostic and prognostic marker, and would aid in studying the basic pathophysiologic processes. Attempts to identify this peak by comparing the chemical shift to genuine compounds, and by using TLC and columns chromatographic methods of PCA extracts were unsuccessful. A ^{1}H-^{31}P correlated 2D NMR spectroscopy of the intact pancreas gave the unequivocal assignment of the signal. In this technique only proton and phosphorous signals which are spin-spin coupled are obtained, and precise assignment of the phosphorous signals by correlating them to the proton chemical shifts of the groups to which they are coupled can be achieved. The new phosphorous peak in the diseased pancreas correlated with two proton signals with chemical shifts of the choline αCH_2 and glycero CH_2 of lecithin. The compound was identified as taurocholate-lecithin complex. A 2D map of prepared taurocholate-lecithin solution was identical. A signal with similar chemical shift was found in the PCA extracts of diseased pancreases; however, the 2D map of the extracts was different. We recently performed ^{1}H-^{31}P correlated 2D NMR studies of experimental pancreatic carcinoma. The ^{31}P spectrum is dominated by the phosphomonoester peaks. 2D measurements demonstrated that this region is governed by phosphocholine (PC) and phosphoethanolamine(PEA), as well as other phosphorous compounds that overlapped the PC and PEA in the ^{31}P spectrum but not in the ^{1}H dimension.

W-PM-D9 DETERMINATION OF CYTOSOLIC FREE MAGNESIUM LEVELS WITH NMR AND FLUORESCENT INDICATORS. Robert E. London, Elizabeth Murphy, Louis A. Levy, Bore Raju, and Charles Steenbergen*, Laboratory of Molecular Biophysics, National Institute of Environmental Health Science, NIH, Research Triangle Park, NC 27709 and *Dept. of Pathology, Duke University Medical Center, Durham, NC 27710

The design of useful indicators for cytosolic ions is subject to a number of constraints including: availability of reasonable loading strategies, good water solubility, a dissociation constant for the ion of interest which is near or slightly above the free ion concentration, dissociation constants for other ions which are very different from, and preferably well above the physiological levels, and useful spectroscopic sensitivity to ion complexation. We have developed several indicators for cytosolic free magnesium ions based on modifications of EDTA in which one of the nitrogen atoms is replaced by an ether oxygen, and the central ethylene bridge is replaced by either a fluorinated benzene to yield an NMR indicator[1], or an aromatic fluorophore.[2] Fluorine 19 NMR studies and fluorescent studies of these indicators indicate that all of the necessary criteria are reasonably satisfied. Studies of perfused rat hearts loaded with the fluorinated indicators have been carried out under basal and ischemic conditions. Basal Mg_i levels averaged 0.85 mM (n=9); between 10 and 15 minutes of ischemia, Mg_i rose nearly three fold to 2.1 mM. This increase occurred over the same time course as the decrease in ATP. Studies of isolated rat hepatocytes loaded with the fluorescent indicator yielded Mg_i value of 0.59 mM.

1. L.A.Levy, E. Murphy, B. Raju, and R. E. London. Biochemistry 27, 4041; 1988.
2. B. Raju, E. Murphy, L. A. Levy, R. D. Hall, and R. E. London. Am. J. Physiol., in press.

W-PM-D10 INFLUENCE OF Li^+ ON FREE INTRACELLULAR Mg^{2+} CONCENTRATION IN HUMAN RED BLOOD CELLS.

Ravichandran Ramasamy and Duarte Mota de Freitas, Department of Chemistry, Loyola University of Chicago, 6525 N. Sheridan Road, Chicago, IL 60626.

Lithium salts are preferred drugs in the treatment and maintenance of both manic and depressive episodes of bipolar patients. Lithium has also been used in a variety of other psychiatric and medical conditions. Several hypotheses exist for the biological action of lithium. One of them is the competition between Li^+ and Mg^{2+} for biomolecules which is based on the existence of a diagonal relationship between Li^+ and Mg^{2+}. We have investigated the influence of Li^+ on free intracellular Mg^{2+} concentrations in human red blood cells (RBCs) by ^{31}P NMR and optical absorbance spectroscopies. In RBCs loaded with 3 mM intracellular Li^+, the chemical shift separation ($\delta_{\alpha\beta}$) between the α and β phosphate resonances of $MgATP^{2-}$ was 0.82 ppm larger than that observed in Li^+ free RBCs. Using a calibration graph, obtained by plotting $\delta_{\alpha\beta}$ versus free intracellular Mg^{2+} from optical spectroscopy on resealed RBC ghosts containing antipyrylazo-III, it was observed that the free intracellular Mg^{2+} decreases upon Li^+ loading in RBCs. Analysis of the interaction of each RBC component with Mg^{2+} and Li^+ indicates that Mg^{2+} is displaced in part from $MgATP^{2-}$ upon addition of Li^+ and that the released Mg^{2+} is bound to the RBC membrane causing an overall decrease in free intracellular Mg^{2+} concentration. These results also indicate that RBC membranes may act as a Mg^{2+} buffer. Effect of presence and absence of Li^+ on ^{31}P NMR resonances of ATP in Mg^{2+}-depleted and saturated RBCs and ideal Li^+ loading conditions will also be presented.

W-PM-D11 **^{1}H-NMR SPECTRA OF ADRENODOXIN: FEATURES OF THE AROMATIC REGION.** **N.J. Greenfield[1], X. Wu[2] and F. Jordan[3]. [1]Department of Physiology and Biophysics, UMDNJ-Robert Wood Johnson Medical School, Piscataway, NJ 08854-5635, and the Departments of Chemistry, [2]Rutgers University, New Brunswick, NJ 08904 and [3]Newark, NJ 07102.**

Adrenodoxin is a two iron-two sulfur mammalian ferredoxin which is a component of several hydroxylase systems. The protein has 3 histidines, 4 phenylalanines, 1 tyrosine and no tryptophans. 1-D ^{1}H-NMR spectra of reduced and oxidized adrenodoxin were recorded as a function of pH. Resonances due to 2 histidines were visible in the spectra. The pK_a values of the resolved histidine resonances in the oxidized protein were 6.64±0.03 and 6.12±0.06. These values were unchanged when adrenodoxin was reduced by the addition of sodium dithionite. The resonances due to the tyrosine were identified using convolution difference spectroscopy. In addition, a DQF COSY spectrum of oxidized adrenodoxin was obtained. The cross peaks of the resonances due to the tyrosine, the 4 phenylalanines, and the same 2 histidines were resolved in the DQF COSY spectrum. Reduction of the protein caused several changes in the aromatic region of the NMR spectra. The resonances assigned to the C4 protons of the two histidines did not shift upon reduction, however the resonances assigned to the C2 proton of the histidine with a pK_a of 6.6 shifted upfield approximately 0.15 ppm. In addition, when the protein was reduced one of the resonances assigned to a phenylalanine residue with a chemical shift of 7.50 ppm appeared to move downfield to 7.82 ppm. The chemical shift of this resonance in the reduced state displayed a pronounced temperature dependence suggesting that one phenylalanine residue is close to an iron atom in the active site of the protein.

W-PM-D12 ONE AND TWO DIMENSIONAL NMR STUDIES OF A SPHINGOLIPID HEAD GROUP FROM SACCHAROMYCES CEREVISIAE. Nathan S. Zingg, Gerald B. Wells, Robert L. Lester, and Judith G. Shelling, Department of Biochemistry, University of Kentucky, Lexington, KY 40536-0084

Sphingolipids have been implicated in the regulation of mammalian cell growth and communication. Higher plants and fungi contain a group of sphingolipids which are not found in animals. They contain a ceramide consisting of a long-chain base, usually hydroxysphinganine (phytosphingosine), that is N-acylated with hydroxy and nonhydroxy fatty acids and with polar head groups consisting of inositol, phosphate, and carbohydrate. Although no function has been ascribed to these charged molecules, the demonstration of a mutant strain of Saccharomyces cerevisiae with an absolute requirement of a long chain base for growth and synthesis of sphingolipids suggests that one or more of these lipids plays a vital role. The focus of this study is the major sphingolipid isolated from Saccharomyces cerevisiae, which has been shown to contain a phytosphingosine-linked head group that consists of two inositol phosphate molecules and a single mannose residue. Preliminary one and two dimensional NMR data on the head group are consistent with the mannose being substituted at two different positions by myo-inositol 1-phosphate (milp). One linkage is the phosphodiester bond milp-α1,6-mannose; the second linkage is mannose-α1,2-milp. Energy minimization and molecular dynamics will being used to examine the three dimensional structure of this head group moiety. (Supported by NIH Grants AI20600 and RR05374)

W-PM-E1 MOLECULAR EXCITON MICROSCOPY

Raoul Kopelman*, Aaron Lewis and Klony Lieberman Department of Applied Physics, The Hebrew University of Jerusalem, Israel; *Department of Chemistry, University of Michigan, Ann Arbor, MI

We will describe the development of a new biologically non-invasive ultraresolution light microscopy, based on combining the well-known energy transfer "spectral ruler" method with the novel micro-movement technology now emplyed in scanning tunneling microscopy (STM). Energy transfer measurements have become a standard for measuring dimensions in macro-molecular complexes which are less than 8nm, using an embedded pair of excitation donor and acceptor molecules. To extend this selective biomolecular spectroscopic ruler to the realm of nanometer imaging the Ångstrom-scale micromovement techniques of STM are integrated with recent methodologies developed for near-field scanning optical microscopy (NSOM)[1], which employs micropipettes developed by biologists for intracellular injection. The resolution limit of NSOM has been 50nm due to the inability of light to travel without appropriate packaging, through dimensions that are much smaller than the wavelength of light.[1] However, we have grown crystals of energy packaging donor molecules in the tips of pipettes that can have apertures smaller than 5nm. These nanometer dimension crystals can be excited to produce light with a variety of excitation methods that overcome the limitation of propagating light in highly confined spaces. Molecular exciton microscopy allows us to extend near-field microscopy beyond the 50nm limit already achieved and thus, permits a new frontier of resolution with light based on the limits of energy transfer measurements. In essence, then, the goal of this research is a spectrally sensitive light microscope that will have the capability to zoom non-destructively and in air from the limits of resolution of lens-based confocal light microscopy (200nm) to molecular dimensions of 1nm.

[1]A. Lewis et al., "Near-field Imaging of Fluorescence," in Spectroscopic Membrane Probes (Vol II) ed. L. Loew, (CRC Press, Florida, 1988) Chap. 12 p. 81-110.

W-PM-E2 PRISMLESS TOTAL INTERNAL REFLECTION FLUORESCENCE AND DETECTION OF PHASE GRADIENTS AND SURFACE FLUORESCENCE WITH UNMODIFIED STANDARD MICROSCOPE OBJECTIVES. Andrea Stout and Daniel Axelrod, Biophysics Research Div. & Dept. of Physics, Univ. of Michigan, Ann Arbor MI 48109

By simple modifications of the pattern of either fluorescence excitation or emission light in an epi-illumination inverted microscope at planes complimentary to the back focal plane of a standard microscope objective, one can achieve a variety of useful effects that traditionally require more specialized optical elements. (1) Total internal reflection fluorescence (TIRF) by evanescent wave excitation can be produced without a special prism by epi-illumination through the periphery of a 1.4 numerical aperture objective. An opaque disk of appropriate size is placed in the illumination path external to the microscope in an easily accessible position so as to cast a sharp real-image annulus at the objective's back focal plane. This annulus then transmits a hollow cone of epi-illumination rays traveling at only supercritical angles toward the glass/water sample plane. In this system, very small TIRF illumination areas can be produced from laser sources, and TIRF can also be produced from standard arc sources. (2) By placing a phase ring or an edge barrier at an accessible plane in the emission light path within the microscope at which the objective's back focal plane forms a real image, any standard bright-field objective can be made to produce phase contrast or schlieren (or Hoffman modulation) contrast, respectively. (3) By placing an appropriately -sized opaque disk at that same emission light plane complimentary to the objective's back focal plane, fluorescence originating from the near-field of emission dipoles near the glass/water sample interface can be selectively detected, even without employing TIRF excitation.

Supported by NSF grant # DMB 8805296 and by a Univ. of Michigan Rackham Faculty Grant.

W-PM-E3 RATIOMETRIC IMAGING OF MEMBRANE POTENTIAL IN A-431 CELLS David Gross, Department of Biochemistry and Program in Molecular and Cellular Biology, University of Massachusetts, Amherst, MA 01003

The membrane-bound, membrane-electric-field-sensitive fluorescent probe di-4-ANEPPS (Hassner, Birnbaum & Loew, J. Org. Chem. 49:2546) exhibits shifts in both absorption and emission spectra which are linearly related to the transmembrane electric field strength in the membrane. I exploit this spectral shift to generate "ratio" images of A-431 cells stained with di-4-ANEPPS. Fluorescence images excited first at 546 nm and then at 436 nm are collected on a charge coupled device by a rapid frame shift technique. The 12 bit images, when processed (546 nm image divided by the 436 nm image), indicate that A-431 cell membranes exposed to 1 uM valinomycin respond to extracellular potassium ion concentration as Nernstian membranes. Variations in di-4-ANEPPS ratio fluorescence in individual cells imply that the transmembrane electric field strength varies by a factor of 3 from region to region laterally along the plasma membrane. If dye response is representative of membrane potential, then the measured V_m relative to rest potential varies from 112 mV hyperpolarized to 66 mV depolarized at different positions along the cell membrane. It appears that portions of plasma membrane contacting other cells are depolarized relative to those facing the medium. The contribution of localized surface charge to the local transmembrane electric field strength in the membrane as well as possible artifacts of the technique will be discussed.

Supported by NSF grant DMB-8803826.

W-PM-E4 A SIMPLE METHOD FOR FOCUSING X-RAYS Daniel J. Thiel*, Aaron Lewis†*, Donald H. Bilderback*, Edward A. Stern¶. *Department of Applied Physics, Cornell University, Ithaca, NY 14853 †Department of Applied Physics, Hebrew University, Jerusalem, Israel ¶Department of Physics, University of Washington, Seattle, Washington 98195.

The need for high intensity x-ray microbeams has motivated researchers to develop sophisticated focusing optics such as zone plates, synthetic multilayer mirrors, and total reflection mirrors. The fabrication of any of these optical elements requires extreme precision; furthermore, their range of operation is limited to a relatively narrow bandpass. A technique has been developed (1) which has the potential of focusing synchrotron radiation with energies as high as 10KeV to diameters less than 0.1 microns with optimal gains greater than 10^5. The optical element is a very gradually tapered glass capillary tube. By multiple total reflections off the inner wall of the tube, impinging radiation propagates down the bore which is gradually decreasing in cross-sectional area thereby giving rise to enhancement of the beam intensity. The bandpass of such tapered tubes is very wide, and their fabrication is surprisingly easy. Experimental results demonstrating the focusing capabilities of various tubes will be presented. Intensity gains as large as 60 have been measured. Tubes which should display much larger gains are currently being fabricated. The availability of such a simple and efficient focusing technique will have an impact on many fields of study. Significant advancements in biophysics should be made in the areas of kinetic XAFS, spatially-resolved x-ray absorption spectroscopy, and microdiffraction.

1. Strern E. A., et al, Applied Optics, in press.

W-PM-E5 MECHANICAL PROPERTIES OF THE HUMAN OCULAR LENS. Christopher A. Cook*$, Jane F. Koretz*, *Center for Biophysics and Biology Department, $Physics Department, Rensselaer Polytechnic Institute, Troy, NY 12180.

Our original modeling method and oscillatory elastometer used in characterizing dynamic Young's moduli have been supplemented with a hydrostatic pressure technique and static technique to provide a bulk modulus and static Young's modulus. Besides being a fundamental mechanical characterization, this information is essential in formulating a dynamic or nonlinear model of accommodation. Apparatus has been constructed which allows direct viewing of the lens in a pressure vessel capable of up to 40 kPsi of hydrostatic pressure. The lens image is digitized and sent to a computer for analysis of geometrical deformation with pressure variation, directly providing an orientation-dependent bulk modulus. Modifications to the existing dynamic elastometer permit direct measurement of force in static deformations. A formulation of a double Hertz contact problem is used to convert static force, displacement and contact area data to a relation from which the Young's modulus may be obtained using the hydrostatic bulk modulus. Several mathematical methods with which a dynamic lens model may be formed from static properties and dynamic data are explored.

Supported in part by NIH grant EY02195.

W-PM-E6 TIME RESOLVED SPECTROSCOPY OF HUMAN BRAIN. Chance, B., Smith, D.S., Leigh, Jr, J.S., Maris, M. & Holtom#, G. Dept. Biochem/Biophys, #Regional Laser Facility, Univ. of Penn. Phila., PA 19104

Blumberg has concluded that photons migrate randomly in tissues (1) and Bonner, Wilson and Patterson predict an exponential decay of intensity with time or distance (2,3). Picosecond laser pulses and fast detectors such as the streak camera or the microchannel plate tube enable resolution of two distinctive features of the pulsed light response of tissues: 1) the "coherent" or non-scattered ray can not be observed to propagate in detectable amounts between input and output, for example, several cm separated on the human forehead. 2) The main component received propagates by efficient random walk [$u=(-1/L)(\log_e I)$], is less than 0.04 cm^{-1} and is spread out over 20 to 100 cm for human brain. The attenuation is largely due to absorption by deoxyhemoglobin, and u = EC according to the Beer-Lambert Law (4). Thus, quantitation of the hemoglobin concentration changes in the tissue is possible. Migration is uniform when sampled on the upper forehead, but models with localized absorbers show discontinuities in the photon decay kinetics. With appropriate input/output geometries, a significant degree of localization of discrete volumes of the absorber appear possible (4). 1. Blumberg W (1987) Biophys J.51:288. 2. Patterson MS, Chance B & Wilson BC (1988) J.Appl.Opt submitted. 3.Bonner, RF et al (1987 J.Opt.Soc.Am.A. 4:423-32. 4. Chance, B et al (1988) PNAS USA 85:4971-5.

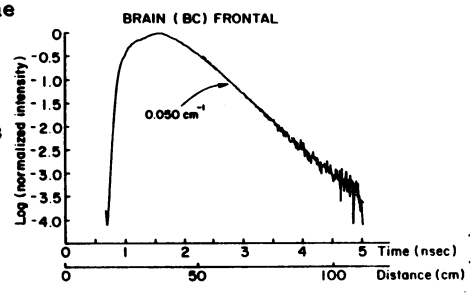

W-PM-E7 IN VIVO NMR IMAGING STUDIES WITH AN OXYGEN-17-PFC-43 (PERFLUROTRIBUTYLAMINE) COMPLEX; S. LASKER, T. ARAI, P. GUPTE, DEPARTMENTS OF MEDICINE AND SURGERY, NEW YORK MEDICAL COLLEGE, VALHALLA, NEW YORK 10595

Oxygen utilization by tissues is usually observed indirectly. The delivery of $^{17}O_2$ in high concentration to an actively metabolizing organ by means of the readily dissociable complex PFC-$^{17}O_2$, permits the conversion of $^{17}O_2$ to $H_2\,^{17}O$ and manifests its presence by T_2 enhancement in a proton imaging system. In 1961 Meiboom showed that splitting of the proton resonance is primarily by spin-spin interaction with quadrapole $^{17}O_2$ and that the proton transfer process is both acid and base catalyzed and fast so that line broadening is observed within a narrow pH range near neutrality. Hopkins in 1988, using $^{17}O_2$ enriched water, was able to demonstrate enhancement of T_2 relaxation in protein solutions and in tissues at physiologic pH confirming the earlier observations of Meiboom. Our preliminary in vivo studies in dogs of T_2 enhancement by metabolic $H_2\,^{17}O$ was accomplished by imaging using a GE 1.5T Signa imaging system (H resonant frequency 63.9 MHz). The inferior vena cava was canulated for delivery of the PFC-$^{17}O_2$ complex. The infusion of 100 ml of PFC emulsion complexed with 36% enriched $^{17}O_2$ was accomplished in 8 minutes. The dog brain was imaged in a volume filling standard knee coil before and after the infusion. Image reconstruction using 2DFT of two excitations of 256 data lines revealed significant global decrease in proton densities of T_2 weighted images compared to the control image. The T_1 weighted images (TE 20, TR 500) did not show proton density changes after infusion of the $^{17}O_2$ complex.

W-PM-E8 IN VIVO LOCALIZED PHOSPHORUS NMR SPECTROSCOPY IN REGIONS OF ARBITRARY SHAPE BY THE SLIM METHOD. Haakil Lee[1] and Paul C. Lauterbur[1,2], Departments of Chemistry[1], Physiology and Biophysics[2], Medical Information Sciences[2] and the Bioengineering program[2], University of Illinois at Urbana-Champaign, Biomedical Magnetic Resonance Laboratory, 1307 W. Park St., Urbana, IL 61801.

Methods now in use to obtain in vivo ^{31}P and other NMR spectra from individual organs or regions are either inefficient and lengthy, such as the various forms of chemical shift imaging, or sample only a portion of the volume of interest by rather complex methods. An alternative method, recently demonstrated for proton NMR spectroscopy by Hu, Levin, Lauterbur and Spraggins, Magn. Reson. Med. (in press), is SLIM (Spectral Localization by Imaging). We have adapted this technique to obtain ^{31}P NMR spectra from multiple regions of arbitrary shape after using proton NMR images to define the boundaries of those regions. Three-dimensional imaging can be used to allow the total spectral intensity from entire organs or regions to be obtained, in times much shorter than those required by chemical shift imaging and with greater sensitivity than other forms of localized spectroscopy. Applications to studies of various structures within the brain are being pursued.

W-PM-E9 VOLUME-SELECTIVE WATER-SUPPRESSED PROTON SPECTRA OF HUMAN TISSUES IN VIVO. M. Bárány, P.N. Venkatasubramanian, J. Capek*, E.Q. Regan, S. Motkur, M. Greenberg*, B.M. Greenberg* and R. Barmada. Col. of Med., Univ. of Illinois, Chicago, IL 60612 and *Greenberg Radiology Inst., Highland Park, IL 60035

A strong water signal masks weaker signals from metabolites in proton spectra of live tissues and, therefore, to obtain metabolite spectra the water signal has to be suppressed. Previously, we have used section-selective water-suppressed proton spectra for human tissues in vivo (Barany et al., Magn. Reson. Imag. 5, 393, 1987; Radiology 167, 839, 1988) which may have included tissues other than that desired to be studied. Now, we have used the STEAM pulse sequence for volume selective spectroscopy (Frahm et al., J. Magn. Reson. 72, 502, 1987) which was combined with two saturation pulses for water suppression. A 1.5 T General Electric Signa whole body MR scanner was used. Spectra were recorded from 4-27 cm^3 regions of the anatomy of interest at 63.86 MHz with the head coil, extremity coil, or surface coils. The water-suppressed STEAM program allowed observation of resonances from the major brain metabolites: $-CH_3$ of N-acetylaspartate (NAA) at 2.0 ppm, $-CH_2-$ of NAA at 2.6 ppm, $=NCH_3$ of phosphocreatine/creatine (PCr/Cr) at 3.0 ppm, and the $(-N(CH_3)_3$ of choline at 3.2 ppm. Furthermore, the minor brain metabolites were also seen: $-CH_2-$ of glutamate at 2.2 ppm, $-SCH_2-$ of taurine at 3.3 ppm, and $-NCH_2$ of glycine at 3.5 ppm. In the muscle, the program allowed observation of resonances from PCr/Cr, choline, and from protons of fatty acyl chains: terminal $-CH_3$ at 0.85 ppm, $(-CH_2-)_n$ at 1.5 ppm, $-COCH_2CH_2-$ at 1.7 ppm, and $-CH=CH-$ at 5.5 ppm. The program was applied for the analysis of cancerous tissues: major changes in the metabolite pattern were observed. (Supported by CTR, MDA and GE).

W-PM-E10 A NEW METHOD FOR DETERMINING PROTEIN STRUCTURE USING SOLID STATE NMR: THE "METRIC METHOD". M. T. Brenneman, C. North, and T. A. Cross. Dept. of Chemistry and the Institute of Molecular Biophysics, Florida State University, Tallahassee, Fl 32306.

A novel method, the metric method, is presented for determining the structure of proteins using solid state NMR dipolar interactions. In analogy to the method of distance geometry, which is based on the general relationships that distances between points must satisfy, a method is developed which makes use of the general relationships that angles between vectors must satisfy. With this method, analytical expressions are derived for the dihedral angles of the peptide backbone, and a way for minimizing the structural ambiguities associated with solid state NMR is also presented. Calculations on a model protein structure reveal the dipolar interactions of only the NH and NC_1 bonds provide insufficient information for uniquely determining dihedral angles, even when constraints arising from long range interactions are employed, but yield a manageable number of solutions when the $C_\alpha H$ interaction is also considered.

W-PM-E11 MODELLING SICKLE CELL VASO-OCCLUSION IN THE RAT LEG USING TECHNETIUM AND MAGNETIC RESONANCE IMAGING: INCREASED TISSUE WATER, T2, AND PROTON DENSITY AND REDUCED PERFUSION. ME Fabry, V Rajanayagam, E Fine, I Cousins, RL Nagel, S Holland, JC Gore and DK Kaul, Depts of Medicine and Nuclear Medicine, Albert Einstein College of Medicine, Bronx, NY 10461, and Dept of Diagnostic Radiology, Yale University School of Medicine, New Haven, Conn 06510.

Sickle cell anemia patients have variable quantities of very dense, non-deformable red cells in their peripheral circulation which are particularly susceptible to polymerization under deoxy conditions. The densest cells (SS4) disappear during sickle cell painful crisis and are the least competent in the microcirculation. We therefore developed an animal model for sickle cell painful crisis which consists of injecting technetium-99m-labelled (Tc), saline-washed, density-defined SS red cells (such as SS4) into the femoral artery of the rat and quantitatively performing both Tc imaging and H-1 magnetic resonance imaging (MRI) at 0.15 Tesla. H-1 T1, H-1 T2, proton density (M_o) and tissue water are all increased and correlated with the absolute volume of cells trapped in the microcirculation of the thigh. Increased T1 is highly correlated with increased proton density (R^2=66.9%) and T2 (R^2=71.4%). The effect of T2 on M_o was calculated and was found to account for less than 30% of the observed increase in M_o. Increased tissue water content can account for less than 10% of the increase. There is still an unexplained increase in apparent proton density which has two possible sources: 1) The control leg exhibited only 40% of the proton density of the reference vials; thus the control tissue has a lower apparent proton density than expected which may be due to perfusion. Decreased perfusion may account for some increase in proton density. 2) The location of the excess tissue water may affect its NMR visibility; extracellular water may have a longer T2 and may thus be more visible.

W-PM-E12 THE APPROPRIATE VISCOSITY IN SEDIMENTATION AND DIFFUSION - Max A.Lauffer, Dept. of Biological Sciences, University of Pittsburgh, Pittsburgh, PA 15260.

Only the liquid in a suspension interacts hydrodynamically with moving particles. The pioneers in sedimentation and diffusion research assumed that the viscosity of the solvent, η_o, is the appropriate term. When η_o is used, sedimentation and diffusion are concentration dependent. The author showed many years ago that, when solution or suspension viscosity, η, is used, sedimentation rates are independent of concentration and proposed that η is the appropriate term.

From Newton's law of flow, the viscosity coefficient can be defined as the force per unit area required to produce unit velocity gradient. This term is η to produce unit gradient of a suspension. Because there is no gradient in the particles, the gradient in the liquid must be $1/(1-\Phi)$, where Φ is the volume fraction of the solvated suspended particles. Thus, the effective viscosity of the liquid component, $\eta' = \eta\,(1-\Phi)$ because this corresponds to unit gradient in the liquid. As pointed out by Schachman and Kauzmann, for sedimentation in a closed system the suspension is forced to move in the direction opposite to sedimentation as a result of the accumulation of solvated particles at the periphery. The observed sedimentation rate, $s_{obs.} = s_{tr}\,(1-\Phi)$ where s_{tr} is the true value. Since s_{tr} is proportional to $1/\eta'$ or $1/\eta\,(1-\Phi)$, s_{obs} is exactly proportional to $1/\eta$. Thus, theoretical analysis confirms that sedimentation and, by analogy, diffusion are inversely proportional to suspension viscosity, η.

W-PM-E13 Modelling the Point Spread Function of a Diffraction-Limited System for Optical Microtomography. Sarah F. Frisken Gibson, and Frederick Lanni. Center for Fluorescence Research in Biomedical Sciences, Carnegie-Mellon University, Pittsburgh, PA 15213.

The use of the light microscope, which was designed for use with 2D planar objects, plus a computer in 3D image collection and object reconstruction is becoming an important tool in studying living cells. Analytic models of image formation in the microscope generally cite one of two classic analyses of a diffraction-limited system. The first is reviewed in Principles of Optics by Born and Wolf (Pergamon, 1959) and extended by Li and Wolf (J.O.S.A. (A1):801-808 (1984)). The second is by Hopkins (Proc. Phys. Soc. (Lond.) A 231:91-103 (1955)), extended by Stokseth (J.O.S.A. 59:1314-1321 (1969)). By extending these analyses to include higher-order terms, it is shown that the two formulations yield equivalent results but the interpretations of these results correspond to two distinct physical situations; moving the detector relative to the lens system, and moving the object relative to the lens system, respectively. The higher-order terms significantly affect the 3D diffraction pattern in microscope systems, particularly with the large degree of defocus expected in optical microtomography. Finally, by reanalyzing the system in terms of spherical coordinates, we find that the 3D diffraction pattern or point spread function, can be represented more accurately and more simply. In particular, in such a coordinate system, the point spread function becomes approximately shift invariant for sources at a constant radius. This suggests a modification of light microscope and detector optics when used for 3D imaging.

Supported by NIH grant GM34639.

W-PM-F1 MONOVALENT IONIC SELECTIVITY OF THE PHOTORECEPTOR cGMP-ACTIVATED CHANNEL IN THE ABSENCE OF DIVALENT CATIONS. R.E. Furman and J.C. Tanaka#. Dept of Neurology and Dept of Biochemistry and Biophysics#, University of Pennsylvania Medical School, Philadelphia, PA 19104.

In the absence of divalent cations, the cGMP-activated channel from Rana pipiens photoreceptors displays relatively small shifts in the reversal potential (E_{Rev}) of excised membrane patch currents with 120 mM biionic substitutions at the cytoplasmic face. The selectivity ratio for Na:K:Li:Rb:Cs is 1:.92:.91:.71:.50 consistent with an Eisenman sequence IX for a high field strength binding site. A different selectivity sequence is determined by conductance ratios derived from macroscopic steady-state currents: Na>K>Cs>Rb>Li.

E_{Rev}'s were also measured under biionic conditions at 20 mM ionic strength. The permeability sequence was the same as at 120 mM. However, the magnitudes of the permeability ratios changed. E_{Rev} for Cs was 16.4 mV at 120 and 2.5 mV at 20 mM. This experiment offers strong evidence that the cGMP channel is a multi-ion channel.

To assess the asymmetry of the free energy profile, we determined permeability ratios under biionic conditions at 120 mM ionic strength for several ion pairs. The E_{Rev} for Cs_i/Na_o was 10.1 mV and for Na_i/Cs_o was 16.4 mV; the respective values for $NH4^+$ substitutions were -14.3 mV and -30.3 mV (n>3). From this we conclude that the channel is asymmetric.

In an attempt to identify an inert cation to maintain ionic strength at low concentrations of [Na^+], we discovered that choline, N-methylglucamine, TEA and TMA at the cytoplasmic membrane face all produce significant block of both inward and outward Na currents suggesting caution when interpreting results from experiments using these ions to substitute for Na^+.

W-PM-F2 ACTIVATION OF THE PHOTORECEPTOR PLASMA MEMBRANE ION CHANNEL BY cGMP AND cGMP-DERIVATIVES J.C. Tanaka*, J.F. Eccleston+ and R.E. Furman#. Dept of Biochemistry and Biophysics and Neurology#, University of Pennsylvania, Philadelphia, PA 19104 and Dept of Biophysical Chemistry+, Mill Hill, England.

We have measured macroscopic currents in the absence of the photochemical machinery by excising membrane patches and directly applying nucleotides at the cytoplasmic face. Examination of the dose-response relation and the IV relation at saturating concentrations provides information on the ligand binding and subsequent channel activation.

We examined a series of derivatives with alterations in C(2), C(6), and C(8) positions on the purine. Most derivatives activated only a fraction of the cGMP-activated current at saturation but all displayed a sigmoidal dose-response function with no significant changes in the N_h among derivates. The $K_{0.5}$'s ranged from 0.8 uM for 8-(5-thioacetamido-fluorescein) -cGMP to > 1.5 mM for cAMP.

We determined that cAMP binds to the same population of channels as cGMP. To further explore the interaction between cAMP and cGMP, we added increasing [cAMP] to a fixed, subsaturating [cGMP]. At both low and intermediate concentrations of cGMP, the current was significantly increased by the addition of concentrations of cAMP that alone would produce no appreciable current. With further titration of cAMP the current rose to a peak at 800 uM before tapering to a lower current plateau characteristic of cAMP alone.

We attribute the cAMP-induced increase in current to the presence of mixed liganded forms of the channel with a single class of binding sites.

W-PM-F3 IDENTIFICATION AND CHEMICAL CHARACTERIZATION OF A PUTATIVE CATION CHANNEL PROTEIN IN ROS PLASMA MEMBRANES. Diane F. Matesic and Paul A. Liebman. Departments of Biochem./Biophys. and Anatomy, University of Pennsylvania, Philadelphia, PA 19104. Introduced by John H. Parkes.

A ~60 kD protein present in ROS membranes was purified by DEAE ion exchange/red dye affinity chromatography[1] and preparative gel electrophoresis for chemical and immunochemical analyses. This protein has previously been identified as a cGMP-dependent cation channel protein subunit by Cook et al.[1] The purified 60 kD protein was resolved into two ~equimolar components on SDS gels which co-migrated with alpha and beta subunits of authentic bovine brain tubulin. Polyclonal and monoclonal tubulin antibodies reacted specifically with the 60 kD protein on immunoblots. One-dimensional peptide maps of electrophoretically purified 60 kD protein matched those of authentic tubulin. Tight association with both ROS membranes and reconstituted liposomes identified this protein as a membrane-associated form of tubulin[2]. The 60 kD tubulin-immunoreactive protein was also identified as a major component of the ROS plasma membrane. These results will be discussed in the context of the cGMP-dependent cation channel protein identification controversy and of the role of membrane-associated tubulin in ROS plasma membrane function. Supported by NIH EY00012, EY01583, and T32EY07035.

[1] Cook, et al. (1987) Proc. Natl. Acad. Sci. 84:585.
[2] Stephens, R.E. (1983) J. Cell Biol. 100:1082.

W-PM-F4 SUBUNIT INTERACTIONS OF RETINAL ROD cGMP PHOSPHODIESTERASE PROBED BY EMISSION ANISOTROPY. Theodore G. Wensel and Lubert Stryer, *Department of Cell Biology, Stanford University School of Medicine, Stanford CA 94305 (Current address of T.G.W., Department of Biochemistry, Baylor College of Medicine, Houston TX 77030)*

The inhibitory γ subunit of cGMP phosphodiesterase (PDE) is removed from the catalytic $PDE_{\alpha\beta}$ complex by the activated (GTP-bound) α subunit of transducin during the light response in rod outer segments. We have measured the steady-state emission anisotropy of a fluorescein-tagged derivative of the γ subunit of PDE (γ^F, Wensel, T.G. & Stryer, L. (1987) *Biophys. J.* **51**:271a.) to study the interactions of γ with $PDE_{\alpha\beta}$ and with the α subunit of transducin. The steady-state emission anisotropy of this relatively small probe subunit (9.7 kd) increases when it binds to the much larger $PDE_{\alpha\beta}$ complex (165 kd). When γ^F is excited with a linearly polarized 476.5 nm laser beam, the anisotropy of the 540 nm emission increases from 0.14 to 0.24 upon binding to trypsin-activated PDE. The reaction is very fast, with a 1/e time of less than 5 s at a PDE concentration of 2.5 nM. The inferred rate constant of 8×10^7 M^{-1}-s^{-1} is similar to that estimated from inhibition kinetics. Addition of excess unlabelled γ reduces the anisotropy, but at a much slower rate. This displacement reaction has a 1/e time of ~440 s. Comparisons were made between complex formation as monitored by anisotropy and PDE activity, in titrations of γ^F with tPDE, as well as in titrations of tPDE with γ^F. The results suggest that γ^F binding to each of the two binding sites for γ on $PDE_{\alpha\beta}$ [Deterre, P.J. *et al.* (1988) *Proc. Natl. Acad. Sci.* **85**: 2424.], abolishes about half of the activity of the complex, and does not appreciably perturb the affinity of the other binding site. The dissociation constants for γ appear to be similar (~ 10 pM).

W-PM-F5 THE STOICHIOMETRY OF THE Na:Ca EXCHANGE IN ROD OUTER SEGMENTS IS $4Na^+:1Ca^{2+},1K^+$ L. Cervetto, L. Lagnado, R.J. Perry, D.W. Robinson & P.A. McNaughton. Physiological Laboratory, University of Cambridge, Cambridge CB2 3EG, UK.

We have measured the activity of the electrogenic Na:Ca exchange, in both forward and reversed modes, from the membrane current produced by its operation. The exchange current is recorded under whole-cell voltage clamp in rod outer segments isolated from the tiger salamander. One charge enters the cell over a wide range of conditions in exchange for every Ca^{2+} extruded (Lagnado, Cervetto & McNaughton, P.N.A.S. 85, 4548, 1988), and the reversed exchange has the same stoichiometry because the charge efflux recorded when the cell is loaded with Ca^{2+} via the reversed exchange is equal and opposite to the influx when the load is extruded. The reversed mode of the exchange is almost completely inhibited by removal of external K^+, and K^+ must be co-transported with Ca^{2+} because alterations in $[K^+]_o$ perturb the equilibrium attained by the exchange in the absence of other membrane Ca^{2+} fluxes. When the exchange is at equilibrium a tenfold reduction in $[K^+]_o$ is balanced by a tenfold elevation in $[Ca^{2+}]_o$ or by a $10^{0.25}$-fold reduction in $[Na^+]_o$. Membrane polarization perturbs the equilibrium in a manner consistent with a single charge being carried per exchange cycle. We conclude that the exchange stoichiometry is $4Na^+:1Ca^{2+},1K^+$. An exchange with this stoichiometry would be capable of supporting calcium extrusion down to levels of $[Ca^{2+}]_i$ approximately 500 times lower than a $3Na^+:1Ca^{2+}$ exchange.

W-PM-F6 SOLUBILISATION AND PROPERTIES OF GUANYLATE CYCLASE FROM RETINAL ROD DISC MEMBRANES
Shereen Hakki and Ari Sitaramayya
Pennsylvania College of Optometry, 1200 West Godfrey Avenue, Philadelphia, PA 19141

In view of several recent reports suggesting the possibility that guanylate cyclase is regulated by calcium and that it may play a significant role in the recovery of dark current, we have attempted to solubilise guanylate cyclase as a prelude to its purification. Rod disc membranes isolated from fresh bovine retinas and washed extensively to remove soluble and peripheral proteins, were used as the source of guanylate cyclase. Solubilisation was achieved by vortexing RDM in Tris buffer at pH 7.6 containing 5% Nonidet P-40, and 1M KCl, followed by centrifugation at 109,000g for 1hr. The supernatant contained 50-65% of the cyclase activity from RDM. The solubilisation was about 50% less when 5 mM Mn^{2+} was present. Solubilised cyclase was very labile, losing about 95% of the activity in 2 days. In the presence of 1 mM DTT, about 50% of the activity remained after 2 days. Mn^{2+} supported the activity of cyclase better than Mg^{2+}. Calcium, Calmodulin and Atrial Natriuretic Factor did not significantly influence the activity. With manganese and GTP at 1:1 in the assays, the enzyme exhibited positive cooperativity with respect to GTP. The n value from Hill plot was 2.5. The solubilised and insoluble fractions of cyclase were similar with respect to all the above properties.

This work was supported by NEI grant EY 07158.

W-PM-F7 DIRECT MEASUREMENT OF INTRACELLULAR pH IN VERTEBRATE ROD PHOTORECEPTORS. R. Wen & B. Oakley II. NBB Program, ECE & Biophysics Depts., University of Illinois at Urbana.

We measured rod intracellular pH (pH_i) in the isolated retina of the toad, Bufo marinus, using double-barrel, pH-sensitive microelectrodes. The electrodes were made from theta tubing, modified to contain a glass fiber in each barrel. After pulling, the electrode tip was bevelled on a dry alumina surface. The pH-sensitive barrel was silanized using TMSDMA vapor (120°C, 1-hr) and then was filled with Fluka #95291 cocktail (containing tri-n-dodecylamine). Both barrels were back-filled with 150 mM KCl. The resistance of the reference barrel was 500-800 megohms, while that of the pH-sensitive barrel was >1000-times larger. The pH-sensitive microelectrodes gave linear responses to pH of 40.0-44.3 mV/decade (mean 42.3, 6 electrodes) over the range of pH 6.8-7.8.

Rods impaled with pH-sensitive microelectrodes had normal photoresponses superimposed upon membrane voltages ranging from -20 to -30 mV. In superfusate containing 10 mM HEPES buffer (pH 7.8), pH_i was 7.2. Superfusion with NH_4Cl was used to verify that the electrodes actually sensed pH_i; superfusion with 20 mM NH_4Cl for 4-min caused an alkalinization of 0.4 pH units; following NH_4Cl treatment, pH_i recovered in 3-min. In other experiments, pH_i varied with the extracellular pH buffer: pH_i acidified reversibly from pH 7.2 to 6.9 (representing a doubling of $[H^+]_i$) upon switching from bicarbonate/CO_2 to phosphate buffer. This intracellular acidification probably was caused not only by the less efficient intracellular pH-buffering by phosphate, but also by the concomitant extracellular acidification that we observed previously. It was interesting to find that removing CO_2 led to intracellular acidificiation. Our results indicate that the extracellular pH buffer system plays an important role in determining rod pH_i. Supported by NIH grant EY04364.

W-PM-F8 EFFECTS OF CYANIDE IONS ON VISUAL PIGMENTS.

Frederick Crescitelli and Béla Karvaly, Department of Biology, University of California, Los Angeles, CA 90024 and Department of Physics, East Carolina University, Greenville, NC 27858-4353

The visual pigment of the Tokay gecko (Gekko gekko) exhibits a number of unusual spectral and photochemical features which clearly distinguish it from rhodopsins. Its major pigment component with its in situ spectral maximum at 521 nm (P-521) is susceptible to relatively mild changes in the environment in a reversible fashion. Properties such as the specific responses to certain anion classes are of particular significance in this respect. In the course of these studies novel phenomena were observed in the presence of cyanide, which we wish to report here.

Cyanide (a pseudohalogenoid) may chemically attack the p-521 pigment in the dark. This is seen as a slow thermal loss of the native photopigment. The following observations have been made on this effec: 1) Only the major (p-521) component responses to the presence of cyanide, the minor (P-467) component seems to be completely resistant to it. 2) Cyanide ions appear to cause no spectral effect on the P-521 pigment. 3) the slow pigment loss in the dark starts occurring above a threshold concentration (40 mM at 15 °C). 4) The disappearance of the P-521 pigment accompanies with the emergence of a new spectral species with maximum absorption at about 330 nm. 5) The same spectral product is seen to be formed when the pigment is photolyzed in the presence of cyanide. 6) The photosensitivity of the pigment is not influenced by the presence of cyanide ions. 7) Unlike the other environmental effects, chloride ions do not provide any protection against cyanide.

The new spectral product is tentatively identified as retinoic acid; the possible reaction mechanisms leading to its formation will be discussed.

W-PM-F9 A BISTABLE PHOTOPIGMENT SYSTEM IN HERMISSENDA TYPE A PHOTORECEPTORS: THE DEPOLARIZING LATE RECEPTOR POTENTIAL (LRP) AND THE PROLONGED DEPOLARIZING AFTERPOTENTIAL (PDA) EXHIBIT CONDUCTANCE CHANGES OF OPPOSITE SIGN. H.-P. Höpp and D.L. Alkon (Intr. by L.B. Cohen). Sect./Neural Systems, Lab. of Biophysics, NINCDS-NIH, Marine Biol. Lab., Woods Hole, MA, USA.

On the basis of anatomy, electrophysiologic properties and synaptic interaction, the 5 photoreceptors in each Hermissenda eye were distinguished (Alkon and Fuortes, 1972) as type A (2) and type B (3). White light elicits depolarizing generator potentials (with early transient and later sustained components) from both types of cells.

Following yellow light adaptation both medial and lateral type A photoreceptors responded to repeated blue stimuli with a reduction (occasionally complete) of all LRP components evoked during the light step and with the emergence of a PDA shortly after the offset of the light step. This PDA could last up to 3 hours. Yellow light reversed all the effects of blue light. The three type B photoreceptors exhibited no comparable changes to blue light. In type A cells the decrease and increase in the early transient depolarizing component of the LRP had separate spectral maxima at 470nm and 570nm, respectively. The low criterion action spectrum had its maximum around 510nm. These results suggest the existence of two distinct visual pigment states, presumably rhodopsin and metarhodopsin, with different absorption maxima.

Membrane conductance was reduced during the PDA evoked by blue light suggesting the shutdown of an outward directed conductance. In contrast the early transient depolarizing component of the LRP was paralleled by an increase in membrane conductance. This increase was eliminated with progressive adaptation to blue light. Supported by DFG Research Fellowship HO 989/1-1.

W-PM-F10 LIGHT AND NUCLEOSIDE TRIPHOSPHATES INFLUENCE cGMP-INDUCED CURRENTS IN EXCISED PATCHES FROM ROD PHOTORECEPTORS. Eric A. Ertel, W.A. Sather & P.B. Detwiler. Univ. of Washington, Dept. Physiol. & Biophy., Seattle, WA.

Our initial goal was to see if GTP or ATP affected the cGMP-gated conductance in inside-out patches of outer segment membrane from *Gekko gekko* rods. The extracellular surface of the excised patch was bathed in 159 mM NaCl, 3.3 mM KCl, 2.8 mM Hepes, 0 added Ca and Mg, pH = 7.4. The cytoplasmic surface was perfused with the same solution containing various nucleotides.

The effect of GTP, but not ATP, on cGMP-gated conductance depends on whether the experiment is done in light or darkness. The conductance activated by 20 μM cGMP in patches obtained in room light is blocked fully by either 50 μM GTP or 1 mM MgATP but is blocked only partially by 1 mM Mg and not at all by 1 mM ATP. The recovery of conductance upon triphosphate removal is generally slow and incomplete. The effect of GTP is reduced but not abolished by 1 mM IBMX. When patches are prepared in darkness, using infrared image converters, 50 μM GTP blocks the 20 μM cGMP-gated conductance only partially or not at all while 1 mM MgATP blocks it completely. In the presence of 50 μM GTP, but not in its absence, the cGMP-gated conductance in 34 out of 46 patches is reduced by light (20 ms, 540 nm). The light-induced decrease in conductance is rapid and followed by slow and typically incomplete recovery. The amplitude and kinetics of the response are graded with light intensity and are reduced but not abolished by 1 mM IBMX. In most but not all cases, light-sensitive patches are membrane blebs drawn 1-10 μm up the pipet during gigaseal formation.

These results indicate that excised patches can contain the transduction machinery necessary for light activation of phosphodiesterase. This is a G protein coupled pathway which can account for the light dependence of GTP block. The explanation for block by MgATP is not clear. It may be a direct effect on the cGMP-gated channel or an indirect effect mediated by biochemical elements associated with the patch. (Supported by PHSNRSA T32 GM07270)

W-PM-F11 CYCLIC GMP-ACTIVATED CHANNELS FROM ROD PHOTORECEPTORS SHOW LITTLE DESENSITIZATION. Gary Matthews & Shu-ichi Watanabe, Dept. of Neurobiology, SUNY, Stony Brook, NY 11794-5230

The transduction channel of vertebrate photoreceptors is an agonist-gated channel activated by internal cGMP. In darkness, there is a steady level of cGMP, which maintains channel activity. Light activates phosphodiesterase that hydrolyzes cGMP, thereby causing channels to close by removing the agonist. Other agonist-gated channels typically show desensitization in the maintained presence of agonist, and if the cGMP-activated channel behaves similarly, then desensitization in darkness and removal of desensitization upon illumination might contribute to the response dynamics of the rod. To examine desensitization of the cGMP-activated channel, inside-out patches from toad rods were exposed to rapid jumps in cGMP applied to the intracellular face by means of a rapid-flow system. Following a step increase in cGMP, the conductance of outer-segment patches rose rapidly to a maintained plateau, with no indication of either rapid or slow desensitization at concentrations ranging from 5 μM to 1 mM.

In addition, in inner-segment patches containing only one cGMP-activated channel (Matthews & Watanabe, 1988, J. Physiol., 403, 389-405), we found little change in channel kinetics during maintained application of cGMP at concentrations ranging from 20 μM to 1 mM. For example, in 5 experiments at 1 mM cGMP, the average proportion of time that the channel was open was 0.20 at early times after application of cGMP and 0.18 at 20 sec. Thus, the cGMP-activated channel shows little desensitization and is capable of faithfully tracking maintained changes in internal cGMP concentration.

(Supported by NIH grant EY03821.)

W-PM-G1 PHYSICAL SIGNIFICANCE OF AMPLITUDE COEFFICIENTS OF THE CHARGING CURVE FOR NONSYMMETRIC MULTIPOLAR NEURONS. *LL Glenn* and *PJ Rebeta*. Intr. by *A. Scarpa*. Dept of Physiology, Ohio Coll Pod Med, Cleveland OH 44106–3082.

The equivalent cylinder model has been used to estimate passive membrane properties and the dendritic electrotonic structure of neurons for over twenty years in a great variety of neurons. In this model, the charging curve, defined as the voltage response to a step of current, can be decomposed into the sum of exponentials, where the boundary conditions determine that amplitude coefficients (C_i) and decay rate (τ_i). The equivalent cylinder model is valid under the condition that the dendrites are symmetric. That is, the time constant of the membrane is uniform across all dendrites and the electrotonic lengths of the dendrites are exactly equal. We derived expressions C_1 as an function of electrotonic length, dendrite–soma input conductance, and dendrite–soma time constant for nonsymmetric multipolar neurons, for any number of dendritic terminations. It was found that the interpretation of C_0 remains the same between symmetric and nonsymmetric neurons, but that the interpretation of C_1 (and all C_i) is modified. In symmetric multipolar neurons, C_1 is dependent upon the input conductance and the electrotonic length of the equivalent cylinder. In this case, the experimentally measured C_1/C_0 ratio can be used to estimate the electrotonic length; in nonsymmetric neurons this no longer holds. Instead, the experimentally measured C_1 depends on the input conductance, length, *and the distribution of denritic lengths*. Thus, all previous estimates of neuron properties based on the C_1 ratio are incorrect. Since many different distributions can give the same C_1, experimental measurements of C_1 have very little value in estimating the membrane properties or electrotonic architecture of neurons. [NIH Grant NS25992]

W-PM-G2 MODULATION OF A TRANSIENT POTASSIUM CONDUCTANCE RESULTS IN CHANGES OF TIMING PROPERTY OF TYPE B PHOTORECETOR IN *Hermissenda*. C. Chen and C. Koch (Intr. by D. Krafte). Computation & Neural Systems, 216-76, Caltech, Pasadena, CA 91125. Associative learning is mediated by cellular interactions between neurons and is stored by modulation of two potassium channels (g_A and g_C). A quantitative model was built to simulate the biophysical mechanisms underlying the temporal specificity of associative learning. The network consists of sensory neurons (photoreceptors and haircells), interneurons and motorneurons. Seven ionic conductances and intracellular second messengers (calcium and diacylglycerol) were modeled by a set of differential equations to predict the receptor potential and channel modulation in B photoreceptors. Light-induced increase of diacylglycerol along with calcium elevation caused by synaptic inputs from haircells activates protein kinase C, reducing g_A and g_C. In addition to the changes in neuronal excitability, the modulation of the fast g_A changes the temporal interval between the onset of an injected current step and the first spike as well as spiking frequency in the photoreceptor. Therefore, ionic channel modulation can modify the gain of neurons as well as their timing properties.

W-PM-G3 TEMPORAL AND SPATIAL INTERACTIONS AMONG OLFACTORY NERVE AXONS FILTER STIMULUS MESSAGES. Robert C. Gesteland, Dept. of Anatomy and Cell Biology, Univ. of Cincinnati, Cincinnati, OH 45267.

Homeostasis of ionic concentration in the olfactory nerve is slow as a result of geometric and energetic factors. Axons are small, unmyelinated and densely packed. Mitochondria are scarce. Schwann cell cytoplasm is sparse. There is little extracellular space. Synchronous activation of the nerve results in elevated extracellular potassium concentrations for many minutes. The capacity for an odorous stimulus to evoke action potentials in an axon depends upon the recent history of activity in that axon, the number of neighboring cells currently and recently active, and the extent of this activity. Under conventional stimulus conditions, the number of stimulus-evoked action potentials, their maximum rate, the latency of the response, and the response threshold are not predictable. A stimulus which evokes a vigorous response can evoke none if delivered a few minutes after a different stimulus to which the cell is unresponsive. This effect is stronger if the second stimulus consists of a mixture of a variety of odorous substances to which the cell is normally unresponsive. Responses to mixtures of odorous chemicals are not summations of the responses of the components delivered separately, because each component can excite the cell and its neighbors to different extents. If the effect on the neighbors is strong excitation, the resulting effect on the cell being studied is a combination of weak direct excitation and strong inhibition resulting from activity in nearby axons. The result is that stimulus intensity changes the function computed by the generator-current-driven axon, not merely the magnitude of the activity. This is accomplished without intervention of junctional complexes, lateral synaptic connections, or interneurons.

This work was supported by NSF Grant BNS-8544025 and NIH Grants NS23523 and NS23348.

W-PM-G4 IONIC CONDUCTANCES IN PIGEON SEMICIRCULAR CANAL HAIR CELLS. D. G. Lang and M. J. Correia (Intr. by A. K. Ritchie). Department of Otolaryngology, UTMB, Galveston, Texas 77550.

Ionic conductances present in the membranes of 25 enzymatically dissociated crista hair cells were studied using the whole cell, voltage clamp mode of the patch clamp technique. We report the presence of two types of voltage-dependent outward K^+ currents and one type of inward Ba^{2+} current. Outward currents were observed when the pipette solution contained (in mM): 140 KCl, 11 EGTA, 2 $MgCl_2$, 1 $CaCl_2$, 10 HEPES, and pH 7.4, and when the bath solution contained (in mM): 152 NaCl, 3.5 KCl, 2.5 $CaCl_2$, 1.0 $MgCl_2$, 17 glucose, 10 HEPES, and pH 7.4. In 68 percent of the hair cells studied, the outward current showed a rapid activation with a time to peak of about 6 ms at 0 mV and a rapid inactivation with time constants of 30 to 90 ms. The steady-state inactivation of this rapid current was half-maximal at -82 mV and was complete at -40 mV. The threshold for activation of this rapid current was between -60 mV and -50 mV with half-maximal activation at -40 mV. In 21 percent of the hair cells studied, the outward current showed a slow activation with a time to peak of about 50 ms at 0 mV and a very slow inactivation. The steady-state inactivation was similar to that of the rapid current; however, the threshold for activation was more positive (-40 mV) with half-maximal activation at -14 mV. The tail currents of the rapid and slow currents reversed at -89 and -83 mV, respectively, which is near the K^+ equilibrium potential (-93 mV). Both of these currents were seen in the absence of external calcium, therefore, they are not Ca^{2+}-activated. Only a small outward current remained when the holding potential was -40 mV, and no "N-shape" of the I(V) curve was detected. Thus, to date, we have no evidence that pigeon semicircular canal hair cells, like hair cells from other species (Ohmori, *J. Physiol.*, 350: 561-581; Art and Fettiplace, *J. Physiol.*, 385, 207-242; Hudspeth and Lewis, *J. Physiol.*, 400: 237-274), show Ca^{2+}-activated K^+ currents. Inward currents could be detected when the pipette solution contained 160 mM CsCl (to block outward currents), and the bath contained 20 mM $BaCl_2$. The inward current showed a very rapid activation and no inactivation during a 100 ms voltage step. The threshold for activation of the inward current was between -50 mV and -40 mV, and the I(V) curve peaked at about -10 mV. The inward currents decreased over time presumably due "run-down." We believe these inward currents are the consequence of Ba^{2+} permeation through voltage dependent Ca^{2+} channels. Ca^{2+} currents with similar characteristics have been previously described in chick hair cells (Ohmori, *J. Physiol.*, 350: 561-581). This work was supported by grants from ONR and NASA.

W-PM-G5 FAST *IN VITRO* MOVEMENT OF OUTER HAIR CELLS IN EXTERNAL ELECTRIC FIELD. K. H. Iwasa and B. Kachar, Biophysics Lab. and Neuro-Otolaryngology Lab., NINCDS, NIH, Bethesda, MD 20892

It has been found that the outer hair cells from the organ of Corti show shape changes and cytoplasmic movements in response to an externally applied ac electric field (Kachar et al., Nature 322: 365, 1986) as well as to a direct current injection into these cells. This is now thought to be the basis of the positive feedback mechanism for the fine tuning of mammalian hearing organs. To test whether the movements in the cytoplasm depend on a direct effect of the electric field on specific charged intracellular components or on the membrane potential, we used digitonin to shunt the membrane resistance. At concentrations of 5 to 20 μM digitonin is capable of permeabilizing biological membranes to ions and low molecular-weight solutes. We observed that the application of digitonin abolished the outer hair cell movements responding to an ac external electric field (10-30 Hz). Coinciding with the abolition of the cytoplasmic response, the nuclear matrix started to oscillate synchronous to the external field. Similar oscillatory movements of the nuclear matrix were also observed when isolated nuclei were directly exposed to the same ac electric field as applied to the cells. Thus the initiation of the oscillatory movements in the nuclei inside of the hair cells is attributable to the rapid increase (of two to three orders of magnitude) of the intracellular electric field when the potential drop across the plasma membrane was reduced due to the permeabilization. If the intracellular electric field were regulating the cell movement, the initiation of the movement of nuclear matrix would have been accompanied by an enhancement of the cytoplasmic movement. Our observation is therefore consistent with the interpretation that a receptor which responds to (local) membrane potential, and not the intracellular electric field, regulates the hair cell movement.

W-PM-G6 **STREPTOMYCIN AFFECTS THE MECHANICS OF INDIVIDUAL HAIR BUNDLES**

W. Denk and W. W. Webb, Cornell University, Ithaca, NY 14853

It has recently been shown that a so called "gating" compliance reduces the stiffness of sensory hair bundles if the mechanosensory channels are allowed to flicker between open and closed states (J. Howard and A. J. Hudspeth, *Neuron*, 1:*189-199*, 1988). Our experiments on frog saccular hair cells show that the Brownian (thermal) motion (W. Denk *et al.*, *Biophys J.*, 49:21a, 1986) of the hair bundles was affected by a transduction channel blocker (Streptomycin) in the expected fashion. Iontophoretic or bath application of Streptomycin reduced the 'rms' amplitude of bundle deflection fluctuations corresponding to a stiffness increase. No spectral changes indicative of a change in the damping coefficient were seen. The stiffness was increased reversibly up to a factor of 1.5 (average = 1.14). In addition we often observed changes of the average bundle position after an iontophoretic current step. The initial fast (≈10 ms) deflection (up to 40 nm) occured in the direction of excitatory bundle displacement in all cases but one. This was frequently followed by a slow response in the opposite direction which usually overshot the pre-pulse resting position. From the direction of the fast mechanical response we conclude that the transduction channel is blocked in its (mechanically) open position. The observed slow response may result from the adaptation mechanism found in those cells (J. Howard and A. J. Hudspeth, *PNAS*, 84:*3064-3068*, 1987). We acknowledge the early help of A.J. Hudspeth, support by NSF, NIH, ONR, and an IBM graduate fellowship for W.D.

W-Pos1 SARCOMERE LENGTH DEPENDENCE OF THE FORCE-VELOCITY RELATION IN SINGLE FROG MUSCLE FIBERS.

Henk L. Granzier*, D.H. Burns and G.H. Pollack. Division of Bioengineering WD-12, University of Washington, Seattle, Wa, 98195, U.S.A. *Present address: Department of Chemistry, University of Texas at Austin, Austin, TX, 78712

In the cross-bridge model of muscle contraction, the characteristics of each force generator are identical to one another and independent of sarcomere length. These features have been tested primarily by measuring the isometric length-tension relation. However, another test of the independent generator concept is to measure the force-velocity relations at different degrees of overlap. If variations of overlap affect only the number of force generators, force-velocity relations at different sarcomere lengths should differ only in scale; shape should remain invariant. We tested this prediction.

The force-velocity relation of single frog fibers was measured at sarcomere lengths of 2.15, 2.65 and 3.15 μm. Sarcomere length was obtained on-line with a system that measures the distance between two markers attached to the surface of the fiber, about 800 μm apart.

Maximal shortening velocity, determined by extrapolating the Hill equation, was found to be similar at the three sarcomere lengths: 6.5, 6.0 and 5.7 μm/sec at sarcomere lengths of 2.15, 2.65 and 3.15 μm, respectively. For loads not close to zero the shortening velocity decreased with increasing sarcomere length. This was the case when force was expressed as a percentage of the maximal force at optimal fiber length or as a percentage of the sarcomere-isometric force at the respective sarcomere lengths.

The force-velocity relation was discontinuous around zero velocity: load clamps above the level that kept sarcomeres isometric resulted in stretch that was much slower than when the load was decreased below isometric by a similar amount. We fitted the force-velocity relation for slow shortening (<600 nm/sec) and for slow stretch (<200 nm/sec) with linear regression lines. At a sarcomere length of 2.15 μm the slopes of these lines was 8.6 times higher for shortening than for stretch. At 2.65 μm and 3.15 μm the values were 21.8 and 14.1, respectively.

At a sarcomere length of 2.15 μm, the velocity of stretch abruptly increased at loads that were 160-170% of the sarcomere isometric load, i.e., the muscle 'yielded'. However, at a sarcomere length of 2.65 and 3.15 μm yield was absent at such loads. Even the highest loads tested (260%) resulted in only slow stretch.

It is concluded that properties of the force generators change with sarcomere length. This is not anticipated by the cross-bridge model of muscle contraction.

W-Pos2 THE DESCENDING LIMB OF THE FORCE-SARCOMERE LENGTH RELATION OF SINGLE FROG FIBERS REVISITED.

Henk L. Granzier*, G. H. Pollack, Center for Bioengineering, University of Washington, Seattle, Wa 98195. *Current address: Department of Chemistry, University of Texas at Austin, Austin, Tx 78712.

The linear descending limb of the force-sarcomere length relation is one of the main predictions by the cross-bridge model. However, ter Keurs et al. (J.Gen.Physiol.,72: 565-592) found that force was much higher than predicted by the degree of filament overlap. Since this result has been criticized for using fixed-end contractions instead of sarcomere-isometric contractions (A.F. Huxley, Ann.Rev.Physiol., 50:1-16) we repeated these experiments and kept sarcomere length constant during contraction.

Sarcomere length was measured simultaneously with two independent methods: a laser-diffraction method and a segment-length method that detects the distance between two markers attached to the surface of the fiber, about 800 μm apart. Both methods were used to keep sarcomeres at constant length during contraction.

Force measured with fixed-end tetani was much higher than predicted by filament overlap, similar to reported by ter Keurs et al. (1978). However, force was much less when sarcomere-isometric tetani were used. Force was now maximal at about 2.1 μm and decreased to zero at about 3.6 μm. At intermediate lengths the descending limb was maximally 80 nm different from predicted based on filament overlap.

We investigated why force of fixed-end contractions was much higher than generated by sarcomere-isometric contractions. The central region of the fiber was found to stretch during the force rise of fixed-end tetani. This was shown to result in a large increase of passive force at sarcomere lengths longer than about 3.2 μm, while beyond overlap (3.6 μm) the increase of passive force was similar to the total force generated by fixed-end contractions at such lengths. This conclusion was confirmed using quick-isotonic release contractions. Furthermore, during the plateau of fixed-end tetani at sarcomere lengths longer than about 2.0-2.2 μm, sarcomeres were not isometric but instead stretched slowly. By measuring the force-velocity relation it was shown that such slow stretch elevates active force far beyond the sarcomere-isometric force.

The laser-diffraction method and segment-length method gave the same result, diminishing the chance that any systematic artifact underlies our findings.

This study supports that the linear descending limb is a characteristic feature of length-clamped sarcomeres.

W-Pos3 MEASUREMENT OF LENGTH AND TENSION IN SINGLE MYOFIBRILS. Marc L. Bartoo, John A. Myers, and Gerald H. Pollack. Center for Bioengineering WD-12, University of Washington, Seattle, WA 98195

An apparatus has been developed for the precise measurement and control of length and tension in single myofibrils. Motor movement and signal digitization are flexibly managed by computer, allowing control of specimen variables in a manner similar to that achieved in whole fiber preparations.

The myofibril is suspended between a fine needle fixed to a piezoelectric motor, and a sensitive optical force transducer. The force transducer is comprised of a 60 μm optical fiber which projects a cone of light from its cut end, and two larger receiving optical fibers. The polished ends of the receivers oppose the cut end of the transmitter across a small gap. The myofibril is attached perpendicularly near the cut end of the transmitter, which bends in response to myofibrillar tension. Small deflections of the transmitter are accurately sensed by differential comparison of the light coupled into each receiver. Results from a 6 mm long beam gave a frequency response of 800 Hz and a resolution of several μg tension.

Phase contrast optics are used to produce an image of the myofibril, which is projected onto a linear photodiode array. The photodiode response is digitized and stored for later analysis using a Macintosh II computer. Algorithms for signal averaging, digital filtering, measurement of sarcomere lengths, and A- and I-band widths have been developed. These are used to improve signal quality and to check for optical or mechanical artifacts during ramp stretch or release. Since all sarcomeres in a short myofibril can be imaged simultaneously, controversial observations such as active tension beyond overlap (de Beer et. al., Am. J. Physiol., 1988) which have been attributed to inhomogeneities or hidden sarcomere populations can be tested with less ambiguity.

W-Pos4 PASSIVE WORK AND VISCOELASTIC PROPERTIES OF ISOLATED RAT DIAPHRAGM MUSCLE
D.A. Syme (Intr. by B.M. Millman)

We measured the passive elastic and viscous properties of isolated rat diaphragm muscle under various strains and strain rates. Their effects on the storage (while lengthening) and release (while shortening) of mechanical potential energy were measured. The muscle was cycled about its rest length by an ergometer, and the passive work done on the muscle to lengthen it, or by the muscle as it shortened, was measured. Increasing strain resulted in increased net energy loss per cycle, but a relatively larger fraction of the potential energy from the stretch was stored (and subsequently released during shortening). Increasing strain rates resulted in increased energy loss per cycle, and decreased storage efficiency. Both effects are due to increased viscous resistance and increased elastic tension at higher strains and strain rates. The effects of increasing strain rate alone (1 to 4Hz) are small relative to the effects of a '10% rest length' increase in cycle strain amplitude or muscle rest length. Muscle movements involving low velocity, small amplitude displacements, at long muscle lengths, are most efficient at conserving passive mechanical energy.

W-Pos5 THE ONSET OF THE INCREASE IN STIFFNESS IN INTACT SKELETAL MUSCLE FIBERS.
D.R. Claflin, D.L. Morgan* and F.J. Julian, Department of Anesthesia Research, Brigham & Women's Hospital, Boston, MA 02115; *Monash University, Australia.

During an isometric contraction, the rise in stiffness of an intact skeletal muscle fiber has been shown to preceed the rise in tension (Ford, Huxley & Simmons, J. Physiol. 372:595, 1986). The onset of the rise in stiffness following stimulation has been reported to occur during latency relaxation (Haugen, Acta Physiol. Scand. 114:187, 1982). The aim of the present study was to relate the earliest stiffness increase following stimulation to the stiffness lead observed during the rise in tension. Experiments were performed at 2.5°C on intact fibers isolated from the tibialis anterior muscle of the frog (R. temporaria). Stiffness was determined at sarcomere lengths between 2.5 μm and 3.2 μm by applying small sinusoidal length oscillations (2kHz, 0.5nm/half-sarcomere) and digitally recording the force responses (50kHz sample rate). Continuous records of stiffness were obtained using digital filtering techniques to isolate, rectify, and then low-pass filter the sinusoidal component of the force response. For the range of sarcomere lengths tested, the onset of the increase in stiffness was independent of sarcomere length and simultaneous with the onset of latency relaxation. Stiffness continued to increase monotonically and lead tension throughout the rising phase of contraction. These results support a crossbridge origin for latency relaxation and suggest a connection between latency relaxation and the "intermediate state" of crossbridges (attached and contributing to stiffness but not tension) postulated to account for the lead of stiffness over tension later in the rise of tension.
Supported by NIH grants AR07972 (DRC) and HL35032 (FJJ).

W-Pos6 THE INTRINSIC BIREFRINGENCE OF SKINNED MUSCLE FIBRES IN AQUEOUS AND NON-AQUEOUS MEDIA.
O. Obiorah & M. Irving. Department of Biophysics, King's College London, London WC2B 5RL.

Muscle birefringence (BF) is of two types: form BF, due to the high refractive index (R.I.) of the oriented contractile filaments relative to that of the bathing solution, and intrinsic BF, due to the polarisation dependence of the R.I. of the filaments themselves. Form and intrinsic BF can be separated experimentally by varying the R.I. of the bathing medium. Rabbit psoas fibres were glutaraldehyde-fixed in rigor, dehydrated in dimethyl sulphoxide, then immersed in non-aqueous media of increasing R.I. (Sato et al., J. Cell Biol. 67, 501, 1975). Both image contrast and BF were minimised in nitrobenzene (R.I.=1.55). After correction for a large irreversible decrease in fibre volume, the minimum BF, which should correspond to the intrinsic BF, was estimated to be 0.9×10^{-3}. This may be compared with the total rigor BF of 2.0×10^{-3}. In order to assess the possible effects of fixation, dehydration and shrinkage on intrinsic BF, we also carried out R.I. matching experiments using metrizamide in aqueous solution. Image contrast of unfixed rigor fibres and myofibrils was minimised in 61% (by weight) metrizamide, R.I.=1.48; this also gave the minimum BF, 1.1×10^{-3}. Fibre diameter was within 2% of that in the absence of metrizamide. The lower matching R.I. in aqueous media is probably due to the retention of a water shell around the filaments, with volume of about one third of the filament volume. This would also explain the slightly higher BF minimum in aqueous than in non-aqueous media, since the water shell is expected to contribute some residual form BF at the R.I. match point. The results therefore suggest that fixation and dehydration have little effect on intrinsic BF. Supported by the M.R.C. and the Royal Society.

W-Pos7 X-RAY OBSERVATIONS CONCERNING THE CROSS BRIDGE ARRANGEMENT IN FROG WHOLE MUSCLE DURING PARTIAL ACTIVATION BY RCC

ALEX.A. STEWART, C.C. ASHLEY, J.D.POTTER AND Y.MAEDA
University Laboratory of Physiology, Parks Road, Oxford OX1 3PT, U.K.,
University of Miami School of Medicine, Maimi, FL, U.S.A. and
EMBL c/o DESY Notkestrasse 85, 2000 Hamburg 52, F.R.G.

Rapid cooling contracture (RCC) (Conway and Sakai, 1960 PNAS,46,897-903) gives graded contractions which are stable over the period required for X-ray exposure allowing data collection using either an electronic X-ray detector or storage phosphor 'imaging plates'.

Following our investigation into the behaviour of the second actin (19.2nm) layer line (Stewart et al ,1988 Biophys.J.53,565a), we have now looked at the 42.9nm first myosin layer line, which is thought to be indicative of the helical track of projections from the thick filament. Plotting the intensity decrease of the layer line against developed tension we find a highly non linear relation, with a layer line intensity of 19% of that in the rest state at a force level of 15% of that during electrical stimulation. This is in contrast to the more linear relation we found for the second actin layer line, which we interperated as indicating considerable cooperativity along the thin filament. We interpret the different behaviour of the two layer lines with a model in which the thin filaments activate as units and a given thick filament loses the larger part of it's contribution to the first myosin layer line as soon as any of the six neighboring thin filaments is active. During maximal electrical stimulation at the cold temperature the layer line intensity is 12-15% of that at rest.

Supported by the MDA and NIH AR37701.
A.A.Stewart is an EMBL predoctoral fellow.

W-Pos8 X-RAY STUDY OF THE STRUCTURAL ROLE OF TITIN AND NEBULIN IN SKELETAL MUSCLE.

H. Tanaka, E. S. Kempner and R. J. Podolsky, NIAMS, NIH, Bethesda MD 20892.

The influence of titin (connectin) and nebulin on the stability of the double hexagonal array of thick and thin filaments in glycerinated rabbit psoas fibers was studied by X-ray diffraction following high energy radiation exposure (1.5 Mrad) which differentially degrades these large proteins (Horowits et al, Nature, 323:160, 1986). Irradiation had no significant effect on the equatorial intensities in the relaxed state at 5 C. Lowering the pH from 7.0 to 5.5 did not affect I(1,0), but caused I(1,1) to drop about 5 fold in both control (Matsuda & Podolsky, J.M.B. 189:361, 1987) and irradiated fibers. Although the effect of lowering pH is fully reversible in control fibers, after irradiation restoring the pH to 7.0 caused I(1,0) to drop by 20% while I_{11} was restored to about 80% of the initial value. Therefore I(1,0) was destabilized by irradiation; the change in I(1,1) with pH, while similar to that in normal fibers, was no longer completely reversible. The lattice spacing changes associated with changes in pH were the same and reversible in both control and irradiated fibers. I(1,0) and I(1,1) were also studied as a function of temperature. In both control and irradiated fibers I(1,0) decreased about 2 fold when temperature was lowered from 20 to 5 C, while I(1,1) increased 2 to 3 fold. These changes were fully reversible in control fibers but only partially reversible in irradiated fibers. Thus, although significant radial order remains after titin and nebulin are degraded by irradiation, the stability of the filament lattice following pH and temperature perturbations is reduced. The results suggest that titin and/or nebulin are involved in radial as well as the axial ordering of the myofilaments (Horowits & Podolsky, J.C.B., 105:2217,1987 and Higuchi,Biophys. J. 52:29,1987).

W-Pos9 ULTRASENSITIVE INTERFEROMETRY REVEALS LARGE REGIONS OF CROSSBRIDGE STATIONARITY IN INTACT SKELETAL FIBERS AT THE PLATEAU OF TETANUS.

Hungyi Lin and Mark Sharnoff, Department of Physics, University of Delaware, Newark, DE 19716

The steady release of heat by isometrically tetanized skeletal muscle is commonly taken to indicate that crossbridges continue to cycle even when internal shortening has ceased. Using dark-field illumination intense enough to guarantee that a typical crossbridge will scatter many quanta into the detector during each exposure, we have made interferometric images of the distributrion of submicroscopic motion in tetanized intact frog toe fibers at the plateau of tetanus. The sensitivity of our previously described methods [Biophys. J. 49, 281 (1986)] has been improved, and we are able to detect displacements as small as 1.2 to 1.5 nanometer in the position of any structure large enough to be resolved optically. When such a structure is at rest, fluctuations in the positions of its submicroscopic components can be detected. In experiments made with a 25X/0.8 objective the "structures" are subsarcomeric, and the submicroscopic components to which the detector is sensitive are principally crossbridges, because the darkfield illumination has largely suppressed light scattered by the filamentary backbones. At the plateau of tetanus we find that large regions (diameter typically 100 micrometer) of our fibers are effectively at rest for intervals as long as 10 msec. Our images suggest either that the crossbridges in these regions are not cycling, that the characteristic time for cross bridge reorientation is quite long in comparison to 10 msec, or that the crossbridge stroke is substantially shorter than 12 nanometer.

W-Pos10 EFFECT OF MECHANICAL STRESS ON THE ORIENTATION OF CROSS-BRIDGES IN MUSCLE FIBERS. Thomas P. Burghardt and Katalin Ajtai, Department of Biochemistry and Molecular Biology, Mayo Foundation, Rochester, Minnesota 55905.

The effect of positive and negative stress on myosin cross-bridge orientation in glycerinated muscle fibers was investigated using fluorescence polarization spectroscopy from the covalent label iodoacetamidotetramethylrhodamine (IATR) specifically modifying sulfhydryl one (SH1) on the myosin heavy chain. With fluorescence polarization spectroscopy, we use the ability to rotate the transition dipole of the fluorescent probe in the molecular frame of the cross-bridge, by excitation wavelength variation, to investigate the three angular degrees of freedom of the cross-bridge. Positive tension was applied by stretching the fiber in rigor. Negative tension was applied in two steps, as described previously (Goldman, McCray and Vallette, J. Physiol. (London), 398:72P, 1988), by relaxing a fiber at resting length and stretching it until the relaxed tension is appreciable, then placing the fiber in rigor and releasing the tension onto the rigor cross-bridges. We found that positive tension has no effect on the fluorescence polarization spectrum from the SH1 bound probe indicating that the cross-bridge did not rotate under these conditions. Negative tension, however, caused a change in the fluorescence polarization spectrum that indicated a probe rotation. The changes in the polarization spectrum from negative stress were reversed by the application of positive stress. It appears that negative tension strains the cross-bridges, or the cross-bridge domain containing SH1, and causes it to rotate. This work was supported by the Mayo Foundation. T.P.B. is an Established Investigator of the American Heart Association.

W-Pos11 FLUORESCENT MODIFICATION AND ORIENTATION OF MYOSIN SULFHYDRYL 2 IN SKELETAL MUSCLE FIBERS Katalin Ajtai and Thomas P. Burghardt, Department of Biochemistry and Molecular Biology, Mayo Foundation, Rochester, Minnesota 55905.

We developed a protocol for the selective covalent labeling of the sulfhydryl two (SH2) on the myosin cross-bridge in glycerinated muscle fibers using the sulfhydryl selective label IANBD. The protocol promotes the specificity of the IANBD using the ability to protect sulfhydryl one (SH1) from modification by binding the cross-bridge to the actin filament and using cross-bridge bound MgADP to promote the accessibility of SH2. We determined the specificity of the probe using fiber extracted proteins to isolate the probe on myosin subfragment 1 (S1), limited proteolysis of the purified S1 to isolate the probe on the 20 kilodalton fragment of S1, and titration of the free SH1's on purified S1 using ^{14}C-iodoacetamide or enzymatic activity measurements. We characterized the angular distribution of the IANBD on cross-bridges in fibers when the fibers are in rigor, relaxation, in the presence of MgADP, and in isometric contraction using wavelength dependent fluorescence polarization. We find that the SH2 probe distinguishes the different states of the fiber such that rigor and MgADP are ordered and maintain a similar orientation throughout the excitation wavelength domain while the relaxed cross-bridge is ordered but has a different orientation. The active isometric cross-bridge is ordered and oriented differently from all of the other states suggesting the presence of a predominant actin bound cross-bridge state that precedes the power stroke during muscle contraction. This work was supported by the Mayo Foundation. T.P.B. is an Established Investigator of the American Heart Association.

W-Pos12 **PHOTON CORRELATION SPECTROSCOPY OF THE POLARIZATION SIGNAL FROM CHEMICALLY ACTIVATED SKELETAL MUSCLE FIBERS.** Shen, S., Yeh, Y., and Baskin, R.J., University of California, Davis, CA 95616

The difference in intensities of the two linearly polarized electric field components of diffracted light has been autocorrelated in time. The measured rapid temporal signals have shown that there exist two components in the relaxed state: One is a relaxational decay at about 5 μs, and the other is a broadly defined oscillation signal at around 350 khz. In previous work, we have shown that both of these signals are related to cross-bridge action. Furthermore, enzymatic digestion by α-chymotrypsin removed both of these signals. Here, we report on the change of these signals upon chemically activating the single, skinned frog fiber. Under sustained activation, the broad but well-defined signal at 350 khz becomes less defined in its spectral content, spreading from very low frequency to approximately 500 khz. The relaxational signal associated with the cross-bridges exhibits a complex exponential profile that cannot be fitted to one relaxational decay time: The original 5 μs correlation intensity signal remained at a reduced level, the amount of remaining signal is a function of the sarcomere length. Due to the spreading of the previously well-defined oscillation signal, slower relaxational components have not been accurately assigned. These results suggest that the 5 μs relaxational signal may be associated with the non-activating cross-bridges while the more complex spectrum, including the spreading of the oscillation signal, is indicative of the activation process. Work is supported in part by NIH AR-26817.

W-Pos13 **DIFFRACTION ELLIPSOMETRY STUDIES ON COMPRESSED MUSCLE FIBERS**

W. L. Kerr, R. J. Baskin, and Y. Yeh, Depts. of Zoology and Applied Science, Davis, California 95616

The change in polarization state of linearly polarized light interacting with a muscle fiber can be described by two parameters: the *differential field ratio* (r), which describes the difference in amplitudes between orthogonally propagating field vectors, and by the *relative phase* (δ) between those fields. This latter quantity can be related to the birefringence (Δn), which is independent of path length. Previously, we have reported on changes in the differential field ratio of relaxed skinned fibers which were compressed by polyvinylpyrrolidone (PVP). We now report on changes in the birefringence in similar conditions.

Birefringence was determined by using a photoelastic modulator to modulate the light impingent upon the fiber. Intensity fluctuations in the first diffraction order were monitored with a photodiode placed after a linear polarizer. The 50kHz and 100kHz components of this signal were measured using lock-in amplifiers. These components can then be related to the phase difference δ. In general, compression of the fibers caused changes in the birefringence dependent upon both the sarcomere length and concentration of PVP. Changes in both r and δ can be described by model calculations which account for both the intrinsic and form contributions to these values.

W-Pos14 **X-RAY DIFFRACTION AND STIFFNESS MEASUREMENTS IN SINGLE MUSCLE FIBRES OF RANA TEMPORARIA.**

G. Cecchi[+], P.J. Griffiths[*], A. Bagni[+], C.C.Ashley[*] & Y. Maeda. EMBL Hamburg, FGR., [*] Univ. of Oxford, UK., [+] Univ. of Florence, Italy.

Cross-bridge kinetics have been studied during contraction and relaxation of skeletal muscle by X-ray diffraction and by stiffness measurements. Unlike previous X-ray measurements on whole muscle, we report time resolved X-ray measurements from single muscle fibres isolated from the tibialis anterior muscle. Aluminium clips were attached to the tendons within 100um of the ends of the cell, so as to reduce tendon compliance and favour the maintainance of isometric conditions during a contraction. The clips were attached to a capacitance force transducer (resonance frequency 50kHz) and a moving coil stretcher (producing a 2um displacement at 4kHz). On exposure to the synchrotron radiation from the source DORIS, equatorial reflections from a single fibre were consistently reproducible and sufficiently strong to provide 25ms time resolution of their intensity changes during activation and relaxation. On transition from relaxation to activation, a decrease in 10 reflection intensity to 0.33x its relaxed value and a 1.58 fold increase in 11 intensity occurred. The intensity changes preceeded the development of tension, and that the I_{10} reflection change led the I_{11} reflection. Intensity changes during relaxation occurred more slowly than the decline of force. Simultaneous stiffness measurements during the tetanus rise suggest its time course is more closely correlated to the I_{11} reflection changes.

W-Pos15 The 2-D X-ray Pattern from Intact Rabbit Psoas Muscle.

Brian Collett†* and Richard J. Podolsky†. †Laboratory for Physical Biology, NIAMS, NIH, Bethesda, MD 20892. *Physics Dept., Hamilton College, Clinton, NY, 13323.

We have obtained two-dimensional X-ray diffraction patterns from small bundles (about 1mm square) of rabbit psoas muscle dissected from fresh muscle, with the ends tied tightly, and stored in a normal skinning solution for periods up to several hours. The muscle membrane in this state appears to be intact; the diffraction pattern is completely impervious to changes in the external ATP concentration. The pattern at room temperature (20°C) resembles the pattern from extensively skinned muscle at the same temperature but has significantly sharper myosin layer lines, as reported by Wakabayashi et. al.[1]. The 143Å and 72Å meridional reflections, which are present in the skinned preparation, are significantly enhanced in the intact muscle and additional reflections appear on the fourth and fifth myosin layer lines. These new meridional reflections are similar in strength to the sixth order reflection (72Å). Such reflections could arise either from some difference in the myosin backbone or from significant perturbations in the helical ordering of the relaxed myosin heads. This latter is unlikely, as the myosin layer lines are at least as strong as in the skinned preparation, so it seems likely that the reflections arise from the myosin backbone, possibly from the S-2 portion of the head or from some extra component which is washed off in the skinning process.

[1] T. Wakabayashi et. al. in Molecular Mechanism of Muscle Contraction eds. H. Sugi and G. Pollack, 1988.

W-Pos16 STRUCTURAL STUDIES OF CONTRACTING SINGLE SKELETAL MUSCLE FIBERS BY FREEZE-SUBSTITUTION . Pieter H.W.W. Baatsen, Karoly Trombitás and Gerald H. Pollack. Center for Bioengineering WD-12, University of Washington, Seattle, WA 98195

Although the A-band of skeletal muscle appears to remain at constant length during isometric contraction, it is not yet clear whether this is the case during activated shortening. To test this, a new setup has been built that allows for control of mechanical conditions, and permits the specimen to be quick-frozen at any instant. The design, based on a principle used earlier by H.E. Huxley, employs a liquid-nitrogen cooled, mirror-polished copper block which moves upward for quick-freezing. The fiber is tetanically stimulated while surrounded by a thin layer of adhering physiological salt solution. Then, it may be frozen during shortening or stretch under constant load, or after redevelopment of tension after reaching its final length. Sarcomere length is measured by laser diffraction. Frozen fibers are freeze-substituted in 2% osmium tetroxide in acetone at -80 °C for 48 hours. Temperature is raised at a rate of 4 °C per hour thereafter. Finally, the specimens are embedded in Araldite, sectioned, stained, and observed in the electron microscope. Freeze-fracture is used as an adjunct method (Baatsen et al., Biophys. J. 51:474a, 1987), but in specimens that are activated, the ends of thick filaments are more difficult to discern using this method than by using freeze-substitution. .

Initial freeze-substitution results show good freeze preservation in the outer layer of the fiber. In a first fiber that had been stretched while activated, some variation in thick filament length was detected (mean length = 1.54 μm, s.d.= 0.09 μm). In the same preparation, mean thin filament length was 0.94 μm (s.d. = 0.04 μm). Additional experiments in which activated fibers are compared with relaxed fibers are underway.

W-Pos17 OBSERVATIONS ON TROPOMYOSIN LOCALIZATION IN FROG SKELETAL MUSCLE. Károly Trombitás, Pieter H.W.W. Baatsen and Gerald H. Pollack. Center for Bioengineering WD-12, University of Washington, Seattle, WA 98195

Single, highly-stretched, mechanically-skinned fibers of frog semitendinosus muscle were labelled with polyclonal antibodies to tropmyosin and observed in the electron microscope. Antigenic sites were localized periodically along the I-filaments, forming 23 or 24 stripes normal to the fiber axis, spaced at about 38 nm intervals. Stripes were prominent in myofibrils near the fiber's surface, decreasing in intensity toward the fiber core where the antibody apparently did not penetrate. In superficial myofibrils, sarcomeres showed less skew than in core myofibrils. This stability implies that the anti-tropomyosin either preserved the naturally existing radial cross-links (Trombitás *et al.*, J. Ultras. & Mol. Str. Res., in press), or created new-cross links that conferred regularity on the lattice. In sarcomeres in which the Z-line was slightly skewed, the stripes followed the skew and remained parallel to the Z-line. But when the Z-line was skewed by more than 10 to 20 degrees, the stripes no longer followed; instead, they remained perpendicular to the fiber axis, indifferent to Z-line skew. Dissociation between Z-line and stripes could be explained if thin filaments had shifted relative to one another by 38 nm or multiples thereof, and cross-links had reattached to new sites. But so specific a shift was not consistently found. A second hypothesis is that the tropomyosin strand is not rigidly bound to the thin filament. With radial interconnections linking them, such 'loose' trompomyosin strands could remain in register while the Z-line broke free and underwent skew. The implication that tropomyosin is not tightly bound to the thin filament is in accord with recent biochemical and crystallographic evidence (Philips *et al.* 1986).

W-Pos18 ULTRASTRUCTURAL STUDY OF A-BAND WIDTH, I-BAND WIDTH, AND SARCOMERE LENGTH IN SINGLE MUSCLE FIBERS. J.E. Anderson and B.H. Bressler, Department of Anatomy, University of Manitoba and Department of Anatomy, University of British Columbia, Vancouver, Canada.

Skinned rabbit psoas single fiber segments were studied in the relaxed state, and following calcium activation. Under isometric and isotonic conditions at 20°C, fibers and segments were fixed in glutaraldehyde or glutaraldehyde plus paraformaldehyde, with or without post-fixation in osmium tetroxide, stained en bloc, and dehydrated for electron microscopy.Sarcomere length (SL) was monitored by laser diffraction. Transmission electron microscope images of longitudinal sections were contrast enhanced and analyzed on a calibrated KONTRON SEM-IPS system. A-band width, half I-band width and SL were measured and recorded separately for each myofibril, field, and fiber segment examined. Shrinkage artifacts were quantified by comparing SL measured by laser diffraction before and after fixation and directly from electron micrographs following sectioning. At SL from 1.82 to 3.97 um, A-band width measured 1.612+ .031 um in segments which produced a successful contracture under both isometric and isotonic conditions. Z-line disruption in unsuccessfully contracted segments was accompanied by skewed A-bands, with an apparent change in A-band width. In addition, for 145 myofibrils under prolonged contracture conditions, the significant correlation between half I-band width and SL indicated A-bands had not migrated toward the Z-line. (Supported by MRC Operating Grant to BHB and MRC PDF to JEA).

W-Pos19 THE EFFECTS OF SITE SPECIFIC PHOSPHORYLATION ON THE SOLUBILITY OF PARAMYOSIN. L.W. Radlick;*#I.S. Green;* M.A. Long#and J.F. Koretz;* Rensselaer Polytechnic Institute* and Russell Sage College#, Troy, New York.

Solubility studies comparing alpha-r-paramyosin, the native protein, and beta paramyosin, a degraded form, have shown that beta paramyosin is more soluble(A.T. Yeung and R.W. Cowgill. Biochemistry 15, 4654, 1976). The lower solubility of alpha-r-paramyosin at neutral pH and low ionic strength is due to a sequence at the C terminus which beta paramyosin lacks.

Since both paramyosins can be phosphorylated by cAMP dependent protein kinases, and additionally, alpha-r-paramyosin can be phosphorylated at a site near the C terminus the effects of phosphorylation on the solubility properties were examined. A comparison of the solubility profiles of alpha-r-paramyosins--non-phosphorylated (NP-A), cAMP dependent protein kinase phosphorylated (CAMP-PM), paramyosin kinase phosphorylated (PMK), and paramyosin kinase + cAMP dependent protein kinases phosphorylated (PMK+CAMP-PM) as well as non-phosphorylated beta (NP-B) paramyosin--were made.

Differences in the solubilities were noted. PMK was the most soluble followed by NP-A. Both of these forms were minimally soluble at 0.05 M ionic strength, pH 7. The least soluble form was CAMP, which demonstrated a solubility minimum over the range 0.05-0.15 M, pH 7. NP-B, with a solubility minimum at 0.1 M, was less soluble than NP-A. Differences in the amounts of covalently bound alkali labile phosphates may account for the fact that non-phosphorylated alpha-r-paramyosin is more soluble than beta paramyosin in our studies. Electron micrographs of the above forms of the paramyosins at different ionic strengths are also included.

W-Pos20 IDENTIFICATION OF EPITOPES ON LIMULUS PARAMYOSIN USING MONOCLONAL ANTIBCDIES. J.L. Woodhead, R.J.C. Levine & H.A. King. Dept. Anatomy, Medical College of PA, Philadelphia, PA 19129.

We have isolated IgGs to different sites on Limulus paramyosin (PM) from the supernatants of mouse hybridoma cultures and used these antibodies to identify the epitopes to which they bind on the purified protein both by Western blots of PM digests according to Cowgill (Biochem. 11:4532,'72; ibid. 14:509,'75) and by direct visualization of IgG binding to isolated protein molecules on rotary shadowed samples, in the electron microscope.

On Western blots, two of the monoclonals bind to all digestion products that contain the amino terminal third of the PM molecule, but do not bind to the lowest molecular weight products of digestion, which probably comprise the sequence closest to and including the amino terminal. In rotary shadowed samples contining IgG plus purified PM, both of these antibodies bind to positions approximately one-third the distance from one end of the rod-shaped molecule. Frequently, two (identical) IgGs bind to this site, producing a butterfly-like image. Presumably, each IgG binds to a specific epitope on one of the two identical polypeptide chains comprising the alpha-helical PM rod. A third monoclonal (IgG) binds to all of the PM digestion products, including those of low molecular weight, on Western blots, and thus, is presumably directed toward the amino terminal itself; this IgG binds specifically to the tip of one end of the isolated molecules, in rotary shadowed images. None of the antibodies cross-reacts with the PM band on Western blots of SDS-PAGels of molluscan striated or catch muscle preparations. We plan to use these antibodies, and others we are currently characterizing, to map exposed PM sites on relaxed and activated thick filaments, both isolated and organized within the A-bands of Limulus sarcomeres. Supported by USPHS grant AR33302.

W-Pos21 INACTIVATION OF THE Ca^{2+} CHANNEL IN GUINEA PIG GASTRIC MYOCYTE IS BOTH Ca^{2+} AND VOLTAGE DEPENDENT. D.A. Katzka & M. Morad, Univ. of Penn, School of Medicine, Philadelphia, PA

In isolated guinea pig gastric myocytes it has been shown that the inward current is carried only by the Ca^{2+} channel (Mitra & Morad, Science 229:269,1985). We investigated the possible existence of more than one population of Ca^{2+} channel and studied the mechanisms of its inactivation. Guinea pig gastric myocytes were isolated (Mitra & Morad, Science 229:269,1985) and studied by the whole cell patch clamp technique (Hamill et al, Pflugers Arch. 391:85,1981). i_{Ca} activated at -20mV, peaked at +10mV and appeared to reverse at potentials positive to +60 mV. The time course of inactivation in EGTA dialyzed solution was described by a fast (t_f=53.4±18.1 ms) and a slow (t_s=175.2±46.1 ms) exponential. Changing the holding potential from -40 to -80 mV enhanced i_{Ca} by 2-3 fold but did not alter the voltage-dependence or the kinetics of inactivation significantly. In myocytes dialyzed with 90 mM citrate the kinetics of the fast component of inactivation (t_f) i_{Ca} were markedly slowed. When Ba^{2+} was the charge carrier a similar slowing of t_f also occurred such that a single time constant (t_s=200 ms) could well describe the time course of inactivation of i_{Ca}. The steady state voltage-dependence of inactivation of i_{Ca} did not change signficantly when Ba^{2+} was the charge carrier or the cells were dialyzed with citrate. Nifedipine, D-600 and diltiazem inhibited i_{Ca} in a voltage-dependent manner. Diltiazem enhanced the inactivation of Ca^{2+} channel, suggesting a time and voltage dependent block of the open channel. At lower concentrations (100 nM) diltiazem enhanced peak i_{Ca} without significant effect on the slowly inactivating component of i_{Ca}. We conclude that gastric myocytes have only one population of Ca^{2+} channel, the inactivation of which is both voltage and Ca_i dependent.

W-Pos22 ENDOTHELIN REGULATION OF INTRACELLULAR FREE CALCIUM IN CORONARY ARTERY SMOOTH MUSCLE CELLS. M Sturek and L Bowman (Intr. by VH Huxley). Department of Physiology and Dalton Research Center, University of Missouri, Columbia, MO 65211.

Endothelin is the most potent constrictor of coronary arteries and is postulated to be an endogenous agonist of voltage-gated Ca channels (Yanagisawa et al. Nature 332:415, 1988). We determined the effects of 10^{-8} M endothelin on smooth muscle cell (SMC) free Ca (Ca_i) in freshly dispersed single bovine coronary artery SMC using fura-2 microfluorimetry. The figure shows that endothelin (E, solid horizontal line) caused a 2-fold enhancement of the 80 mM K-induced (80K) increase in Ca_i, consistent with its action as a Ca channel agonist. However, in normal physiological saline endothelin caused a 63% increase in Ca_i above resting and the increase was only attenuated by 50% in either Ca-free solution or normal saline containing 0.2 mM lanthanum (La). These data suggest that endothelin may also release Ca from the sarcoplasmic reticulum and that inhibition of Ca_i buffering and other Ca influx mechanisms should be considered.

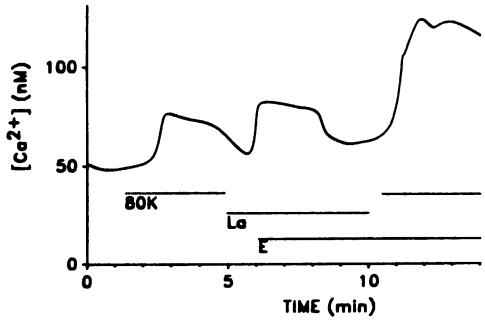

W-Pos23 BUFFERING OF INTRACELLULAR FREE CALCIUM BY THE SARCOPLASMIC RETICULUM IN CORONARY ARTERY SMOOTH MUSCLE CELLS. M Sturek, KR Kunda, and L Bowman. Department of Physiology and Dalton Research Center, University of Missouri, Columbia, MO 65211.

We determined whether the sarcoplasmic reticulum (SR) buffers (attenuates) the increase of intracellular free Ca (Ca_i) resulting from Ca influx through voltage-gated Ca channels. Ca_i was measured with fura-2 in freshly dispersed single bovine coronary artery smooth muscle cells (SMC). The figure shows that depolarization of SMC with 30 or 80 mM K for the duration indicated by the solid horizontal line elicited small rises in Ca_i. Caffeine (CAF, 5 mM) released Ca from the SR and depleted the Ca store as shown by the large, transient increase of Ca_i. In the continued presence of CAF (or 10 μM ryanodine), Ca_i buffering by the SR is inhibited and exposure to K caused larger increases of Ca_i than K alone. The augmented K-induced increase of Ca_i during inhibition of Ca_i buffering by the SR was abolished in Ca-free external solution and inhibited 80% by 0.2 mM lanthanum (La). These data indicate a significant role for Ca_i buffering by the SR.

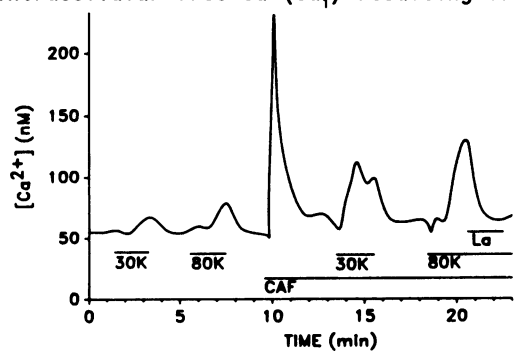

W-Pos24 CHANGES IN $[Ca^{2+}]_i$ IN VASCULAR SMOOTH MUSCLE CELLS ISOLATED FROM COARCTATION-HYPERTENSIVE RATS. Panos Papageorgiou and Kathleen G. Morgan (Intro. by Jeanne Y. Wei). Departments of Physiology and Medicine, Harvard Medical School, Boston, MA 02215.

Increased blood pressure acts as a growth stimulus and induces hypertrophy of the rat aortic media. The hypertrophy is accompanied by modified contractile responses. To further define the role of Ca^{2+} in growth and contraction processes, we examined the intracellular $[Ca^{2+}]$ in single, freshly isolated smooth muscle cells from aortas of normotensive (NR) and coarctation-hypertensive rats (CHR). Rat thoracic aortas were inverted, tied at the ends and incubated at 34° C into Hank's solution containing collagenase, elastase and trypsin inhibitor. Single cells were incubated in 1uM fura-2 AM for 20min. Digital cell-images were acquired after excitation at 350nm and 390nm, and ratio-values were obtained after appropriate background subtraction. Data are expressed as means ± S.E.M. Resting $[Ca^{2+}]_i$ in single cells from NR was 201±27 nM (n=18), whereas cells from CHR had significantly higher resting $[Ca^{2+}]_i$ of 324±53 nM (n=11, p=0.03). The CHR cells were also significantly shorter. In response to 51mM K^+, cells from NR increased their $[Ca^{2+}]_i$ by 24%±6% (n=8) from the basal levels, as opposed to a 61%±13% increase observed in cells from CHR (n=6, $p<0.02$). Further studies are in progress to determine if the higher $[Ca^{2+}]_i$ and shorter length of the CHR cells could be due to damage from the cell-isolation procedure. However, we think this is unlikely since the same procedure was used for both cell types. The present data suggest that increased wall tension modifies the excitation-contraction characteristics of vascular smooth muscle cells, possibly through changes in mechanisms regulating Ca^{2+} homeostasis. [Support: Ryan Fellowship to PP, NIH HL 31704 and AHA EI to KGM].

W-Pos25 PROLONGED $[Ca^{2+}]_i$ ELEVATION ENHANCES THE RATE OF DECLINE OF $[Ca^{2+}]_i$ IN SINGLE SMOOTH MUSCLE CELLS. Peter L. Becker, Fredric S. Fay, Joshua J. Singer, & John V. Walsh. Department of Physiology, University of Massachusetts Medical Center, Worcester, MA.

The processes which regulate cytosolic $[Ca^{2+}]$ play an important role in controlling contraction of smooth muscle. We have used a high time resolution microfluorimeter to monitor $[Ca^{2+}]$ in fura-2 loaded smooth muscle cells that are voltage clamped with a single conventional microelectrode. Brief depolarizing pulses generate a short-lived Ca^{2+} current elevating the $[Ca^{2+}]_i$ which then allows the decline in $[Ca^{2+}]_i$ to be studied in the absence of stimulated calcium influx. Plots of $d[Ca^{2+}]/dt$ vs $[Ca^{2+}]_i$ constructed from the $[Ca^{2+}]_i$ data during the decline of $[Ca^{2+}]_i$ show a relation which was less steep at higher $[Ca^{2+}]_i$'s, indicating that the underlying processes were saturable. The observed relationship is consistent with an underlying process having a K_m near 200-300 nM. Repetitive, closely spaced depolarizing command pulses could elevate the $[Ca^{2+}]_i$ to a higher level for a prolonged period of time. Following these more prolonged $[Ca^{2+}]_i$ elevations, the rate of decline of the $[Ca^{2+}]_i$ at any given cytosolic $[Ca^{2+}]$ was greater when compared to the rate measured following a brief elevation, indicating that the underlying processes were enhanced. This enhancement persisted for 20 to 25 seconds, well after the $[Ca^{2+}]_i$ returned to "rest", and in fact the resting $[Ca^{2+}]$ was somewhat lower during this period. Thus, it appears that the processes responsible for lowering the cytosolic $[Ca^{2+}]$ are stimulated by, and display a "memory" for, the immediately preceding period of $[Ca^{2+}]_i$ elevation. Supported by NIH (HL-14523, AM07807, DK31620), NSF (DCB8511674), and MDA.

W-Pos26 Na GRADIENT REDUCTION POTENTIATES VASOCONSTRICTOR-INDUCED $[Ca^{2+}]$ TRANSIENTS IN VASCULAR SMOOTH MUSCLE CELLS: A FURA-2/DIGITAL IMAGING STUDY. S. Bova, W.F. Goldman & M.P. Blaustein, Physiology Department, University of Maryland School of Medicine, Baltimore, MD 21201.

Reduction of external Na^+ usually enhances the contractile responses of vascular smooth muscle (VSM) to vasoconstrictors. The mechanism of this effect is unknown, but may be related to the Na/Ca exchange-mediated regulation of intracellular Ca^{2+}. Digital analysis of images of fura-2 fluorescence was used to measure intracellular $[Ca^{2+}]$ in single cells from the A_7r_5 cell line. The responses to various agonists were investigated under conditions of an altered $[Na^+]_o/[Na^+]_i$ gradient. When $[Na^+]_o$ was reduced from 138 to 1.2 mM, Na^+ was replaced by isosmotic Li^+ or N-methylglucamine (NMG); 1-3 mM ouabain or K-free media were used to increase $[Na^+]_i$. Resting $[Ca^{2+}]$ (normally about 100 nM) increased by 20-30% when $[Na^+]_o$ was decreased or $[Na^+]_i$ was increased. When $[Na^+]_o$ was reduced, the amplitudes of the $[Ca^{2+}]$ transients evoked by serotonin, vasopressin and high $[K^+]_o$ were increased and the rates of decline of $[Ca^{2+}]$ during the falling phase of the transients were slowed. Reintroduction of 138 mM Na^+ during the falling phase cause a prompt increase in the rate of $[Ca^{2+}]$ decline. Similar effects on the $[Ca^{2+}]$ transients were obtained when $[Na^+]_i$ was elevated. These data suggest that reduction of the Na^+ gradient may increase $[Ca^{2+}]$ in VSM via Na/Ca exchange; much of the entering Ca^{2+} is apparently stored in the sarcoplasmic reticulum since the amplification of the $[Ca^{2+}]$ transients is greatly attenuated by caffeine. The increased availability of intracellular Ca^{2+} and diminished Ca^{2+} extrusion under reduced Na^+ gradient conditions could explain the enhanced $[Ca^{2+}]$ transients and amplified responses to agonists. (Supported by AHA-Md Affiliate, MDA and NIH)

W-Pos27 EFFECTS OF SEROTONIN ON THE DISTRIBUTION OF CALCIUM IN SINGLE CULTURED VASCULAR SMOOTH MUSCLE CELLS. W.F. Goldman & S. Bova, Department of Physiology, University of Maryland School of Medicine, Baltimore, MD 21201.

A rise in cytosolic free Ca^{2+} is the trigger for contraction in vascular smooth muscle (VSM). Ca^{2+} can enter the cytosol from the extracellular fluid (ECF) and/or via release from the sarcoplasmic reticulum (SR). We are using fura-2 and digital imaging microscopy to study the spatial distribution of intracellular Ca^{2+} in cultured A_7r_5 cells and the changes elicited by activation with serotonin (5-HT). The apparent distribution of Ca^{2+} in A_7r_5 cells is heterogeneous reflecting, in part, separate pools of intracellular Ca^{2+} in the nucleus, SR and cytosol. This is especially evident in the nuclear region where large differences exist between the nucleus, containing the lowest apparent Ca^{2+}, and the reticulum rich, perinuclear region containing some of the cells' highest Ca^{2+} levels. 5-HT evokes Ca^{2+} transients that reach a peak within 24 sec, and subsequently decline to near basal levels within 5 min. Ca^{2+} transient amplitudes vary, depending on the size of the intracellular Ca^{2+} store, ranging from approximately 1 uM to >1.9 uM (signal saturation). In the presence of 10 mM caffeine, SR Ca^{2+} stores are depleted; 5-HT-evoked Ca^{2+} transients are then markedly inhibited, and instead, 5-HT induces small, stable increases in Ca^{2+} (100-300 nM) that result from an influx of Ca^{2+} from the ECF. This influx is blocked in the absence of extracellular Ca^{2+}, as are 5-HT-induced Ca^{2+} transients. These observations indicate that 5-HT evokes both an influx of Ca^{2+} from the ECF and release of Ca^{2+} from the SR. They also suggest that Ca^{2+} influx from the ECF may play a role in mediating 5-HT-induced release of Ca^{2+} from the SR. (Supported by grants from the AHA/MD Affiliate to W.F. Goldman; MDA & NIH to M.P. Blaustein.)

W-Pos28 INTRACELLULAR HEPARIN INHIBITS PHARMACOMECHANICAL CALCIUM RELEASE IN SMOOTH MUSCLE, S. Kobayashi, A.V. Somlyo, T. Kitazawa, A.P. Somlyo. PA Muscle Inst., Univ. of PA Med. Sch., Phila., PA 19104-6083 and Dept. of Physiol., Univ. of VA, Charlottesville, VA 22908

Heparin, a specific blocker of inositol 1,4,5-trisphosphate-induced Ca^{2+} release in smooth muscle (Kobayashi et al., 1988, Biochem. Biophys. Res. Commun. 153, 625), and Fura-2 acid, an intracellular Ca^{2+} indicator, were loaded into longitudinal smooth muscle of guinea-pig ileum by reversible permeabilization (Rembold & Murphy, Circ. Res. 63, 593, 1988), with a minor modification. Simultaneous recordings of Ca^{2+} transients (the ratio of Fura-2 signal excited at 340 and 380nm) and force development were carried out by the method of Himpens & Somlyo (J. Physiol. 395, 507, 1988) in small (100-200µm diameter) strips mounted in a "bubble" chamber (Horiuti, J. Physiol. 398, 131, 1988). In the presence of extracellular Ca^{2+}, the responses to 10µM carbachol (expressed as % of high K^+ response) were inhibited in 1-50mg/ml heparin-loaded cells by 30% (tension) and 10% (Ca^{2+} signal). In high K^+, Ca^{2+}-free solution, carbachol responses were inhibited by 50% (tension) and 75% (Ca^{2+} signal). Reversible permeabilization in the absence of heparin had no effect on the tension evoked by high K^+ or 10µM carbachol. The results suggest that heparin inhibits intracellular Ca^{2+} release mediated by pharmacomechanical coupling. Supp. by grant HL15835 to PA Muscle Inst.

W-Pos29 RECEPTOR OCCUPANCY AFFECTS CHANGES IN INTRACELLULAR FREE CA^{2+} ($[Ca^{2+}]_i$) AND MYOSIN PHOSPHORYLATION CAUSED BY MUSCARINIC ACTIVATION OF CANINE TRACHEAL SMOOTH MUSCLE. S.J. Gunst, M.H. Al-Hassani and W.T. Gerthoffer. Dept. of Physiology, Mayo Fndn., Rochester, MN 55905, and Dept. of Pharmacology, Univ. of Nevada School of Med., Reno, NV.

Although acetylcholine (ACh) and McN-A-343 both activate pirenzepine-insensitive (M2) muscarinic receptors in canine tracheal muscle, ACh can elicit maximal force by occupying only 4% of receptors, whereas 61% occupancy is needed by McN-A-343 (Gunst, et al., Physiologist, 1988). $[Ca^{2+}]_i$ and myosin light chain phosphorylation were compared during contractions with concentrations of McN-A-343 (10^{-4}M) and ACh (10^{-5}M) that elicited equivalent force. In 9 muscles loaded with aequorin, ACh elicited a large initial transient in the Ca^{2+} signal accompanied by rapid force development (peak dF/dt = 0.78 ± 0.11 g/s), whereas contraction with McN-A-343 elicited a slow gradual rise in $[Ca^{2+}]_i$ and a much slower rate of force development (peak dF/dt = 0.16 ± 0.04 g/s). The ratio of the average magnitude of the light signal during the first 30 s of contraction to that during the first 300 s of contraction was 3.4 ± 0.6 for ACh but only 0.46 ± 0.09 for McN-A-343. Myosin phosphorylation was significantly lower for McN-A-343 than for ACh during the first 3 min of contraction. Phosphorylation reached a peak of 0.507 ± 0.037 moles Pi/mole light chain 20 s after stimulation with ACh, but did not reach its maximum of 0.435 ± 0.014 moles Pi/mole light chain until 3 min after stimulation with McN-A-343. Differences in subcellular effects elicited by muscarinic agonists acting on the same receptor subpopulation may be due to differences in their ability to elicit the release of second messengers such as IP_3.

Supported by HL29289 and HL35805.

W-Pos30 CATECHOLAMINE EFFECTS ON Ca^{2+}-ACTIVATED K^+-CHANNELS OF GUINEA PIG TAENIA COLI MYOCYTES. S.F. Fan[2], S.L. Hu[1] and C.Y. Kao[1], [1]Department of Pharmacology, SUNY Downstate Medical Center, Brooklyn, NY 11203 and [2]Department of Anatomical Sciences, HSC, SUNY at Stony Brook, NY 11794.

Activation of both α and β adrenergic receptors in the guinea pig taenia coli is said to involve increases of membrane K^+ conductance (Bülbring and Tomita, Pharmacol. Rev. 39:49, 1987). In multicellular preparations, a more negative E_K but no change in the slope conductance of the tail I_K was observed upon β-activation (Kao et al., INSERM [Paris] symposium 50:165, 1976). In cell-attached membrane patches of freshly dispersed myocytes, the probability of opening (P) of the Ca^{2+}-activated K^+-channel is enhanced by isoproteronol (ISO, 2.5-4.7 μM), and is depressed by both phenylephrine and epinepherine (EPI). In all cases, the unitary conductance is unaltered. The ISO-induced rise of P is prevented by bath-additions of Cd^{2+}, Co^{2+} and Mn^{2+}. Forskolin (50-100 μM) also increases P. KF alone at 1 mM has no detectable effect on P, but enhances the effect of ISO. In a solution with pCa = 8, detaching the patch from the cell is accompanied by a marked increase of P that is not suppressed by Ca^{2+} -free medium, but is suppressed by treating the cell with ISO (4.7 μM) before detachment. After detachment, the ISO-suppressive effect declines with a time-constant of about 10 min. Cd^{2+}, Co^{2+}, Mn^{2+} added with ISO before detachment abolish the suppressive effect. ISO added after detachment has no effect on the increased P. It appears that (1) ISO increases P of the Ca^{2+}-activated K^+-channel through some Ca^{2+}-mediated activation of adenyl cyclase, and (2) ISO suppresses P of the Ca^{2+}-activated K^+-channel in detached patches through some Ca^{2+}-activated sarcoplasm-related mechanism (Supported by NIH grant HD-00378).

W-Pos31 EFFECTS OF STIMULANTS AND CYCLIC AMP-RELATED RELAXANTS ON CYTOSOLIC CALCIUM LEVEL IN VARIOUS SMOOTH MUSCLES H. Karaki, H. Ozaki, M. Tazimi, S.-C. Kwon and A. Abe. Department of Veterinary Pharmacology, Faculty of Agriculture, The University of Tokyo, Bunkyo-ku, Tokyo 113, Japan

In isolated smooth muscle tissues of rabbit and rat aortas, dog trachea and guinea-pig taenia coli, cytosolic Ca level ([Ca]i) and muscle tension were measured simultaneously with fura-2-Ca fluorescence. High K induced sustained increments in both [Ca]i and muscle tension in these smooth muscles. Similar sustained increments were induced by norepinephrine in aortas and by carbachol in trachea and taenia. In aortas and trachea, forskolin and isoproterenol did not change or slightly decreased resting [Ca]i without or with a slight decrease in resting tension. In taenia, these inhibitors decreased spontaneous rhythmic changes in both [Ca]i and muscle tension. In norepinephrine-stimulated aortas and carbachol-stimulated trachea and taenia, forskolin and isoproterenol decreased [Ca]i and, more strongly, muscle tension. These inhibitors decreased high K-stimulated muscle tension without or with only a small decrease in [Ca]i. These results suggest that (1) sustained contraction in smooth muscle is due to sustained increase in [Ca]i and (2) cyclic AMP-related relaxants inhibit contraction by decreasing [Ca]i and by decreasing the sensitivity of contractile elements to Ca. It has been shown using aequorin that receptor-agonists induce only a transient increase in [Ca]i during sustained contraction, and forskolin and isoproterenol increase [Ca]i without muscle contraction in aorta and trachea (Morgan & Morgan, 1984; Takuwa et al., 1987). These results may indicate the different distribution of fura-2 and aequorin in smooth muscle cytoplasm.

W-Pos32 MEASUREMENT OF INTRACELLULAR [NA^+], WITH SBFI, AND NA^+ REGULATION IN SMOOTH MUSCLE CELLS. Moore, E.D.W., Minta, A., Tsien, R.Y. and Fay, F.S. Dept. of Physiology, U. Mass. Medical Center., Worcester, MA, 01655 (Intr. by Raul Pedron)

We have undertaken a study of the intracellular [Na^+] and its regulation in single cells that were freshly isolated from the stomach of the toad Bufo marinus. The $[Na^+]_i$ was measured with sodium binding fluorescent indicator (SBFI), a sodium-sensitive fluorescent dye recently developed by Tsien et al.. Cells were incubated at room temperature with the acetoxymethylester form of the dye for up to three hours before recording. Intracellular dye concentrations were no greater than 900 μM. Images of the cells were captured with a digital imaging microscope and a thermoelectrically cooled CCD camera. The calibration curve of the dye is different in vivo and in vitro, and varies between cells, possibly reflecting different degrees of de-esterification between cells. We have therefore developed an approach which allows us to record the fluorescence from a single cell and then calibrate the dye from that cell. The dye distributed throughout the cytoplasm, but concentrated in the nucleus and in mitochondria. The ratio images indicated that the intracellular Na^+ concentration was uniform at 12 mM ± 3 mM (N=27). Local application of ouabain increased the Na^+ concentration uniformly in the cell 10 min. after application. We also applied isoproterenol by puffer pipette and observed a significant decrease in the intracellular Na^+ concentration. This observation is consistent with the hypothesis that β-adrenergic relaxing agents stimulate the Na^+-K^+ ATPase, lowering the intracellular Na^+ concentration, increasing the transmembrane Na^+ gradient which is used to extrude Ca^{2+} via the Na^+-Ca^{2+} exchange mechanism. Supported by; MDA and NIH (HL14523).

W-Pos33 WHOLE CELL PATCH CLAMP EXPERIMENTS ON HUMAN UTERINE SMOOTH MUSCLE. R. C. YOUNG, (INTRA BY R. CROUCH)

Human uterine tissue was obtained from pregnant women at the time of Cesarean section delivery. Primary cell culture was performed and electron microscopy was used to demonstrate smooth muscle morphology. Whole-cell patch clamp experiments were performed on cells between the second and sixth pass. Action potentials were seen in bathing solutions containing 25 mM barium or 10 mM calcium. Voltage clamp experiments were performed which demonstrated voltage activated inward currents followed by outward rectification. Ion substitution experiments identified these currents as probably due to inward voltage dependent calcium channels and outward calcium dependent potassium channels.

W-Pos34 AFFINITITES OF SMOOTH MUSCLE TROPOMYOSIN AND HEAVY MEROMYOSIN TO CALDESMON. Kurumi Y. Horiuchi* and Samuel Chacko, Department of Pathobiology, University of Pennsylvania Philadelphia, PA 19104. (Intr. by Dr. S. Takashima).

Caldesmon, an actin-binding protein which also binds to calmodulin in the presence of Ca, inhibits the actin-activation of the Mg-ATPase of myosin, and this inhibition is pronounced in the presence of tropomyosin. In order to study the interactions of caldesmon to other muscle proteins, cysteine residues of caldesmon were labeled with fluorescent reagent, N-(1-pyrene) maleimide, as described (Horiuchi and Chacko, Biochemistry, 1988, Nov. issue).

Smooth muscle tropomyosin and heavy meromyosin (HMM) induced changes in the fluorescence spectra of pyrene-caldesmon indicating the conformational changes associated with the interaction between caldesmon and these proteins. The binding constants of caldesmon were $5x10^6$ M^{-1} for tropomyosin, 3.4 x 10^7 M^{-1} for phosphorylated HMM, 4.8 x 10^7 M^{-1} for unphosphorylated HMM and $7x10^5$ M^{-1} for skeletal S1 in the absence of salt. Mg-ATP had no effect on the affinity of caldesmon to these proteins. Affinities of caldesmon to these proteins decreased on increasing the ionic strength. At ionic strengths close to physiological conditions, the affinity for tropomyosin was decreased 20-fold, whereas the affinity for both phosphorylated and unphosphorylated HMM showed a 40-fold decrease. In the presence of actin, there was a 5-fold increase in the affinity of caldesmon to tropomyosin. (Supported by NIH Grants HL 22264 and DK 39740).

W-Pos35 THE 37K CYANOGEN BROMIDE FRAGMENT OF CHICKEN GIZZARD CALDESMON MAY BE DIFFERENT FROM THE SIMILAR-SIZED CHYMOTRYPTIC FRAGMENT C.-L. Albert Wang, Dept. of Muscle Research, Boston Biomedical Res. Inst., Boston, MA 02114

Limited treatment of chicken gizzard caldesmon (CaD) with either cyanogen bromide or chymotrypsin results in a fragment of about 40K in the apparent molecular weight which is able to interact with calmodulin (CaM). In an attempt to determine whether the 37K cynaogen bromide fragment (CB40) is identifiable with its chymotryptic counterpart (CT40), we have purified both fragments and treated them with chymotrypsin. After 20 min of digestion CB40 yielded 2 major peptides that migrated upon gel electrophoresis in the presence of $NaDodSO_4$ with apparent molecular weights of 30K and 24K, respectively. Under the same experimental conditions CT40 yielded 3 major fragments of 30K, 24K and 18K as described by Szpacenko & Dabrowska (1986). When the chymotryptic subfragments of CB40 were subjected to a CaM-affinity column, none of the peptides were found to bind to the column, whereas in the case of the chymotryptic digest of CT40 both the 24K and 18K subfragments were retained in the CaM-column. Thus the two similar-sized peptides (24K) derived from the two fragments behave differently toward CaM-binding. It is possible that after further chymotryptic cleavage the peptide derived from CB40 has a much weakened affinity for CaM. Alternatively, the two peptides of fortuitously similar molecular sizes may be derived from different parts of the parent molecule; this would in turn suggest that CB40 and CT40 represent 2 different regions of CaD. More recently, we have obtained information on the amino acid composition of both CB40 and CT40; the former has a Lys:Arg ratio of 0.65, while the latter has a much greater value of 5.2, suggesting that they are indeed quite different. Since both fragments are able to interact with CaM in the presence of Ca^{2+}, these results are consistent with our recent observation that there are more than one CaM-binding domains in the CaD molecule (Supported by grants from NIH and AHA).

W-Pos36 IMMUNOLOGICAL STUDIES OF MYOSIN LIGHT CHAIN KINASE BY USING MONOCLONAL ANTIBODIES. Hiroshi Tokumitsu, Tomohiko Ishikawa, Masatoshi Hagiwara, Koji Onoda and Hiroyoshi Hidaka. Department of Pharmacology, Nagoya University School of Medicine, Showa-ku, Nagoya 466, Japan.

Myosin light chain kinase (MLCK) is a Ca^{2+}-calmodulin dependent enzyme that phosphorylate the P-(phosphorylatable) light chain of myosin. This phosphorylation of myosin appears to be important for initiation of smooth muscle contraction. We have produced monoclonal antibodies against chicken gizzard MLCK for using immunological, structural and functional studies of this enzyme. Immunoblot analysis revealed that twelve antibodies (MM-1 to MM-12) cross-reacted with the enzyme (130 kDa) from chicken intestinal and vascular smooth muscles, whereas five (MM-1,3,4,9 and 12) or three (MM-1,3 and 4) of twelve antibodies did not cross-react with chicken cardiac muscle or with blood platelet MLCK (130 kDa), respectively. None of these antibodies showed cross-reactivity against skeletal muscle MLCK. As for mammalian species, MM-10 and 11 cross-reacted with MLCK of vascular smooth muscle (140 kDa) and MM-11 cross-reacted with enzyme (140 kDa) from cardiac muscle of rat and rabbit. These data suggest that the existence of at least four subspecies of MLCK in chicken tissues and the heterogeneity of tissue- and species-specific isozyme forms. One monoclonal antibody (MM-13) cross-reacted with 150 kDa peptide of bovine aortic actomyosin preparation and inhibited actomyosin superprecipitation dose-dependently in accordance with the suppression of 20 kDa myosin light chain phosphorylation by endogenous kinase. Furthermore, MM-13 also inhibited both kinase activity of purified chicken gizzard and bovine aortic MLCK (150 kDa) *in vitro*. These antibodies are expected to be useful tools for detecting native MLCK and assessing its function in relation to actomyosin in smooth muscle.

W-Pos37 LOCATION OF THE INHIBITORY DOMAIN OF SMOOTH MUSCLE MYOSIN LIGHT CHAIN KINASE. M. Ikebe, S. Maruta and S. Reardon, Department of Physiology and Biophysics, Case Western Reserve University, Cleveland, OH 44106.

Previously it has been shown that the trypsin proteolysis of smooth muscle myosin light chain kinase (MLCK), in the absence of calmodulin, produces the inactive fragment of MLCK which is converted to the calmodulin independent active fragment with further proteolysis (Ikebe et al., J. Biol. Chem. 262, 13828 (1987)). The effects of calmodulin binding on the proteolysis of MLCK were studied. In the presence of calmodulin, the production of the inactive fragment (64 kDa) was inhibited and the Ca^{2+}-calmodulin dependent fragment (66 kDa) was produced. The Ca^{2+}-calmodulin dependent fragment was further proteolyzed in the absence of calmodulin to produce the inactive fragment. With prolonged digestion, the calmodulin independent active fragment (61 kDa) was produced in the presence of calmodulin, however, the production of the calmodulin independent fragment was 6 times faster than in the absence of calmodulin. To determine the cleavage sites to produce these fragments, the C-terminal and N-terminal amino acid sequences of these fragments were determined. The N-terminal sequence of these fragments were not found in the reported partial sequence of MLCK. The sequence of the 66 kDa fragment was KKAPKTPPKAATPPGITQF. The c-terminus of the 5th lysine and 9th lysine were cleaved for the production of the 64 kDa and the 61 kDa fragments, respectively. The sequences of the peptides from C-terminus were investigated using carboxy peptidase A, B and Y digestion. As a result, the C-terminus end of the fragments were determined as lysine 473 for the 56 kDa active fragment, lysine 490 and arginine 494 for the 59 kDa inactive fragment and arginine 522 for the calmodulin dependent active fragment. The results indicate that the inhibitory region and calmodulin binding region of MLCK are 473-490 and 495-522, respectively. (Supported by NIH, AHA and Syntex).

W-Pos38 ALTERATION OF THE ACTIVITY OF GIZZARD MYOSIN LIGHT CHAIN KINASE BY A MONOCLONAL ANTIBODY WHICH RECOGNIZES CALMODULIN BINDING REGION. Y. Araki, J. Nestor+, and M. Ikebe. Department of Physiology and Biophysics, Case Western Reserve University School of Medicine, Cleveland, OH 44106. +Syntex corporation, Palo Alto, CA 94303.

The functional domain of smooth muscle myosin light chain kinase (MLCK) was studied using monoclonal antibodies. 22 antibody producing clones were identified by high affinity to MLCK in the screening assay (ELISA and immunoblot). Among them a monoclonal antibody designated LKH18 was found to inhibit MLCK activity in the presence of calmodulin. The activity was reduced 10-15 fold and the inhibition was not reversed by the addition of excess calmodulin. This suggests that the antibody binding to MLCK is not competitive to the binding of calmodulin to MLCK. This was confirmed by gel filtration at which MLCK, calmodulin and the antibody were found to have comigrated. On the other hand, LKH18 induced the MLCK activity in the absence of calmodulin although the activity is not quite as active as in the presence of calmodulin. The antibody binding site was studied using the proteolytic fragments of MLCK and synthetic peptide analogs. Immunoblot analysis revealed that LKH18 reacted on the 66 kDa calmodulin dependent active fragment but neither on the 64 kDa inactive fragment nor on the 61 kDa calmodulin independent active fragment. Furthermore LKH18 reacted on the peptide 493-512 but neither on the peptide 483-498 nor on the peptide 493-504. Therefore, it is reasonable to conclude that the LKH18 binding site is the amino acid sequence of 505-512. These results suggest that LKH18 binds to MLCK irrespective to the calmodulin binding and induces the change in MLCK conformation to partially active. LKH18 would provide a good probe to study the functional domain of MLCK. (Supported by NIH, AHA and Syntex).

W-Pos39 PROTEOLYSIS OF SMOOTH MUSCLE MYOSIN LIGHT CHAIN KINASE. M. Ito and D.J. Hartshorne, R. Pearson and B. E. Kemp, Muscle Biology Group, University of Arizona, Tucson, AZ 85721 USA and St. Vincents Inst. Med. Res. Fitzroy, Vic 3065, Australia.

Studies with myosin light chain kinase (MLCK) have identified different regions including the calmodulin-binding site, the active site and the sites of phosphorylation. A partial cDNA was sequenced (Guerriero et al., Biochemistry 25, 8392 [1986]), and correlations between sequence and functions suggested. It was proposed that a pseudosubstrate sequence existed (Kemp et al., J. Biol. Chem. 262, 2542 [1987]) that was inhibitory in the apoenzyme. This is consistent with the finding that an inactive tryptic fragment of 64 kDa was converted into an active calmodulin-independent 61 kDa fragment (Ikebe et al., J. Biol. Chem. 262, 13828 [1987]). Our studies are focussed on further defining this region. Proteolysis by thermolysin generated as a limit peptide an inactive fragment of 58 kDa. Further digestion with trypsin or endoproteinase lys-C (endo Lys-C) produced an active independent fragment (54 kDa). Digestion of native MLCK by endo lys-C also generated the inactive and active fragments. These fragments were purified and N-terminal sequences determined. Cleavage at the N-terminal end of MLCK to produce all of the inactive and active fragments occurred within a span of 13 amino acids in a proline-rich region. The pseudosubstrate site therefore occurs towards the C-terminal end of the molecule. Identification of some C-terminal residues have helped define this region. The inactive fragments produced by trypsin, thermolysis and endo lys-C end at Arg 505, Ala 503 and Lys 499. This defines a C-terminal limit to the inhibitory region. Cleavage to produce the independent-fragment occurs at Lys 445 or Arg 459 (trypsin) Lys 445 or Lys 457 (endo Lys-C). Supported by NIH grants HL 23015 and HL 20984.

W-Pos40 KAEMPFEROL SPECIFICALLY INHIBITS MYOSIN LIGHT CHAIN KINASE. John C. Rogers and David L. Williams, Jr., Biological Chemistry, Merck Sharp and Dohme Research Laboratories, West Point, PA 19486. Kaempferol, 3,5,7-trihydroxy-2-(4-hydroxyphenyl)-4H-1-benzopyran-4-one, was found to inhibit bovine aorta myosin light chain kinase with a Ki of 300-500 nM. It was found to be competitive with ATP and non-competitive with isolated myosin light chains. This inhibitor is relatively specific for myosin light chain kinase as compared with cAMP dependent protein kinase and protein kinase C (IC50 = 15 uM for both enzymes). It appears not to interact strongly with calmodulin binding proteins such as Ca^2-calmodulin dependent phosphodiesterase (IC50 = 45 uM), and had little effect on actin-activated myosin subfragment-1 ATPase activity (IC50$>$ 100 uM). Due to its in vitro specificity, this compound may be useful in physiological studies of the function of myosin light chain kinase in cells and animals.

W-Pos41 ISOLATION AND CHARACTERIZATION OF A NOVEL Ca^{2+}-BINDING PROTEIN (11 KDa) FROM SMOOTH MUSCLE. R.S. Mani and C.M. Kay, MRC Group in Protein Structure and Function, Department of Biochemistry, University of Alberta, Edmonton, Alberta.

A low molecular weight Ca^{2+} binding protein has been isolated from chicken gizzard using phenyl sepharose affinity chromatography in a homogeneous form. Molecular weight studies by both sedimentation equilibrium in 6 M Gdn-HCl and 15 percent SDS polyacrylamide gel electrophoresis indicated the subunit molecular weight to be around 11000. A molecular weight of 21000 was obtained in native solvents in the ultracentrifuge suggesting that the protein exists as a dimer in benign medium. The amino acid composition of this protein is very different from other low molecular weight Ca^{2+} binding proteins (the monomer of S-100, the intestinal Vit. D-dependent protein, parvalbumin or oncomodulin). The ratio of Phe to Tyr is one and for this reason, its U.V. absorption spectrum is not characterized by the fine structure that one usually observes in the 250 to 270 nm region with Ca^{2+} binding proteins. 11 K protein undergoes a conformational change upon binding Ca^{2+}, as revealed by UV difference spectroscopy and near UV CD measurements. In the presence of Ca^{2+}, the tyrosine residues are perturbed and move to a more nonpolar region. Upon excitation of the protein at 280 nm, the tyrosine fluorescence emission was centered at 306 nm. Ca^{2+} addition resulted in a nearly 20 percent decrease in intrinsic fluorescence intensity. Fluorescence titration with Ca^{2+} suggests that this protein binds calcium with high affinity ($K_d \sim 0.2$ μM). In non-SDS gels, the protein moves faster in the presence of EDTA, suggesting that Ca^{2+} binding affects its mobility similarly to other calcium binding proteins.

W-Pos42 OKADAIC ACID AND CALYCULIN-A: INHIBITORS OF PROTEIN PHOSPHATASE, H. Ishihara[1], D. J. Hartshorne[1], H. Karaki[2], H. Ozaki[2], M. Hori[2], S. Watabe[2], B. Martin[3] and D. Brautigan[3]. [1]Muscle Biology Group, Univ. of Arizona, Tucson, AZ 85721; [2]Dept. of Vet. Pharm. Univ. of Tokyo, Tokyo 113, Japan; [3]Div. Biol. and Med., Biochem. Sect. Brown Univ, Providence, RI 02912.

Okadaic acid (OA) and calyculin-A (Cl-A) are cytotoxic compounds isolated from marine sponges. Several groups have shown that OA induces contraction of smooth muscle fibers in the absence of Ca^{2+} and part of this effect is due to inhibition of phosphatase activity. Cl-A also induces contraction in the absence of Ca^{2+} and promotes phosphorylation of myosin. The objectives of this study are to investigate inhibition of protein phosphatases by OA and Cl-A and to identify the phosphatase activity dominant in smooth muscle fibers. Acid phosphatase (potato and bovine semen) alkaline phosphatase (bovine liver, intestinal mucosa, kidney and E. coli) and protein phosphotyrosine phosphatase were not inhibited by OA (10 M) or Cl-A (1 M). However, the activity of the catalytic subunits of Type 1 and Type 2A phosphatase were inhibited. Phosphorylated light chains, phosphorylated myosin and phosphorylase a were used as substrates. With Type 2A the IC50's for OA and Cl-A were similar, approximately 1 nM. However, for Type I activity the IC50's with Cl-A were 1-2 nM, but the IC50's for OA were 0.6 to 5 x 10^{-7} M. The distinctive pattern of inhibition was used to identify the phosphatase dominant in myosin B and it was found that the IC50 for OA was about 0.2 x 10^{-7} M and about 0.3 nM for Cl-A. The activation of contractile activity of skinned smooth muscle fibers in the absence of Ca^{2+} was more sensitive to Cl-A than OA. These results suggest that the dominant phosphatase activity (toward myosin) in myosin B and in fibers is the Type 1 activity. Supported by NIH grants HL 23615 and HL 20984 (to DJH) and DK 31374 (to DB).

W-Pos43 INTERACTION OF A FLUORESCENT MASTOPARAN WITH CALMODULIN.

John S. Mills, Lynn Reece, and J. David Johnson. Dept. of Physiological Chemistry, The Ohio State University Medical School, Columbus, Ohio.

Mastoparan x was labeled with 1.0 stoichiometry with acrylodan to produce ADAN-MSP. ADAN-MSP and mastoparan x were equally effective as inhibitors of calmodulin dependent phosphodiesterase (I50 = 3 nM). ADAN-MSP underwent a 9-fold increase in fluorescence with its calcium dependent association with calmodulin. The dissociation constant of ADAN-MSP for calmodulin was determined to be 3.7 nM in the presence of 1 mM Ca^{++}. Ca^{++} titrations of CaM in the presence of ADAN-MSP showed half-maximal binding occurred at pCa = 6.2 in the absence of Mg^{++} or at pCa = 5.5 in the presence of 3 mM Mg^{++}. Melittin, calmidazolium, mastoparan and mastoparan x dissociated the ADAN-MSP-CaM complex with calculated dissociation constants of 3 nM, 5 nM, 8 nM, and 13 nM, respectively. Displacement of ADAN-MSP from calmodulin by melittin, calmidazolium, or mastoparan x in the presence of 1 mM Ca^{++} at 4^{o} C occurred with a rate of 1.4 s-1. Dissociation of ADAN-MSP from calmodulin by EGTA exhibited biexponential kinetics with dissociation rates of 3.1 s-1 and 0.28 s-1, with relative amplitudes of 57% and 43%, respectively. This fluorescent calmodulin antagonist peptide has proven very useful for characterizing calmodulin's interaction with this model peptide.

W-Pos44 CONTROL OF PROTEIN PHOSPHORYLATION IN JUNCTIONAL SARCOPLASMIC RETICULUM. A. Chu, C. Sumbilla, G. Inesi, Dept. Biol. Chem., Univ. of Maryland Medical School, Baltimore, MD. 21201.

Using purified rabbit skeletal muscle subfractions of longitudinal tubules (LSR) and junctional terminal cisternae (JTC), we studied cAMP- (cAK) and calmodulin- (CaMK) dependent protein kinase (PK) phosphorylation of various membrane proteins and related cleavage by protein phosphatases (FFT). Protein phosphorylation (with Mg^{2+}) by added cAK (in EGTA) was slightly less than that in the presence of added Ca^{2+} (without any added PK). In autoradiograms of SDS-PAGE of JTC, a ~60 kDa and >330 kDa protein were phosphorylated by cAK regardless of whether Ca^{2+} was present. On the contrary, addition of CaM (without added PK) produced marked phosphorylation of many JTC proteins, and to a lesser extent, of LSR proteins. JTC proteins around ~170 kDa, Ca^{2+} pump region (~98-120 kDa), ~60 kDa and ~22 kDa were most heavily phosphorylated. The ~400 (>350) kDa (ryanodine receptor) protein was also phosphorylated. Phosphorylation was promoted by micromolar Ca^{2+} and depressed by millimolar Ca^{2+}. Cleavage of phosphorylated proteins was very slow in the absence of added FFT, but was accelerated by addition of FFT 1A, 2A (catalytic subunit) (without Ca^{2+}) and calcineurin (with Ca^{2+}). Our experiments indicate that the purified JTC subfraction contains significant amounts of a membrane-bound CaMK system, which is readily autophosphorylated and/or by other PK's. Micromolar Ca^{2+} and CaM are additive in regulating phosphorylation by this system. Direct binding of CaM to a ~60 kDa protein has been demonstrated [M.G.P. Vale, J. Biol. Chem. 263, 12872-77, 1988; B.S. Tuana & D.H. MacLennan, FEBS Lett. 235, 219-23, 1988]. Control of dephosphorylation, however, must rely on cytoplasmic FFT. [Supported by NIH and MDA grants (to G.I.) and AHA fellowship-Calif. Affl. (to A.C.)]

W-Pos45 CALCIUM UPTAKE, CAFFEINE-INDUCED CALCIUM RELEASE, AND RYANODINE BINDING OF ISOLATED UTERINE MUSCLE SR. L. Toro[1], C. Dettbarn[2], P. Palade[2] and E. Stefani[1], [1]Dept. of Physiology and Molecular Biophysics, Baylor College of Medicine, Houston, TX 77030 and [2]Dept. of Physiology and Biophysics, University of Texas Medical Branch, Galveston, TX 77550.

Uteri from non-pregnant swine were cleaned of endometrium. The myometrium was homogenized in the presence of protease inhibitors. Following removal of debris at 700 x g for 30 min, a second centrifugation for 40 min at 14,000 x g yielded supernatant (S) and pellet (P) fractions which were pelleted or washed and pelleted, respectively, prior to centrifugation on a discontinuous 20/25/30/35/40% sucrose gradient overnight at 67,500 x g. All P fractions displayed low levels of SR marker activity: ryanodine binding (≤0.02 pmol/mg) and low rates of phosphate-supported Ca^{2+} uptake (<7 nmol Ca/mg·min). Ryanodine binding was maximal (1.5 pmol/mg) in the heaviest S fraction (35/40% interface) and substantial (0.44 pmol/mg) in the next lightest fraction. In the presence of 40 mM KCl, 62.5 mM K-phosphate, 1 mM MgATP, 10 mM phosphocreatine, 40 µg/ml CPK and 0.25 mM antipyrylazo III, 8 mM MOPS, pH 7.0, both these fractions demonstrated high rates of Ca^{2+} uptake (~300 nmol/mg·min; considerably higher than the vast majority of published values for smooth muscle microsomes (~10 nmol/mg·min)) and a ruthenium red-insensitive caffeine-induced Ca^{2+} release in the presence of 1 mM vanadate. Lighter S fractions displayed much lower rates of Ca uptake (~10 nmol/mg·min) and caffeine-induced Ca^{2+} release. The relative ruthenium red-insensitivity of the caffeine-induced Ca^{2+} release by uterine smooth muscle SR stands in marked contrast to that displayed by skeletal muscle SR. Authors thank Dr. S. Hamilton[1] for assistance with ryanodine binding determinations. Supported by AHA, Texas Affiliate and by NIH.

W-Pos46 HETEROGENOUS PROPERTIES OF TRIAD JUNCTION OF SKELETAL MUSCLE. Kyungsook C. Kim, Anthony H. Caswell, and Neil Brandt, Department of Pharmacology, University of Miami, School of Medicine, P.O.Box 016189, Miami, FL 33101.

It has been recognized that a number of protocols may cause breakage of the triad junction and separation of the constituent organelles. We describe a fraction of junctions which are peculiarly refractory to the known protocols for disruption. Triads which were enriched in junctional components were passed through a French press and dissociated organelles were separated on a continuous sucrose density gradient, which was assayed for the distribution of PN200-110 (PN), ouabain, iodocyanopindolol (CYP) and ryanodine. The distribution pattern of ryanodine showed a single peak at the isopycnic point of heavy TC. On the other hand external membrane markers, PN, ouabain and CYP, bound in two defined peaks: one at the isopycnic point of free transverse tubule (TT), and the other at that of light TC (LTC). Similar two peak patterns of PN and ouabain binding were observed when triadic junctions were broken by the Ca^{2+}-dependent protease, calpain, which selectively hydrolyzes the junctional foot protein. To investigate the nature of TT activity in LTC region, LTC was subjected to three different means of junctional breakage - French press, protease digestion using trypsin or calpain, and 0.6M Na gluconate treatment. Assays for PN and ouabain on sucrose gradients showed no shift of these activities into free TT region by the French press, calpain, and 0.6M Na gluconate which all are known to release TT from triads. Only trypsin treatment at high concentration (0.03mg/ml for 10 min at 37°C) caused a partial shift of ouabain into the density of free TT indicating that TT activities in LTC were due to incomplete breakage of junction and the remaining junction was unusually resistant to breakage. Maximum number of PN sites in LTC and TT was 40 pmol/mg and 66 pmol/mg respectively. Since TT in LTC region is likely to be a minor constituent, it suggests that PN receptors are enriched in the TT subfraction of LTC compared to the free TT. Supported by Lucille P. Markey Fellowship, NIH training grant HL07188, NIH grant AR-21601 and American Heart Association, Florida Affiliate.

W-Pos47 DOXORUBICIN OR CAFFEINE ACTIVATES CALCIUM RELEASE CHANNELS FROM CANINE CARDIAC SARCOPLASMIC RETICULUM. Do Han Kim and Barbara E. Ehrlich. Departments of Medicine and Physiology, University of Connecticut Health Center, Farmington, CT 06032

Mechanisms for activation of calcium (Ca^{2+}) permeable channels in canine cardiac sarcoplasmic reticulum (SR) by doxorubicin or caffeine were studied using SR vesicles and SR incorporated into planar lipid bilayers. With $^{45}Ca^{2+}$-flux measurements, SR released 25-40% of the loaded $^{45}Ca^{2+}$ after addition of doxorubicin ($C_{1/2}$ =5 uM) or caffeine ($C_{1/2}$=0.7 mM). Both Ca^{2+} releases were inhibited by known Ca^{2+} release inhibitors such as ruthenium red ($C_{1/2}$ =0.5 uM), ryanodine ($C_{1/2}$ =10 uM) or tetracaine ($C_{1/2}$ =0.7 mM). The extent of Ca^{2+} release by 50 uM doxorubicin (40% of that loaded) was not increased by addition of 2 mM caffeine. To determine whether these Ca^{2+} releases are channel-mediated, SR was incorporated into planar lipid bilayers (PE:PS =3:1; 53 mM Ca^{2} trans, 100 nM Ca^{2} cis). In the presence of 100 nM free Ca^{2} cis alone, channels were open <2% of the time (slope conductance measured at 0 mV = 75 pS). Subsequent addition of 5 uM doxorubicin or 0.5 mM caffeine increased the percent open time to 40%. Ruthenium red (0.5 uM) blocked the bilayer-incorporated Ca^{2+} channel activity when activated by either 5 uM doxorubicin or 0.5 mM caffeine. These results suggest that doxorubicin or caffeine-induced Ca^{2+} release in the cardiac SR is channel-mediated and that doxorubicin and caffeine share the same receptor.

Supported by NIH Grant HL-33026, Grant-in-Aid from AHA-Connecticut Affiliate. BEE is a PEW Scholar in the Biomedical Sciences.

W-Pos48 ULTRASTRUCTURE OF THE CALCIUM RELEASE CHANNEL (CRC) FROM HEART SARCOPLASMIC RETICULUM. Akitsugu Saito, Makoto Inui and Sidney Fleischer (Intr. by John Wikswo). Department of Molecular Biology, Vanderbilt University, Nashville, TN 37235.

The ryanodine receptor has been purified from cardiac sarcoplasmic reticulum (SR) and found to be equivalent to the feet structures involved in junctional association to form the dyad/triad junctions [M. Inui, A. Saito and S. Fleischer. J. Biol. Chem. 262, 15637 (1987)]. This receptor is an oligomer composed of a single high molecular weight polypeptide (M_r ~ 340 KD). The purified receptor has been incorporated into bilayers and found to have the characteristics of the CRC in SR [L. Hymel, M. Inui, H.G. Schindler and S. Fleischer. BBRC 152, 308 (1988)]. New ultrastructure of the purified CRC can now be discerned using negative staining with uranyl acetate (see photo). The feet structures have four-fold symmetry with dimensions of 260 x 260 x 150 Å. Extensive structural information of the SR CRC from heart can be observed which is similar to that previously reported for skeletal muscle. There is a dense central core enclosed by a frame having a pin wheel appearance. A central circular pore (~ 20 Å) can be observed in the square face. (Supported by NIH HL 32711.)

W-Pos49 ORGANIZATION OF TRIAD JUNCTIONAL STRUCTURE IN SKELETAL MUSCLE. A.H. Caswell, N.R. Brandt, Jane Talvenheimo, Shu-Ron Wen and Kyungsook C. Kim, Department of Pharmacology, University of Miami. School of Medicine, P.O. Box 016189, Miami, FL 33101.

Evidence from three different experimental approaches support the view that glyceraldehyde phosphate dehydrogenase (GAPDH) and aldolase bind specifically to the junctional foot protein (JFP) of the triad junction: 1) Detergent dissolved T-tubular proteins were affinity chromatographed on the JFP attached to Sepharose. The JFP specifically retained GAPDH and aldolase. Aldolase bound to JFP-Sepharose can be specifically eluted with inositol 1,4,5-trisphosphate (IP_3). 2) T-tubular proteins were electrophoresed, electroblotted onto nitrocellulose and overlayed with [^{125}I] JFP. The JFP bound to GAPDH and less strongly to aldolase. Blotted triad proteins were overlayed with [^{125}I] aldolase which bound to the JFP; this binding was inhibited by the IP_3 analog, 2,3 diphosphoglycerate. 3) The photoactivable heterobifunctional disulfide-bridged reagent (SASD) was iodinated and covalently attached to the JFP. The JFP-SASD complex was incubated with T-tubules and then illuminated. The JFP-SASD-T-tubule products were electrophoresed in the absence and presence of reducing agents. Mercaptans break the disulfide linkage of SASD, transferring the iodinated residue from the JFP to the photo linked moiety. GAPDH was identified as the major specifically labelled product. GAPDH liganded to a noncleavable heterobifunctional reagent (NHS-ASA) crosslinked to JFP in triads. Binding of GAPDH to T-tubules was investigated by affinity chromatography and protein overlay. Both techniques indicate binding of GAPDH to proteins of M_r 100,000 and 72,000. In addition overlay of [^{125}I] GAPDH on partially purified dihydropyridine (DHP) receptor shows binding to the α_1 subunit but not the α_2 subunit. JFP did not bind to this electroblotted receptor unless the DHP receptor blots were pre-incubated with GAPD. Under these conditions the α_1 subunit bound [^{125}I] JFP. We conclude that GAPDH and aldolase bind directly to junctional foot protein at the junction. The DHP receptor binds indirectly to the JFP through GAPDH to form the junctional complex. Supported by NIH grants AR21601, HL36029 HL07188, and by a Lucille P. Markey Fellowship.

W-Pos50 EFFECT OF Mg^{2+} AND ATP ON [^{3}H]-RYANODINE BINDING AND $^{45}Ca^{2+}$ FLUX OF JUNCTIONAL SARCOPLASMIC RETICULUM. Alice Chu, Mary Jane Hawkes and Susan L. Hamilton. Department of Medicine, Cardiovascular Sciences Section and Department of Physiology and Molecular Biophysics, Baylor College of Medicine, Houston, TX 77030. Intr. by Julius C. Allen.

We have correlated the binding of [^{3}H]-ryanodine with the effect of ryanodine on $^{45}Ca^{2+}$ flux of rabbit fast-twitch skeletal muscle junctional sarcoplasmic reticulum. We find that 1 mM ATP and AMP-PNP enhance the rate of association of ryanodine with its binding site. Conversely, Mg^{2+} (1 mM) slows the rate of association. Kinetic analysis of [^{3}H]-ryanodine binding under different buffer conditions predicts dissociation constants which are in agreement with equilibrium binding studies. Under these binding conditions, the net $^{45}Ca^{2+}$ uptake (both by passive and active loading) is relatively constant. Ryanodine at low concentrations (1 μM) inhibits uptake and at high concentrations (100 μM) increases uptake. These observations are consistent with the previously described activation and inhibition of the calcium release channel by low and high concentrations of ryanodine (G. Meissner, J. Biol. Chem. 261, 6300-6306, 1986). Our observations show that ATP increases the rate of both activation and inhibition of the Ca^{2+} release channel by ryanodine, while Mg^{2+} (1 and 10 mM) slows the rate at which these actions occur. The data suggests that ATP favors a conformation of the Ca^{2+} release channel in which the ryanodine binding site is more accessible than it is in the absence of ATP or in the presence of Mg^{2+}. This would predict that the sensitivity to ryanodine of the Ca^{2+} channel would be modulated by ATP and Mg^{2+}.
[Supported by grants from AHA-Texas Affiliate to A.C. and MDA to S.L.H.]

W-Pos51 HEPARIN INHIBITS INOSITOL 1,4,5-TRISPHOSPHATE INDUCED CALCIUM RELEASE FROM AORTIC SARCOPLASMIC RETICULUM IN VESICLES AND PLANAR BILAYERS. James Watras* and Barbara E. Ehrlich#. Departments of Medicine*# and Physiology#, University of Connecticut, Farmington, CT

We tested compounds that have been suggested to inhibit the calcium release channel found in the sarcoplasmic reticulum (SR) of smooth muscle. SR vesicles, isolated from canine aortic smooth muscle, accumulate calcium in the presence of ATP, and release calcium upon addition of inositol 1,4,5-trisphosphate (IP_3). Heparin (50 ug/ml) completely blocked the IP_3-induced calcium release, but had no effect on calcium uptake. Half-maximal inhibition of IP_3-induced calcium release occurred at 4 ug/ml heparin. Lineweaver-Burk analysis showed that heparin acts as a competitive inhibitor. De-N-sulfated heparin (50 ug/ml) had no effect on IP_3-induced calcium release, suggesting that the N-sulfate is critical for inhibition by heparin. When aortic SR vesicles were incorporated into planar lipid bilayers, IP_3-gated channel openings were observed. Heparin (10 ug/ml) on the cis side of the bilayer reduced the probability of finding the channel open by 80%, but did not alter single channel conductance (10 pS). This contrasts with results using skeletal SR where heparin (500 ug/ml) does not inhibit calcium channels in vesicles and in planar lipid bilayers (125 pS). Thus, heparin acts a competitive inhibitor of IP_3-induced calcium release, decreasing the open probability of the IP_3-gated channel in smooth muscle. The results provide additional evidence that the calcium release channels of skeletal and smooth muscles are strikingly different.

Supported by NIH grant HL-33026. BEE is a PEW Scholar in the Biomedical Sciences.

W-Pos52 EARLY OVEREXPRESSION OF LOW AFFINITY [3H]RYANODINE RECEPTOR SITES IN JUNCTIONAL SARCOPLASMIC RETICULUM FROM DYSTROPHIC CHICKEN PECTORALIS MAJOR

Isaac N. Pessah and Mary J. Schiedt. Dept. of Veterinary Pharmacology and Toxicology, University of California, Davis, 95616.

Junctional sarcoplasmic reticulum (JSR) vesicles enriched in [^{3}H]ryanodine (RY) receptor have been isolated from pectoralis major (PM) of normal (line 412) and dystrophic (line 413) chickens by the method of Inui and coworkers (JBC 262, 1740, 1987). Yields of JSR from birds 2 days ex ovo are similar with both lines 412 and 413 (80 vs. 96 mg JSR protein/100g PM). JSR from 2 day line 412 but not line 413 exhibit nonlinear Scatchard plots which can be resolved into high (K_{D1}= 18nM) and low (K_{D2}=530nM) affinity RY binding sites having similar capacities (B_{m1}=1.7 & B_{m2}=2.6 pmol/mg protein, respectively), while 2 day PM from line 413 has a single class of high affinity RY binding sites (K_D=31nM; B_m=2.1pmol/mg). By 2 weeks ex ovo, a dramatic drop in yield of JSR from line 412 is observed (to 24mg JSR protein/100g PM) and is associated with disappearance of low affinity RY binding sites (K_D=17nM; B_m=3.5pmol/mg). In contrast JSR recovered from paired line 413 PM increases significantly (to 167mg JSR protein/100g PM) & parallels the appearance of low affinity, high capacity binding sites (K_{D1}=17nM, B_{m1}=1.5pmol/mg; K_{D2}=725nM, B_{m2}=15.4pmol/mg). These pronounced differences are accentuated in birds 5 weeks ex ovo when line 412 PM yields 7-fold lower recovery of JSR protein than line 413 PM (28 vs 190mg/100g), and greater discrepancies in RY receptor composition (line 412: K_D=14nM, B_m=0.24pmol/mg; line 413: K_{D1}=32nM, B_{m1}=2.1pmol/mg; K_{D2}= 7,000nM, B_{m2}=21pmol/mg). Overexpression of low affinity RY binding sites in dystrophic PM corresponds to increased intensity of the high molecular weight RY receptor doublet (MW 340 and 320 kDa) on SDS gels stained with Coomassie blue. Sponsored in part by a UC Davis New Faculty Research Award.

W-Pos53 BETA ADRENERGIC RECEPTOR AND PHOSPHOINOSITIDE TURNOVER IN ISOLATED PERFUSED GUINEA PIG HEARTS. I. Edes*, E.G. Kranias*, and R.J. Solaro#, Department of Pharmacology and Cell Biophysics*, University of Cincinnati, Cincinnati, Ohio 45267 and Department of Physiology and Biophysics#, University of Illinois, Chicago, Illinois 60680.

β-adrenergic agonists increase the inotropy and relaxation of the heart by involving cAMP-dependent protein phosphorylation. Guinea pig hearts were perfused with Krebs-Henseleit buffer containing [^{32}P]Pi and freeze-clamped at different times during the positive inotropic response to isoproterenol. Myofibrillar proteins, sarcoplasmic reticulum and phospholipids were isolated from the same hearts. Stimulation of the hearts with isoproterenol was associated with time dependent increases in cAMP levels and in the degree of ^{32}P-incorporation into phospholamban, troponin-I and phosphatidylinositols (PI, PIP and PIP_2). However, ^{32}P-labeling of inositol trisphosphates in the same hearts decreased with time upon isoproterenol stimulation. Examination of the phosphoinositide specific phospholipase C (PI-PLC) activity in these hearts revealed that β-adrenergic stimulation was associated with a decrease in the membrane-bound enzymatic activity at pCa 6.5 and 5.0, using [^{3}H]-PIP and [^{3}H]-PIP_2 as substrates. These findings suggest that the changes in phosphatidylinositol turnover in perfused, beating hearts are associated with β-receptor stimulation and may be mediated, at least in part, by inhibition of the PI-PLC enzymatic activity. (Supported by NIH Grants HL26057, HL22231 and HL22619.)

W-Pos54 IS THE SKELETAL MUSCLE TRANSVERSE TUBULAR (TT) MEMBRANE Mg^{2+}-ATPase A DIACYLGLYCEROL RECEPTOR? J-J. Kang, C. Jachec-Schmidt, A. Priest, R. A. Sabbadini, and A. S. Dahms, Depts. of Chemistry and Biology & Molecular Biology Institute, San Diego State University, San Diego, California, 92182

The chicken TT membrane contains a very active vanadate-insensitive, lectin-stimulated Mg^{2+}-ATPase that exhibits several kinetic and thermodynamic anomalies which are abolished by Con-A through a putative nucleotide regulatory site; severe inhibition by sub-cmc levels of Triton and relieval thereof by Con-A are consistent with Triton serving as a nucleotide-mimetic agent at this site (Moulton et al., JBC 261, 12244 [1986]). Evaluation of the inhibitory effects of possible regulatory agents which possess combined hydrophobic and nucleotide properties show that fatty acyl CoA's can serve as potent activators of the Mg^{2+}-ATPase at sub-cmc levels ($K_{0.5}$ palmitoyl-CoA and oleoyl-CoA, 1.0 and 1.1 uM, respectively). Free fatty acids (FFA's), in turn, are potent inhibitors of the Mg^{2+}-ATPase with $K_{0.5}$'s for palmitic, oleic, and arachodonic acids of 5.0, 2.0, and 1.5 uM, respectively, with $K_{0.5}$'s raised at least 4-15 fold higher with Con-A. It is speculated that the Mg^{2+}-ATPase may be regulated intracellularly by the fatty acyl CoA/FFA ratio. The high affinity of regulatory site(s) for amphiphiles has led us to explore the effects of other significant regulatory lipids. The chicken TT-Mg^{2+}-ATPase is inhibited by octanoyl acetyl glycerol (DAG) and phorbol 12-myristate 13-acetate (TPA) ($K_{0.5}$'s, 1.7 uM and 0.5 uM) which is also protected by Con-A ($K_{0.5}$'s >15 uM). The 4-alpha phorbol 12,13-didecanoate is as inhibitory as TPA, thus distinguishing the Mg^{2+}-ATPase site from the TPA- and DAG-responsive activation site on protein kinase C. Whether the inhibition of the Mg^{2+}-ATPase by DAG is indirectly achieved through events mediated by possible TT protein kinase C has yet to be determined. The possible role of DAG in E-C coupling and relaxation will be discussed. (Supported in part by NSF DCB 8613881, NSF INT 8515846, and The California Metabolic Research Foundation).

W-Pos55 MAMMALIAN SARCOPLASMIC RETICULUM K CHANNELS RECORDED IN SKINNED FIBERS. P.G. Stein[1], T.E. Nelson[2] and P.T. Palade[1]. [1]Department of Physiology and Biophysics, University of Texas Medical Branch, Galveston, TX 77550 and [2]Department of Anesthesiolgy, University of Texas Health Science Center, Houston TX 77225. (Introduced by R. David Baker).

Swine skeletal muscle fibers (gracilis) skinned in a K_2SO_4 relaxing solution to which Ca^{2+} (1 mM) is added produce sarcoballs as described previously. Recording with 100 mM K_{bath} vs 52.5 mM $Ca_{pipette}$, we observe the sarcoplasmic reticulum K^+ channel recorded by Miller and others previously in lipid bilayers. In sarcoballs, the predominant conductance state of these channels is about 100 pS and they exhibit a less frequent subconductance state of about 60 pS. They are highly impermeable to Ca^{2+} (P_K / P_{Ca} > 1000) and are only weakly sensitive to potential. 100 uM decamethonium applied to the presumptive lumenal surface causes an apparent 50% reduction in unitary conductance. Increased open channel noise suggests that this apparent reduction is due to a rapid flicker block of the channel. Analysis of current fluctuations (filtered at 1 kHz) indicates that the open time is well fit by a single exponential (τ = 36 msec) while the closed times are described by at least 3 exponentials with time constants of 3 msec, 23 msec and one less easily resolved on the order of seconds). These kinetic results differ markedly from the first kinetic descriptions of this channel in bilayers. The fundamental similarities of these channels to those reported previously suggests that they are not vastly altered by the bilayer paradigm. At the same time, however, it is clear that the patch-clamp allows a more detailed view of high frequency events than is attainable in the bilayer. This work done during the tenure of a Grant-in-Aid from AHA-Wyeth-Ayerst Laboratories (AHA 881114) and funded in part by 1PO1 HL37044.

W-Pos56 SARCOPLASMIC RETICULUM CALCIUM CAN BE REPLETED BY ELECTRICAL STIMULATION FOLLOWING DEPLETION BY RYANODINE. W.H. DuBell, H.A. Spurgeon, E.G. Lakatta and B. Lewartowski. Laboratory of Cardiovascular Science, Gerontology Research Center, Baltimore, MD.

Recent studies have shown that ryanodine (R) can deplete the sarcoplasmic reticulum (SR) of Ca^{2+} during rest. We examined whether the SR could be reloaded with Ca^{2+} following electrical stimulation in single rat ventricular myocytes loaded with Indo-1 AM. Figure shows the Ca^{2+} transients elicited (arrows) by picospritzes of caffeine (15mM in pipette) in the rested cell before (A) and 40 min. after .05 μM R (B), indicating that no Ca^{2+} is released after R. Following a period of electrical stimulation in the presence of R (C), diastolic Ca^{2+} increases and a sizable caffeine-induced release can be elicited (D, showing the last stimulated and the caffeine-induced (arrow) Ca^{2+} transients). These results suggest that while SR Ca^{2+} retention is compromised by R, the SR pump is operative and the SR can be reloaded with Ca^{2+}.

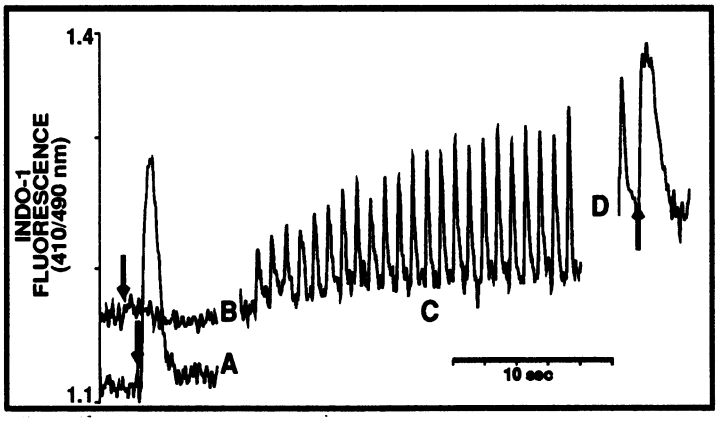

W-Pos57 **INFLUENCE OF THE 53kDa GLYCOPROTEIN ON COOPERATIVE BEHAVIOR OF THE SARCOPLASMIC RETICULUM CA^{2+}ATPase.** Kimberly L. Boyd, Qing Xu, Christopher P. Weis, and Howard Kutchai. Department of Physiology and Program in Biophysics, University of Virginia, Charlottesville, VA. 22908.

Previous results from this laboratory suggest that the 53kDa glycoprotein (GP-53) of rabbit skeletal muscle sarcoplasmic reticulum membrane (SR) may modulate coupling between Ca^{2+} transport and ATP hydrolysis by the Ca^{2+}-ATPase. (Leonards and Kutchai, 1985, Biochemistry 24, 4876; Kutchai and Campbell, submitted) Consistent with this hypothesis, we have shown that GP-53 influences the cooperative behavior of the Ca^{2+}-ATPase. The ATPase demonstrates a negative cooperative dependence (Hill coefficient n<1) of Ca^{2+}-stimulated ATPase activity on [Mg-ATP] and a positive cooperative dependence (n>1) of activity on $[Ca^{2+}]_{free}$. We have determined the degree of cooperativity for native SR vesicles, SR preincubated with antiserum against GP-53 or preimmune serum, and KCl-cholate extracted preparations. Our results show that SR incubated with preimmune serum or SR treated with low [KCl]-cholate (rich in GP-53) demonstrate a cooperative dependence of ATPase activity on both [ATP] and $[Ca^{2+}]$ at levels similar to that of native SR. Preincubation of SR with antiserum (which causes an uncoupling of Ca^{2+} transport from ATP hydrolysis) or high [KCl]-cholate extracted preparations (depleted of GP-53) yield a decrease in both [ATP] and $[Ca^{2+}]$-dependent cooperativity and alters K_m.

Hill Coeff.	Normal SR	SR plus preim. serum	SR plus antiserum	Lo [KCl]-cholate SR (rich in GP-53)	Hi [KCl]-cholate SR (Poor in GP-53)
$n_{[Ca++]}$	1.95	1.71	1.43	1.97	1.47
$n_{[ATP]}$	0.364	0.425	0.650	0.372	0.565

W-Pos58 REGULATION OF CARDIAC SARCOPLASMIC RETICULUM Ca^{2+}-ATPase BY PHOSPHOLAMBAN IN RECONSTITUTED VESICLES. H.W. Kim, N.A.E. Steenaart, G. Szymanska, and E.G. Kranias, Dept. of Pharmacology and Cell Biophysics, University of Cincinnati, Cincinnati, Ohio 45267-0575

The Ca^{2+}-ATPase in cardiac sarcoplasmic reticulum (SR) is under regulation by phospholamban (PLB), a polymeric proteolipid. Phosphorylation of PLB increases the affinity of the Ca^{2+}-ATPase for Ca^{2+}. To determine the molecular mechanism by which PLB regulates the Ca^{2+}-ATPase, we developed a reconstitution system, using a freeze-thaw sonication procedure. The Ca^{2+}-ATPase was purified by a method which yields an active enzyme preparation essentially free of PLB. Initially, various detergents and phospholipids were used to develop optimal conditions for reconstitution. We obtained the best rates of Ca^{2+} uptake in the presence of cholate and phosphatidylcholine (PC) when the ratio of cholate/Ca^{2+}-ATPase/PC was 2/1/80. The rate of Ca^{2+} uptake was 700 nmol/min/mg of reconstituted vesicles compared to 800 nmol/min/mg of SR vesicles. The EC_{50} values for Ca^{2+} were 0.05 μM for both Ca^{2+} uptake and Ca^{2+}-ATPase activity in the reconstituted vesicles compared to 0.8-0.9 μM Ca^{2+} in native SR vesicles. To determine the effect of PLB on the Ca^{2+}-ATPase activity in the reconstituted vesicles, purified PLB was added to the cholate/Ca^{2+}-ATPase mixture prior to combining it with liposomes. Inclusion of PLB was associated with a significant inhibition of the initial rates of Ca^{2+} uptake, assayed over a wide range of Ca^{2+} concentrations. Furthermore, the degree of Ca^{2+}-uptake inhibition appeared to increase when the PLB/Ca^{2+}-ATPase ratio increased. These preliminary results suggest that PLB is an inhibitor of the Ca^{2+} pump in cardiac SR. (Supported by NIH grants HL26057 and HL22619.)

W-Pos59 THE THYROID HORMONE RECEPTOR OF MUSCLE SARCOPLASMIC RETICULUM. L. Fliegel, K. Burns, K. Wlasichuk and M. Michalak. (Intr. by S. Grinstein). Dept. of Pediatrics and Biochemistry, University of Alberta, Edmonton, Alberta, Canada.

Specific, saturable high-affinity binding sites for 3,3',5-triiodo-L-thyronine (T3) have been identified in a variety of animal and human tissues, including muscle cells. These sites have been detected on the plasma membrane, in mitochondria, in the cytosol and on the nuclear envelope. The diverse biological effects of T3 may be initiated not only by nuclear but also by other cellular sites. To study the presence of T3 binding protein in cardiac and skeletal muscle sarcoplasmic reticulum (SR) membranes, we have examined T3 binding to isolated SR vesicles. SR vesicles from rabbit skeletal muscle and sheep cardiac muscle bind thyroid hormone, but the binding requires the partial solubilization of the membrane with Triton X-100. No binding is observed to intact SR membranes. This suggests that the T3 receptor exists within the lumen of this membrane system similar to its occurrence in endoplasmic reticulum. To examine the T3 binding proteins of muscle SR we have isolated two cDNA clones encoding for the muscle form of T3 binding protein. Clone 1 originated from a rabbit slow-twitch muscle lambda gt11 expression library and was 1.7 kb in size. It was used to isolate clone 2 (2.4 kb) from a rabbit neonatal skeletal muscle Okayama-Berg cDNA library. Northern blots analysis of skeletal muscle shows that mRNA encoding for muscle T3 binding protein is approximately 2.8 kb in size. Partial sequence analysis of these clones shows that there is very strong homology between them and bovine and human T3 binding protein in both deduced amino acid sequence and nucleotide sequence, suggesting we have isolated cDNA of the skeletal muscle form of T3 binding protein (Supported by AHFMR, AHSF and MRC).

W-Pos60 HALOTHANE INCREASES CALCIUM LEAK FROM SARCOPLASMIC RETICULUM OF SAPONIN-SKINNED RAT VENTRICULAR TRABECULAE BY OPENING CALCIUM CHANNELS. JS Herland, DG Stephenson*, and FJ Julian, Dept. of Anesthesia Research Laboratories, Brigham & Women's Hospital, Boston MA, 02115 and *Dept. of Zoology, LaTrobe University, Bundoora, Victoria 3085, Australia.

Right ventricular trabeculae of female rats were dissected and skinned in 50 μg/ml saponin for 5-10 minutes. Sarcoplasmic reticulum (SR) function was investigated by loading for 7-10 minutes in 0.5-1.0 μM weakly buffered [Ca^{2+}]. The area under the force transient produced by exposure to 30 mM caffeine was used to indicate the amount of releasable Ca^{2+}. Ca^{2+} leak was investigated by exposure to an ATP-free leak solution immediately after loading and prior to caffeine-stimulated release. Halothane (0.5 mM, 2 mM) added to the leak solution caused a reversible dose-dependent decrease in releasable Ca^{2+}. When 10 μM Ruthenium Red (RRed), a known Ca^{2+} channel blocker, was included in both the loading and leak solutions, halothane's effect was blocked. AMP (11 mM) included in the leak solution caused a decrease in releasable Ca^{2+} similar in magnitude to that caused by 0.5 mM halothane. The effect of AMP was blocked when 10 μM RRed was included in both the loading and leak solutions. The results suggest that: 1) both halothane and AMP reversibly increase the permeability of cardiac SR to Ca^{2+}; 2) since each effect can be completely blocked by RRed, it appears that either AMP or halothane specifically stimulates Ca^{2+} efflux through the Ca^{2+}-specific release channel; 3) since there is no obvious source of adenine nucleotide to support Ca^{2+}-induced Ca^{2+} release (CICR) in the absence of ATP, halothane stimulates Ca^{2+} efflux through a mechanism different from enhancing CICR. This work supported by NIH Grant HL35032 (FJJ).

W-Pos61 MOLECULAR CLONING OF cDNAs ENCODING THE SARCOPLASMIC RETICULUM GLYCOPROTEINS. Ekkehard Leberer and David H. MacLennan, Banting and Best Department of Medical Research, Charles H. Best Institute, University of Toronto, Toronto, Ontario M5G 1L6, Canada.

A combination of antibody and synthetic oligonucleotide screening was used to isolate cDNAs encoding the 53 and 160 kDa glycoproteins of rabbit skeletal muscle sarcoplasmic reticulum. Sequence analyses and RNA blot hybridizations indicate that both glycoproteins derive from the same gene by alternative splicing. The 53 kDa glycoprotein cDNA encodes a largely hydrophilic protein of 453 amino acids with Mr of 52,421 and a 19 residue amino-terminal signal sequence. Structural prediction of the deduced amino acid sequence suggests that the 53 kDa glycoprotein is an extrinsic membrane protein bound peripherally to the luminal side of the sarcoplasmic reticulum membrane. The 160 kDa glycoprotein contains the complete sequence of the mature 53 kDa glycoprotein but the amino-terminal signal sequence is replaced by a much longer sequence characterized by juxtapositions of acidic amino acid residues similar to those found in calsequestrin (Fliegel et al., PNAS 84, 1167, 1987). Like calsequestrin, the 160 kDa glycoprotein binds Ca^{2+}, as detected by the Ca^{2+} overlay technique. We assume that the abundant negative charges provide the molecular basis for Ca^{2+} binding, suggesting that the 160 kDa glycoprotein could be involved in Ca^{2+} storage in the lumen of the sarcoplasmic reticulum.

W-Pos62 PATCH-CLAMP RECORDINGS OF K+ CHANNELS FROM MEMBRANE BLEBS ("SARCOBALLS") FROM SKINNED FROG SKELETAL MUSCLE FIBERS. *Michel B. VIVAUDOU, Christophe ARNOULT, and Michel VILLAZ*
Laboratoire de Biophysique Moléculaire et Cellulaire, C.E.N.G., 85X, 38041 Grenoble, FRANCE.

Recently, Stein & Palade (1988. *Biophys.J.* 54:357) reported that, after mechanical skinning of muscle fibers in millimolar Ca^{++}, membrane blebs developed which were large enough for patch-clamp recording. These blebs, termed "Sarcoballs", contained, in addition to large-conductance Cl^- channels, Ca^{++} channels with some properties expected from the Ca^{++}-release channels of the sarcoplasmic reticulum (SR). On this basis, sarcoballs were identified as extrusions of the SR membrane. However, K^+ channels which are abundant in the SR membrane were not seen.

In our hands, formation of sarcoballs was best achieved when fibers were skinned in nominally Ca^{++}-free solutions (PCa>8). These sarcoballs, which could be of a different origin than those obtained in Ca^{++}, were studied using the patch-clamp technique mostly in the excised inside-out mode (i.e., cytoplasmic side facing the inside of the pipette). The pipette always contained (in mM): 106 K^+, 6 Cl^-, 100 $Gluconate^-$, 10 Pipes, 1 EGTA. In symmetrical ionic conditions, a channel with a predominant conductance of 52 pS was observed. The Cl^- channel blocker DIDS (1 mM) on either side of the patch did not affect this channel. Neither did ionic substitution of $Gluconate^-$, an anion impermeant through Cl^- channels, with Cl^-. Replacement of all external K^+ with either Ca^{++} or Tris resulted in a shift in reversal potential with an almost complete rectification of the currents flowing from the sarcoplasmic side. Qualitatively similar effects of much less magnitude were produced when Na^+ replaced K^+. These results suggest that we are recording a channel which is selective for K^+ over other cations. Preliminary studies indicate that its opening probability is not strongly voltage-dependent and is not affected by Ca^{++}(<1 uM) or ATP(1-3 mM) on the cytoplasmic side. Further work is necessary to study the regulation of this channel as well as other channels and determine if our preparation consists of SR membrane.

W-Pos63 SITE-SPECIFIC MUTAGENESIS OF PHOSPHOLAMBAN. STUDIES OF RESIDUES INVOLVED IN PENTAMER FORMATION AND PHOSPHORYLATION. Junichi Fujii, Kei Maruyama, *Michihiko Tada, and David, H. MacLennan. Banting and Best Department of Medical Research, Charles H. Best Institute, University of Toronto, Toronto, Ontario M5G 1L6, Canada and *First Department of Medicine and Department of Pathophysiology, Osaka University School of Medicine, Osaka 553, Japan

The cloned cDNA encoding phospholamban, a regulatory protein of cardiac muscle sarcoplasmic reticulum Ca^{2+}-ATPase, has been expressed in COS-1 cells. The microsomal proteins isolated from cDNA-transfected cells were dissociated in SDS and subjected to polyacrylamide gel electrophoresis. The expressed phospholamban was pentameric and was phosphorylated by cAMP-dependent protein kinase. In order to identify amino acid residues responsible for stabilization of the pentamer, several amino acid residues were substituted by site-specific mutagenesis. Changes of each of the intramembranous polar amino acids Cys^{36}, Cys^{41} and Cys^{46} to Ser and Ala diminished the stability of the pentameric form, but mutations of Cys^{41} altered the stability of the pentamer most strongly. These results, together with the observation that mutations of Gln^{22}-Gln^{23}, Gln^{26}-Asn^{27}, and Gln^{29}-Asn^{30} to Ser, Asp or Ala had no effect on pentameric stability, suggest that the intramembranous cysteine residues might be responsible for the intermolecular interactions which prevent SDS from binding to the hydrophobic portion of the pentamer. The potential phosphorylation sites, Ser^{16} and Thr^{17}, and several positively charged amino acids were also altered. Through these mutations, we have confirmed that Ser^{16} is the amino acid residue uniquely phosphorylated by cAMP-dependent protein kinase and that Arg^{13}-Arg^{14} are necessary for phosphorylation.

W-Pos64 Ca^{2+} AND CALCIUM TRANSPORT IN CARDIOMYOPATHIC SYRIAM HAMSTER. J. Lopez, M. Mendoza, V. Sanchez. CBB, IVIC, Apdo. 21827, Caracas 1020A, Venezuela. There has been considerable interest about a postulated generalized membrane defect in muscular dystrophy. Intracellular free Ca was measured by means of calcium selective microelectrodes in the superficial fibers of the Extensor Digitorum Longus (EDL) isolated from cardiomyopathic Syriam Hamster (BIO 14.6) as well as control animals (WIB) at 3,6,9 and 12 months of age. In addition calcium uptake was measured in crude microsomal sarcoplasmic reticulum (SR) fractions from the same population of animals, using the Millipore filtration technique. The Ca^{2+} in the control muscle fibers was 110+20 nM (m+SEM, n=30) independently of the age. In the cardiomyopathic skeletal muscle fibers Ca^{2+} was 306 +30 nM at 3 months, 380 + 20 nM at 6 months, 860+60nM at 9 months, and 920+90 nM at 12 months. At 3 months of age, there were no difference in calcium uptake in SR vesicles from control or myopathic skeletal muscle. However, by 6,9 and 12 months the calcium uptake was significantly depressed, both in its initial rate and capacity. The results of this study provide some direct evidence about alteration in the regulation of intracellular calcium concentration in cardiomyopathic hamster which became more evident as the animal get older. It is interesting to notice that the changes in Ca^{2+} were detected at an early age than the changes in Ca uptake by the SR. This suggest that other mechanisms of intracellular Ca homeostasis in addition to the malfunction of the SR may be affected in these animals. (CONICIT, MDA and Elmor de Venezuela)

W-Pos65 SARCOPLASMIC CALCIUM ION CONCENTRATION IN NEUROLEPTIC MALIGNANT SYNDROME. J.R.Lopez[1], V.Sanchez[2], M.J.Lopez[1] [1]Centro de Biofisica y Bioquimica, IVIC, Aptdo. 21827, Caracas 1020A, Venezuela. [2]Dpt. of Biochemistry, UT Memphis, TN 38163. The neuroleptic malignant syndrome(NMS)is an uncommon but serious adverse effect of antipsychotic medication. Similarities in the clinical picture and muscle alteration between NMS and malignant hyperthermia(MH)suggest common mechanisms underlying both disorders. Intracellular free calcium concentration was measured by means of Ca++ selective microelectrodes in intercostal muscle fibers isolated from NMS patients and from subjects without evidence of neuromuscular disease, who served as controls The mean resting membrane potential and Ca++ i were -85+1 mV and .10+.01 uM (mean+SEM)in the control subjects. Similar determinations carried out in NMS fibers showed a mean value fo -83+1 mV and .49+.02 uM (mean+SEM) for the resting membrane potential and Ca++ i respectively. Only the difference in Ca++ i was significant. The incubation of NMS muscle bundles in dantrolene (10^{-6}M) induced a reduction on Ca^{2+} i to .20+.02 uM. These results show an alteration in sarcoplasmic ionic Ca^{2+} in NMS muscle fibers, suggesting that a dysfunction in skeletal muscle plays some role in the pathogenesis of NMS. (Supported by grants from CONICIT of Venezuela (S1 -1277), Muscular Dystrophy Association and Elmor de Venezuela)

W-Pos66 **PATCH CLAMP OF STRETCH-INDUCED SPHERES FROM FROG SKELETAL MUSCLE FIBERS.**

P.G. Stein and P.T. Palade. Department of Physiology and Biophysics, University of Texas Medical Branch, Galveston, TX 77550.

Stretching frog skeletal muscle fibers to the breaking point causes the rapid formation of numerous, large spheres of membrane (5-80 μm in diameter) on the fiber surface. Spheres appear immediately upon recoil of the broken fiber and thereafter increase in both size and number. The membrane composing the spheres forms gigaohm seals against 15-20 megaohm patch pipettes allowing low noise recording of patch currents. Currents recorded from excised, inside/out patches isolated from these spheres indicate that they contain a variety of channels including: a) a 12 pS Na^+-selective channel (P_{Na} / P_K ≈ 6) seen in the presence of 50 μM veratridine, b) a 21 pS (103 K_{bath} vs. 53 $Ca_{pipette}$) K^+-selective (P_K / P_{Na} ≈ 80) channel which exhibits only one open current level, appears in clusters and is rapidly blocked by 1 mM Mg-ATP and c) a relatively large (200 pS) Cl^- channel which exhibits voltage dependent gating, several subconductance states, is completely blocked by 5-10 mM Zn^{2+} on the cytoplasmic side of the membrane and has limited in selectivity over other anions (P_{Cl} / P_{MOPS} ≈ 4). Similar channels have been described previously in other preparations and identified as markers for skeletal muscle sarcolemmal membrane (SL). Accordingly, this technique represents an improvement in existing methods for studying SL channels because it allows rapid and direct recording of channels in the SL membrane without first having to pretreat fibers with proteolytic enzymes to render the membrane accessible to patch-pipettes.

This work done during the tenure of a Grant-in-Aid from AHA-Wyeth-Ayerst Laboratories (AHA 881114) and funded in part by 1PO1 HL37044.

W-Pos67 PHORBOL ESTER ALTERS $[Ca^{2+}]_i$ IN VENTRICULAR CELLS. Osami Kohmoto and William H. Barry (intr. by John L. Walker), Division of Cardiology, University of Utah, Salt Lake City, UT 84132

It has been reported that activation of protein kinase C has a negative inotropic effect in cultured ventricular cells, but the mechanism is not well understood. We studied the effects of the protein kinase C activator 12-O-tetradecanoyl-phorbol-13-acetate (TPA) on $[Ca^{2+}]_i$ (Indo-1 fluorescence), cell contraction (video motion detector), and Ca influx (^{45}Ca) in cultured chick embryo ventricular cells. Exposure to 80nM TPA decreased the amplitude of $[Ca^{2+}]_i$ transients and cell contraction within 60 seconds. In the cells rendered quiescent by exposure to verapamil, TPA did not have significant effect on resting $[Ca^{2+}]_i$. TPA decreased ^{45}Ca uptake in a first 60 seconds but, unlike verapamil, did not reduce rapidly exchangeable Ca content. These effects of TPA on $[Ca^{2+}]_i$, contraction, Ca flux and Ca contents resemble those produced by ryanodine in these spontaneously contracting cells, suggesting that TPA might be altering sarcoplasmic reticulum function. We therefore examined the effects of TPA on oscillatory cell motion induced by Ca overload, reported due to phasic Ca release from sarcoplasmic reticulum via ryanodine sensitive channels. Exposure to TPA resulted in marked slowing or cessation of cell motion oscillation induced by exposure to solution containing zero Na_o, and this effect was manifest within 60 seconds. These results indicate that TPA decreases the $[Ca^{2+}]_i$ transient in cultured ventricular cells, and that protein kinase C activation may inhibit Ca^{2+} induced Ca^{2+} release from sarcoplasmic reticulum.

W-Pos68 SIMULTANEOUS RECORDINGS OF $[Ca^{++}]_i$ AND pH_i IN PERFUSED RABBIT HEARTS CONTAINING INDO-1 AND BCECF. Rajendra Mohabir, Hon-Chi Lee, William T. Clusin. Cardiology Division, Stanford University School of Medicine, Stanford, California.

Continuous measurements of intracellular calcium and pH (pH_i) were made from isolated perfused rabbit hearts using the fluorescent calcium indicator Indo-1 and the pH_i indicator BCECF. These indicators were introduced by arterial perfusion with the acetoxymethylester forms. Indo-1 fluorescence was recorded from the epicardial surface of the left ventricle at an excitation wavelength of 360 nm and emission wavelengths of 400 and 550 nm. BCECF fluorescence was recorded at an excitation wavelength of 490 nm and an emission wavelength of 530 nm. Global ischemia decreased contractility and caused a rapid (first 2 min.) increase in both the systolic and end diastolic level of the calcium transients. The initial increase was followed by a decline to a level higher than baseline (2-5 min.). A secondary rise in the calcium transients occurred between 5 and 15 min. of ischemia. In contrast to the effects on the calcium transient, ischemia caused a monotonic decrease in pH_i (n=4 hearts) from a baseline of 7.03 $\pm$ .06 to 6.83 $\pm$ .02 after 2 min., 6.32 $\pm$ .01 after 10 and 6.11 $\pm$ after 15 min. To elucidate the role of cytoplasmic acidification in mediating increase in $[Ca^{++}]_i$ during ischemia, hearts were simultaneously loaded with Indo-1 and BCECF. Perfusion of hearts with acidified (hypercarbic) saline increased the systolic and diastolic values, but only when pH_i surpassed a threshold value, which was more acid than values achieved during the first 2 min. of ischemia (6.83 $\pm$ .03). Lesser degrees of acidification caused a decrease in contractility but did not affect the calcium transients. These results suggest that cytosolic acidification may contribute to the increase in $[Ca^{++}]_i$ during the first 15 minutes of global ischemia, but that some other factor mediates the increase during the first 2 minutes.

W-Pos69 REST DEPENDENT CA LOSS FROM SARCOPLASMIC RETICULUM OF INTACT CARDIAC MUSCLE. Lyle G. Walsh and John McD. Tormey, Dept. of Physiology, UCLA, Los Angeles CA 90024-1751

We have used electron probe x-ray microanalysis (EPMA) to measure changes in the Ca content of ventricular JSR and SR. The SR of rabbit papillary muscles was maximally loaded with Ca using optimized paired-pulse stimulation, and the redistribution of electrolytes that occurs over prolonged periods of rest was observed. We hypothesized that Ca is lost from the SR at a rate that correlates with contractility. Between rest periods of 30 and 600 sec, the cell Ca concentration decreased by 0.7 mmol/kg dry weight (-53%, $P \leq .05$), confirming results obtained by Bridge (J. Gen. Physiol. 88:437, 1986) using wet chemical analysis. Na and Cl concentrations declined by 30% and 16% respectively. Little of the Ca decrease came from myofibrils, mitochondria, T tubules or SL. On the other hand, the JSR Ca concentration decreased dramatically, from 13.4 to 2.4 mmol/kg dry weight ($P \leq .001$). This correlates closely with the concurrent fall in strength of the first post rest beat, from 69% of steady state after 30 sec to 9% after 600 sec rest. We also carried out a compartment analysis similar to that used previously (Walsh & Tormey, Cellular compartmentation in ischemic myocardium: Indirect analysis by electron probe, A.J.P., 255:H929, 1988). It indicated that the total SR represents 66% of the cell Ca content after 30 sec rest but only 29% after 600 sec. We conclude that: (a) Ca is lost from the SR of resting rabbit myocardium with a halftime on the order of 100 sec, (b) Ca concentration in the JSR correlates closely with contractility, (c) the SR contains sufficient Ca to fully activate the myofibrils, (d) a major part of this Ca is stored outside the JSR. Supported in part by NIH grant HL31249.

W-Pos70 **INWARD CALCIUM CURRENTS AND MYOPLASMIC CALCIUM TRANSIENTS IN FROG SKELETAL MUSCLE.** M. Amador, J. García & E. Stefani. Dept. Physiology and Molecular Biophysics, Baylor College of Medicine, Houston TX, 77030.

Ca^{2+} transients were recorded in single fibers with 0.5 mM $[APIII]_i$ and 0.1 mM $[EGTA]_i$. Ca^{2+} signals with 200 ms pulses had an initial fast rising phase and a later slower one. Only the late phase was increased (50%) when $[Ca^{2+}]_o$ was raised from 2 to 10 mM. The Ca^{2+} transient increase was associated with the I_{Ca} increment. Equivalent results were obtained when we added 2 μM Bay K 8644 (BK) to the extracellular solution, with either 2 or 10 mM Ca^{2+}. The decay of Ca^{2+} transients at the end of the pulse became slower in high Ca^{2+} or with BK. In other experiments with 1.0 mM $[EGTA]_i$, Ca^{2+} transients progressively decreased and became slower with repetitive stimulation (250 ms pulses to 0 mV, 0.02-0.03 Hz). The relationship between Ca^{2+} transients and I_{Ca} was more evident as the transients became smaller. Furthermore, with a large pulse to +100 mV they became smaller during the pulse. Addition of BK caused a parallel increase of I_{Ca} and Ca^{2+} transients. In conclusion, Ca^{2+} transients could be directly related to I_{Ca} which may contribute to a small fraction (≈10%) of the myoplasmic Ca^{2+} transients. The figure shows Ca^{2+} transients (upper traces) and I_{Ca} (lower traces) in 10 mM Ca^{2+} (A) and after the addition of BK (B). Supported by NIH.

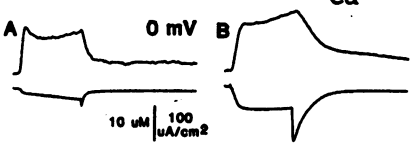

W-Pos71 SARCOPLASMIC IONIC [CA] MEASURED IN VIVO IN MALIGNANT HYPERTHERMIA SUSCEPTIBLE PATIENTS. EFFECTS OF DANTROLENE. J.R. Lopez[1], M. Lopez[2], P.D. Allen[3], [1]CBB, Instituto Venezolano de Investigaciones Cientificas (IVIC), Caracas 1020A, Venezuela, [2]Servicio de Medicina Interna, Hospital A. Larralde, Valencia, Venezuela, [3]Department of Anesthesia, Brigham and Women's Hospital, Boston, MA.

Malignant hyperthermia (MH) is a disorder of skeletal muscle triggered when susceptible patients are exposed to volatile anesthetic agents and/or depolarizing muscle relaxants. We have used Ca selective microelectrodes to measure the sarcoplasmic ionic [Ca] in vivo in the sartorius muscle in 3 MH susceptible patients, before and after the administration of dantrolene. MH susceptibility was confirmed by a high resting serum CPK and a positive caffeine contracture test from a previous muscle biopsy. All patients received epidural anesthesia with bupivacaine before the measurements were carried out. The mean resting ionic [Ca] of these patients was 480 ± 38 nM (M ± SEM n = 11) with a mean resting membrane potential of -83 ± 0.8 mV. The administration of 0.5, 1.5, and 2.5 mg/kg of dantrolene intravenously (cumulative dose) reduced the sarcoplasmic ionic [Ca] to 259 ± 34, 203 ± 12 and 85 ± 5 nM respectively, without a significant change in the resting membrane potential. These results extended our previous findings that susceptibility to MH is associated with an abnormally high resting sarcoplasmic ionic [Ca]. The administration of dantrolene produced a dose dependent reduction in the sarcoplasmic ionic [Ca]. We conclude that the effectiveness of dantrolene as a prophylactic and therapeutic agent might be associated with its ability to reduce the resting ionic [Ca] in MH skeletal muscle. (Supported by Grants from CONICIT of Venezuela S1-1277, Muscular Dystrophy Association).

W-Pos72 EFFECTS OF CAFFEINE, DANTROLENE, NITRENDIPINE AND TETRACAINE ON $[CA^{2+}]i$ IN SKELETAL MUSCLE FROM NORMAL AND MHS SWINE. [1]J.R. Lopez, [2]J. Contreras, [1]V. Sanchez, [3]P. D. Allen, [3]J. F. Ryan, [4]F.A. Sreter. [1]CBB, IVIC, Caracas, Venezuela, [2]Dept. de Anestesia, Hospital de Maracaibo, [3]Dept. of Anesthesia, Harvard Medical School, Boston, MA, [4] Boston Biomedical Research Institute, Boston, MA.

We have measured the intracellular free calcium concentration ($[Ca^{2+}]_i$) using calcium selective microelectrodes in the superficial fibers of the peroneus longus muscle isolated from normal and malignant hyperthermia susceptible (MHS) swine. The calcium microelectrodes were prepared using neutral carrier (ETH 1001 or 129). The isolated muscle preparation was placed in a temperature controlled chamber (37°C) and the sarcomere length was held at 2.2 μm. The resting $[Ca^{2+}]_i$ in the normal swine was 120 ± 10 nM(M ± SEM, n = 20) and it was 312 ± 20 nM (n = 20), in the MHS swine. The addition of 1 mM caffeine caused a significant increase in the $[Ca^{2+}]_i$ in both groups, to 218 ± 40 nM (n = 16) in the normals and 930 ± 30 nM (n = 18) in the MHS swine. The effect induced by caffeine was blocked by 1 mM tetracaine or 50 μM dantrolene, in both groups of muscle fibers. The addition of nitrendipine in the bathing solution from 25 to 200 μM did not modify the increment in $[Ca^{2+}]_i$ associated with the caffeine effect. These results extend our previous work in which we have shown that the resting $[Ca^{2+}]_i$ in MHS skeletal muscles is much higher than normal. The increment of $[Ca^{2+}]_i$ in the presence of caffeine, was much higher in the MHS (2.98 times) muscle than in the normal (1.8 times) swine, which might be related to the reduced threshold for caffeine observed in MHS skeletal muscle fibers. These data add further evidence that the Ca^{2+} increase seen with caffeine comes from intracellular stores and not through sarcolemmal calcium influx. (MDA, CONICIT S1-1277 and NIH GM 15904).

W-Pos73 ACTIVATION OF RYANODINE-SENSITIVE CALCIUM CHANNELS FROM FROG SARCOPLASMIC RETICULUM (SR) BY INOSITOL (1,4,5)-TRISPHOSPHATE (IP_3) IS STRONGLY CALCIUM DEPENDENT. B.A.Suárez-Isla[1], R. Bull and J.J.Marengo. [1]Centro de Estudios Científicos de Santiago, P.O.B. 16443, and Faculty of Medicine, Dept. Physiol. & Biophysics. University of Chile, P.O.B. 70055, Santiago, Chile.

The large conductance calcium channel (LCC channel) present in SR vesicles from frog (100 pS in 37 mM trans barium or calcium, incorporated in POPE/PS/PC Mueller-Rudin bilayers) is gated by IP_3, a postulated internal agonist in excitation-contraction coupling (1), that increases fractional open time (Po) in a concentration dependent manner (2). We have found that: a) increments in Po are mainly due to an IP_3 dependent decrease of a slow time constant (τ_{slow}) of closed interval distributions that accounts for >60% of all closures. At pCa 7.0, 1 μM IP_3 decreases τ_{slow} from 27.2 ± 3.9 ms to 17.3 ± 0.9 ms, while 3 μM IP_3 brings the value down to 13.1 ± 0.5 ms, without change in τ_{fast} or in the relative proportion of short and long closures. b) inositol (1,4)-bisphosphate (10 μM) or inositol (1,4,5,6)-tetrakisphosphate (10 μM) did not activate the channel. c) Increments in Po by IP_3 are strongly calcium dependent: at pCa 7.0, 10 μM IP_3 increases Po from 0.13 to 0.61 (n_H = 0.5, $K_D \approx 3$ μM); in contrast, at pCa 4.3, Po increases from 0.08 to 0.19 (n_H=1.6, $K_D \sim 12$ μM), while at pCa 8.0 no agonist effect was observed. d) ATP activation was also calcium dependent (K_D = 0.2 mM at pCa 6.0 and 2 mM at pCa 7.0). e) All agonists (including calcium itself) decreased τ_{slow} in a concentration dependent manner. Thus, τ_{slow} can plausibly be associated with agonist binding and channel activation steps. These results suggest a role of calcium as a modulator of LCC channel gating by IP_3 and ATP. (1) Vergara et al., PNAS, 82, 6352 (1985), (2) Suárez-Isla et al., Biophys J. 54 (1988). Supp. by NIH GM35981, MDA, FONDECYT 598 and U. de Chile DTI 2123.

W-Pos74 Na^+/Ca^{2+} EXCHANGE IN SMOOTH MUSCLE CELLS: ROLE IN Ca^{2+} REGULATION IN HUMAN ARTERIAL MUSCLE AND ENERGY DEPENDENCE. Jeffrey Bingham Smith and Lucinda Smith. Dept. Pharmacology, University of Alabama at Birmingham, UAB Station, Birmingham, AL 35294.

Smooth muscle cells were cultured from explants of umbilical arteries. The identity and homogeneity of the cells was indicated by >95% staining with an antibody (GCA7) to the α isoform of actin. 45Ca uptake depended on the Na gradient; loading the cells with Na stimulated 45Ca uptake only when assayed in the absence of external Na (Na_o). The presence of Na_o or dimethylbenzamil (DMB) prevented the stimulation of 45Ca uptake. DMB inhibited Na gradient-dependent 45Ca uptake by 50% at 1.7 μM. The effect of the Na gradient on cytosolic free Ca (Ca_i) was examined in cells that were grown on cover glasses and loaded with fura-2. Incubating the cells ouabain for 30 min to increase cell Na had no significant effect on Ca_i (146 ± 6 nM compared to 127 ± 6 nM for cells with basal Na, n=14, p>0.05). Replacing Na_o with choline transiently increased Ca_i; the Ca_i peaks were 363 ± 23 (10) and 776 ± 46 (14) for cells with basal or increased Na, respectively. Removing external Ca strongly inhibited the effect of Na_o removal on Ca_i in the Na-loaded cells; peak Ca_i after Na_o removal in the absence of external Ca was 210 ± 18 (4). Monensin (3 μM) slightly increased basal Ca_i. Removing Na_o 2 min after adding monensin evoked a large spike in Ca_i which depended on the presence of external Ca. The Ca_i peaks produced by Na_o removal were 1001 ± 113 (8) and 188 ± 12 (5) in the presence and absence of external Ca, respectively. Human skin fibroblasts had no detectable DMB-inhibitable 45Ca uptake that depended on the Na gradient. Previously we reported that Na_o removal releases stored Ca in human fibroblasts. Na_o removal also released stored Ca from the muscle cells, but to a much smaller extent than in the the fibroblasts. Na^+/Ca^{2+} antiport activity in rat aortic muscle cells was strongly inhibited by energy poisons. Rotenone decreased cell ATP slightly more rapidly that it decreased antiport activity. The presence of glucose prevented rotenone from decreasing ATP and antiport activity. Adding glucose after ATP depletion restored ATP and antiport activity to control levels. A small amount of antiport activity was maintained in the absence of detectable ATP. (Supported by Grants DK39258 and HL01671 from the NIH and a Grant-in-Aid from the American Heart Association.)

W-Pos75 CHANGES IN $[Ca^{2+}]_i$ MEASURED IN VENTRICULAR MUSCLE CELLS OBTAINED FROM HEART TRANSPLANTED PATIENT. J. R. López[1], R. Espinoza[2], V. Parthé[1], M. Penso[2], G. Cordovez[1]. [1]CBB, IVIC, Apartado 21827 Caracas, Venezuela. [2]Unidad de Cardiología, Hospital Miguel Pérez Carreño, Caracas, Venezuela.

Endomyocardial biopsy is the only dependable method of diagnosis rejection on cardiac recipients. We have measured the intracellular free calcium concentration ($[Ca^{2+}]_i$) by means of calcium selective microelectrodes in right ventricular cells, obtained with a Stanford Caves Schultz bioptome, from 3 heart trasplanted patiens as part of the program of early diagnosis of rejection. The mean resting $[Ca^{2+}]_i$ in the muscle biopsies obtained 8, 16, 24, 32 and 40 days after the trasplant were 531 ± 66 nM (M ± SEM, n = 8), 454 ± 42 nM (n = 9), 336 ± 42 nM (n = 6), 228 ± 49 nM (n = 6) and 140 ± 9 nM (n = 8). Histological studies carried out with hematoxylin-eosin, methyl green pyronine and trichrome stains revealed interstitial and intermiofibrillar edema, fibrosis, areas of hiper contractions and lipid droplets. Morphological changes that reverted as a function of time, reaching a normal appearance at the last biopsy. In the muscle biopsies obtained after 40 days of heart trasplant the effect of acidosis on $[Ca^{2+}]_i$ was studied. Acidification produced by increasing $[CO_2]$ in the external medium, induced a detectable increment in the $[Ca^{2+}]_i$, from 140 ± 9 nM (n = 8) to 245 ± 32 nM (n = 6). These results show that the inflamatory process observed in the early period of heart trasnplant seem to be associated to significant increment in intracellular $[Ca^{2+}]_i$. In addition, acidification produced a measurable increase in resting $[Ca^{2+}]_i$. (Supported by CONICIT S1-1277 MDA and Elmor of Venezuela).

W-Pos76 DEPOLARIZATION-INDUCED Ca^{2+} RELEASE IN SINGLE MAMMALIAN CARDIAC MYOCYTES REQUIRES Ca^{2+} INFLUX THROUGH THE Ca^{2+} CHANNEL. M. Näbauer, G. Callewaert, L. Cleemann & M. Morad, Univ. of Pennsylvania, Dept. of Physiology, Philadelphia, PA.

In absence of $[Ca^{2+}]_o$, contraction in cardiac muscle is completely suppressed. We have recently shown that intracellular Ca^{2+} release is gated primarily by the Ca^{2+} current (Callewaert et al., PNAS 85:2009, 1988). Here we examine the specificity of transport of Ca^{2+} vs. other charge carriers (Ba^{2+}, Na^{+}) through the Ca^{2+} channel in regulating Ca^{2+} release and development of tension. Rat or guinea pig ventricular myocytes were enzymatically isolated and were dialyzed with fura-2 (0.5 mM) or 0.1 mM BAPTA, for measurement of respectively intracellular Ca^{2+} transients or cell shortening. Ca^{2+} current was activated repetitively at 0.2 Hz by depolarizing pulses from -80 to +10 mV. A rapid perfusion system (50-100 ms) was used to alter the extracellular concentration of Ca^{2+} or to add drugs. Replacement of Ca^{2+} containing solution with one containing nominal Ca^{2+} (10 uM) reduced i_{Ca} and abolished Ca^{2+} release or cell shortening within 200 ms. Replacement of normal Ringer with one containing Ca^{2+} activity < 10^{-8}M ("0" Ca^{2+} + 5mM EGTA) activated a larger Na^{+} current through the Ca^{2+} channel, but did not activate Ca^{2+} release or cell shortening. In such Ca^{2+}-poor solutions Ca^{2+} release or cell shortening could be serially induced with application of caffeine (1-5 mM), suggesting that intracellular stores were fully intact. Similarly, rapid replacement of Ca^{2+} by Ba^{2+} as the charge carrier through the Ca^{2+} channel failed to activate release. Our results therefore show that transport of Na^{+} or Ba^{2+} through the Ca^{2+} channel cannot gate the release of Ca^{2+} from the intracellular stores when the stores are intact and suggests a Ca^{2+}-specific mechanism for the release of Ca^{2+}.

W-Pos77 CHARACTERISTICS OF CALCIUM TRANSIENTS AND ELECTROPHYSIOLOGY IN HUMAN VENTRICULAR MYOCYTES. Q. Li, B. Biagi, R. Starling, C. Hohl, R. Altschuld and B. Stokes (Intr. by D. Jung). Department of Physiology and Division of Cardiology, The Ohio State University, Columbus, Ohio 43210.

Calcium tolerant ventricular myocytes were isolated from excised end-stage failing human hearts. When perfused in Krebs-Henseleit buffer at 35° C, pH 7.2 - 7.4, the human myocytes had resting membrane potentials of -68.5 ± 1.4 mV (X ± SE, n = 24). Action potential duration evaluated at 50% (APD_{50}) and 90% recovery (APD_{90}) was 678 ± 72 and 801 ± 75 msec, respectively. Resting free Ca^{2+} measured by single cell fura-2 fluorescence microscopy averaged 126 ± 15 nM (n = 29 cells). Small and prolonged free Ca^{2+} transients could be recorded from single human myocytes during electrical stimulation (A). A distinctive and temporally fast component of the calcium transient (L1) was evident when the cell was treated with 1 μM isoproterenol (Iso) (B), but was abolished by 10 mM caffeine (C). We conclude therefore that the L1 phase in human myocytes predominantly reflects Ca^{2+} handling by the sarcoplasmic reticulum. APD_{50} and APD_{90} were also increased by 1 μM Iso to 200% and 145%, respectively. Human myocytes can therefore be examined individually and show pharmacological responses similar to multicellular preparations. (Supported by HL36240, USPHS-10165 and The Central Ohio Heart Chapter, Inc.)

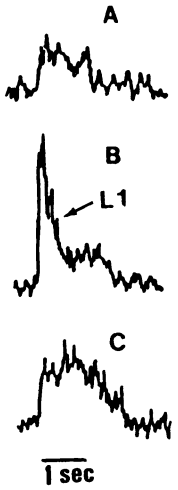

W-Pos78 **INTRACELLULR CALCIUM IN VOLTAGE-CLAMPED GUINEA PIG VENTRICULAR MYOCYTES MEASURED WITH INDO-1.** L.M. Crespo and M.B. Cannell. Dept. of Pharmacology, Univ. Miami Sch. Medicine, Miami, FL 33136.

Enzymatically dissociated guinea pig ventricular myocytes were voltage clamped with a single microelectrode technique. The electrode filling solution contained (in mM/l) 83 KGlutamate, 20 CsCl, 5 glucose, 30 PIPES, 3.3 KATP, 5 $MgCl_2$, 10 TEA & 0.05 K-Indo-1, pH 7.2. Fluorescence from a 20 μm diameter spot was split at 450 nm to allow simultaneous measurement at 400 and 500 nm. With fluorescence excitation at 350 nm, voltage clamp depolarization resulted in changes in fluorescence at both wavelengths (see figure), consistent with a $[Ca]_i$ increase. We are also able to monitor cell shortening by illuminating the cell at 650 nm without contaminating the fluorescence record. We find that resting $[Ca]_i$ is increased by depolarization, but that the amount of calcium released from the SR (in response to fixed size depolarizations) is decreased by this increase in $[Ca]_i$. Experiments are currently in progress to determine if this phenomenon arises from calcium-inactivation of calcium release. Supported by the AHA and NIH R01 HL39733-01A1.

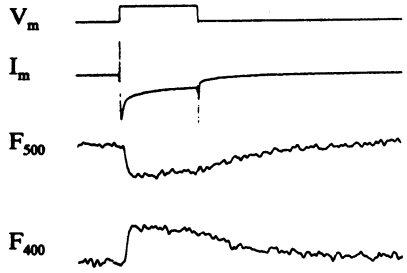

Fig. showing unaveraged response to a 160 msec step from -55 to 0 mV. Peak Ca current is 1.2 nA.

W-Pos79 NOREPINEPHRINE AND GTPγS INCREASE MYOFILAMENT SENSITIVITY TO CALCIUM IN α-TOXIN PERMEABILIZED ARTERIAL SMOOTH MUSCLE. Junji Nishimura and Cornelis van Breemen. Department of Pharmacology, University of Miami, School of Medicine, Miami FL 33101.

A new method for preparing permeabilized smooth muscle fibers from rabbit mesenteric artery has been developed using α-toxin, a transmembrane pore-making exo-protein produced by Staphylococcus aureus. After α-toxin treatment, the fibers developed tension as a function of Ca^{2+} concentration (EC_{50}= 890 nM). Fibers could not contract without added ATP, indicating loss of endogenous ATP from the permeabilized cells. When the sarcoplasmic reticulum (SR) was loaded with $5x10^{-7}$ M Ca^{2+} solution, norepinephrine(NE) with 100 μM GTP induced a transient contraction in 2 mM EGTA 0 M Ca^{2+} solution and a transient and maintained contraction in $5x10^{-7}$ M Ca^{2+} solution. NE with 100 μM GTP caused a sustained contraction in 10^{-7} M Ca^{2+} solution even after the SR was depleted. However, NE could not contract the fiber in the presence of 100 μM GDPβS, non-hydrolysable GDP analog, in 10^{-7} M Ca^{2+} solution. GTPγS, a non-hydrolysable GTP analog, substitutes for NE in producing these contractile effects. The contraction induced by GTPγS could be reversibly inhibited by 20 μM H-7, an inhibitor of protein kinase C (PKC). The analysis of the relationship between Ca^{2+} and maintained tension revealed that NE and GTPγS increased the Ca^{2+} sensitivity of the myofilaments shifting the EC_{50} to 280 nM and 160 nM, respectively. These results indicate that signal transduction through α-adrenoceptors is mediated by a G protein. Activation of this G protein by either NE or GTPγS induces an increase in myofilament sensitivity to Ca^{2+} which probably involves PKC mediated phosphorylation of elements of the contractile apparatus. This constitutes the first report on a permeabilized smooth muscle preparation with intact receptor and transducing mechanisms.

W-Pos80 INOSITOL TRISPHOSPHATE. METABOLISM IN SKELETAL MUSCLE MEMBRANES AND POTENTIAL-DEPENDENT EFFECTS IN SKINNED FIBERS. Cecilia Rojas, Ximena Sánchez, M. Angélica Carrasco, Cecilia Hidalgo and Enrique Jaimovich. Centro de Estudios Científicos de Santiago, P.O. Box 16443, Santiago 9, Chile, and Departamento de Fisiología y Biofísica, Facultad de Medicina, U. de Chile, P.O. Box 70055, Santiago 7, Chile.

Inositol trisphosphate (IP3) has been proposed as a chemical messenger in E-C coupling in skeletal muscle (Vergara et al, PNAS. USA. 82, 6352, 1985; Volpe et al, Nature 316, 347, 1985). We have carried out experiments in mechanically skinned fibers or in membrane fractions isolated from frog skeletal muscle to test this model. In skinned fibers, IP3 causes fast calcium release, detected by means of aequorin light signals; IP3-induced calcium release requires a pCa of 7 and is synergistic with caffeine. Ion substitution affects the IP3-induced responses. Thus, uM concentrations of IP3 fail to produce release when fibers are skinned in high sodium solutions and tested in high potassium solutions (polarized fibers). In contrast, fibers skinned in high potassium and tested in high sodium (depolarized fibers) release calcium following addition of very low (sub uM) concentrations of IP3. These results agree with those of Donaldson et al. (PNAS USA, 85, 5749, 1988) and suggest that the effect of IP3 is under control of the transverse tubule (T-tubule) membrane potential. Experiments carried out in isolated muscle membranes revealed significant IP3-ase activity, which is enriched in T-tubules but is also present in sarcoplasmic reticulum vesicles. Furthermore, only T-tubule membranes phosphorylate phosphatidylinositol to phosphatidylinositol bisphosphate, and hydrolyze the latter although with low specific activity. These combined results support a role of IP3 as chemical transmitter in E-C coupling.
Supported by NIH GM35981, MDA, Fondecyt and DTI.

W-Pos81 QUALITATIVE AND QUANTITATIVE COMPARISON OF SYSTOLIC AND DIASTOLIC CALCIUM LEVELS IN AEQUORIN-LOADED PAPILLARY MUSCLES VERSUS INTACT WORKING HEARTS OF FERRETS. Yasuki Kihara, William Grossman, and James P. Morgan. Harvard-Thorndike Laboratory of Beth Israel Hospital and Harvard Medical School, Boston, MA 02215.

We recently reported a technique for loading the bioluminescent Ca^{2+} indicator aequorin (Aq) into ferret papillary muscles (PM) and isolated perfused whole hearts (WH) that involves macroinjecting (MACRO) Aq beyond the epimysium and into the interstitium (Kihara and Morgan, 1988. J Gen Physiol 92:47a). In the present study, we compare the Ca^{2+} transients and levels obtained with MACRO in WH (Kihara and Morgan, 1988. J Mol Cell Cardiol 20:S59) and PM. In both preparations, the Aq-light signal rose to a peak and declined towards baseline before the corresponding isometric tension/left ventricular pressure response. MACRO did not affect the mechanical responses of either the PM or WH. The Aq-signals from WH showed equivalent time courses to those from PM at 30° C in 1 mM $[Ca^{2+}]_o$. Moreover, end-diastolic and peak systolic $[Ca^{2+}]_o$ determined by the method of fractional luminescence were similar in both preparations and lay in the range of 2-3 x 10^{-7} M and 0.8-1 x 10^{-6} M, respectively. The effects of drugs (including isoproterenol, increases in $[Ca^{2+}]_o$, and cardiotonic steroids) and interventions (extrasystolic stimuli) had similar effects on the Aq-light signals and mechanical activity of both preparations. These studies indicate that MACRO provides similar qualitative and quantitative results in both PM and perfused WH. (Support: HL31117, DA05171, HL01611, to JPM, and awards from the Jap. Fnd. Metab. Dis., and AHA Mass. Affiliate to YK).

W-Pos82 COMPARISON OF MEASUREMENTS OF INTRACELLULAR Ca^{++} CONCENTRATION WITH ION-SELECTIVE MICROELECTRODES AND AEQUORIN IN THE SAME INTACT ISOLATED FROG SKELETAL MUSCLE FIBERS. L.A. Blatter and N.K.M. Lee (Intr. by J.R. Blinks). Department of Pharmacology, Mayo Foundation, Rochester, MN 55905.

Calcium-selective microelectrodes (single-barrelled; Ca^{++} sensor ETH 1001, PVC mixture) and the bioluminescent Ca^{++} indicator aequorin (microinjected intracellularly) were used in the same intact single skeletal muscle fibers of the frog (Rana temporaria) to compare the two different methods for measuring intracellular calcium ($[Ca^{++}]_i$) levels. EGTA-buffered solutions with an ionic composition similar to that of the intracellular fluid were used to calibrate the electrodes and the aequorin signal (concentrations in mmol/l: K^+ 130; Na^+ 8.2; Mg^{++} 1; Cl^- 130.1; EGTA 1; PIPES 5; pH 7.0; Ca to give concentrations between pCa 7.4 and 5.4; the logs of the apparent association constants for the Ca-EGTA complex estimated with the electrodes and with aequorin were 6.43 and 6.39, respectively). Signals recorded from fibers in normal physiological salt solution ($[K^+]_o$ 2.5 mmol/l) could not readily be compared for two reasons: (1) $[Ca^{++}]_i$ was so low that the calibration curves for both indicators were nearly flat, and experimental points falling below the calibration curves gave indeterminate values; (2) the aequorin signal was consistently below the level of calcium-independent luminescence expected for the amount of aequorin in the fiber (by 0.3 log unit). Preliminary experiments with cut fibers in vitro revealed that the Ca^{++}-independent luminescence of aequorin was reduced by exposure to myoplasm, but that the Ca^{++}-stimulated luminescence was not. Therefore, $[K^+]_o$ was raised to 12.5 mmol/l; this increased the aequorin signal well above the level of Ca^{++}-independent luminescence, but did not cause a detectable contracture. In each fiber the aequorin signal was recorded immediately before and after a microelectrode measurement. (The electrode was calibrated before and after the impalement.) With $[K^+]_o$ 12.5 mmol/l the results obtained with the two indicators were not significantly different: in eight muscle fibers $[Ca^{++}]_i$ determined with electrodes was 41 nmol/l. $[Ca^{++}]_i$ measured with aequorin before and after impalement by the electrodes was 37 and 41 nmol/l, respectively. (Support: USPHS grant HL12186).